The role of the AhR signaling pathway in regulation of gut-associated immune cells

Dissertation

zur Erlangung des Doktorgrades (Dr.rer.nat)

der

Mathematisch-Naturwissenschaftlichen Fakultät

der

Rheinischen Friedrich-Wilhelms-Universität Bonn

vorgelegt von

Jan Oliver Schanz

aus

Schwerte

Bonn, Januar 2018

Angefertig mit Genehmigung der Mathematisch-Naturwissenschaftlichen Fakultät der Rheinischen Friedrich-Wilhelms-Universität Bonn

1. Gutachter: Prof. Dr. rer. nat. Irmgard Förster

2. Gutachter: Prof. Dr. Natalio Garbi

Tag der Promotion: 29.05.2018

Erscheinungsjahr: 2018

Eidesstattliche Erklärung

Hiermit erkläre ich an Eides statt, dass

die vorgelegte Arbeit – abgesehen von den ausdrücklichen bezeichneten Hilfsmitteln – persönlich, selbstständig und ohne Benutzung anderer als der angegbenen Hilfsmittel angefertigt wurde,

die aus anderen Quellen direkt oder indirekt übernommenen Daten und Konzepte unter Angabe der Quelle kenntlich gemacht sind,

die vorgelegte Arbeit nicht bereits anderweitig als Dissertation eingereicht worden ist,

ich keine früheren Promotionsversuche unternommen habe,

für die Erstellung der vorgelegten Arbeit keine fremde Hilfe, insbesondere keine entgeltliche Hilfe von Vermittlungs- oder Beratungsdiensten in Anspruch genommen wurde.

Bonn, den_____ _____

Jan Oliver Schanz

Table of Contents

Abstract/ Summary

The aryl hydrocarbon receptor (AhR) is an important sensor for environmental polyaromatic chemicals and plays an essential role in immune regulatory processes, including maintenance of intestinal barrier integrity. AhR activity is regulated through the AhR repressor (AhRR), which is encoded by an AhR target gene. Regulation and interplay of AhR and AhRR, however, remain largely elusive. Using AhRR/EGFP-reporter mice it could be shown that the AhRR is specifically expressed in immune cells of barrier organs, but not in intestinal epithelial cells, different from the more widespread expression of the AhR. Similar to AhR-knockout mice, AhRR-deficient mice are highly susceptible to dextran sodium sulfate (DSS)-induced colitis.

In this PhD thesis it could be shown that enhanced colitis susceptibility in AhRR-deficient mice was accompanied by enhanced Th17/Tc17 and reduced Th1/Tc1 frequencies in the gut. In contrast, AhR-deficiency resulted in accumulation of both Th17/Tc17 and Th1/Tc1 cells in the intestine. A decreased frequency of intestinal ILC3s, previously held responsible for colitis susceptibility in $AhR^{-/-}$ mice, was not observed in AhRR-deficient mice. Yet, significantly elevated IL-1β levels could be detected in steady-state colon tissue of AhRR-deficient mice, indicating enhanced activation of the innate immune system. Using conditional macrophage- and neutrophil-specific AhRR-knockout mice, it could be shown that these cells types do not convey the enhanced DSS colitis susceptibility noticed in complete AhRR-deficient mice.

Moreover, it was shown that cell type-specific AhRR expression in intestinal immune cells is driven by dietary AhR ligands, whereas depletion of microbiota by treatment with broad-spectrum antibiotics had no effect on AhRR expression. Further, it could be confirmed that lack of dietary AhR ligands deteriorates the mucosal intestinal barrier, whereas AhR ligand supplementation improves barrier integrity and protects from DSS-induced colitis. Interestingly, other synthetic diets like High fat diet and matched control diet protect against DSS-induced colitis, despite low AhR ligand content, highlighting the existence of other diet related pathways besides AhR signaling with great importance for the intestinal barrier function.

Overall the findings of this thesis underline the physiologic importance of cell-type-specific balancing of AhR/AhRR signaling in response to microbial, nutritional and inflammatory stimuli.

Zusammenfassung

Der Arylhydrocarbon Rezeptor (AhR) ist ein wichtiger Sensor für polyaromatische Umweltchemikalien und spielt eine wesentliche Rolle bei immunregulatorischen Prozessen, einschließlich der Aufrechterhaltung der Integrität der Darmbarriere. Die AhR-Aktivität wird durch den AhR-Repressor (AhRR) reguliert, der durch ein AhR-Zielgen kodiert wird. Regulierung und Zusammenspiel von AhR und AhRR bleiben jedoch weitgehend unklar. Mit AhRR/EGFP-Reporter Mäusen konnte gezeigt werden, dass der AhRR spezifisch in Immunzellen von Barriere Organen exprimiert wird, jedoch nicht in Darmepithelzellen, was sich von der weiter verbreiteten Expression des AhR unterscheidet. Ähnlich wie AhR-Knockout-Mäuse sind AhRR-defiziente Mäuse sehr anfällig für Dextran-Sodium-Sulfat (DSS)-induzierte Colitis.

In dieser Dissertation konnte gezeigt werden, dass eine erhöhte Colitis-Anfälligkeit bei AhRR-defizienten Mäusen mit einer erhöhte Th17/Tc17- und reduzierter Th1/Tc1-Frequenz im Darm assoziiert war. Das Fehlen des AhR führte zur erhöhten Frequenzen von sowohl Th17/Tc17- als auch Th1/Tc1-Zellen im Darm. Eine verringerte Häufigkeit von intestinalen ILC3s, die für die Colitis-Empfindlichkeit bei $AhR^{-/-}$ Mäusen verantwortlich gemacht wird, konnte bei AhRR-defizienten Mäusen nicht beobachtet werden. Dennoch konnten signifikant erhöhte IL-1β Spiegel im Kolongewebe von unbehandelten AhRR-defizienten Mäusen als Hinweis für eine verstärkte Aktivierung des angeborenen Immunsystems nachgewiesen werden. Mit Hilfe von Makrophagen- und Neutrophilen-spezifischen AhRR-Knockout-Mäusen konnte gezeigt werden, dass diese Zelltypen nicht die erhöhte DSS-Colitis-Empfindlichkeit vermitteln. Darüber hinaus wurde gezeigt, dass die zelltypspezifische AhRR-Expression in intestinalen Immunzellen durch AhR-Liganden in der Nahrung gesteuert wird, während die Reduktion der Mikrobiota keinen Einfluss auf die AhRR-Expression hatte. Weiterhin konnte bestätigt werden, dass der Mangel an diätetischen AhR-Liganden die Darmbarriere Integrität verschlechtert, während AhR-Ligand-Supplementation die Barriere Funktion verbessert und vor DSS-induzierter Colitis schützt. Andere synthetische Diäten wie eine fettreiche Diät und angepasste Kontrolldiät schützen trotz niedrigem AhR-Ligandengehalt gegen DSS-induzierte Colitis, was die Existenz anderer ernährungsabhängiger Signalwege mit großer Bedeutung für die Darmbarriere unterstreicht. Insgesamt zeigen die Ergebnisse dieser Arbeit die physiologische Bedeutung zelltypspezifischer Balancierung von AhR/AhRR Expression als Reaktion auf mikrobielle, Ernährungs- und Entzündungsreize.

List of Abbreviations

2-1′H-indole-3′-carbonyl)-thiazole-4-carboxylic acid methylester	ITE
2,3,7,8-tetrachlordibenzo-ρ-dioxin	TCDD
4',6-diamidino-2-phenylindole	DAPI
6-formylindolo[3,2-b]carbazol	FICZ
AhR nuclear translocator	ARNT)
AhR repressor	AHRR
Antigen presenting cell	APC
Antimicrobial peptide	AMP
Aryl hydrocarbon receptor	AhR
Aryl hydrocarbon receptor interacting protein	AIP
benzo[a]pyrene	B[a]P
C-C chemokine receptor	CCR
Cluster of differentiation	CD
Cryptopatch	CP
cullin 4B	CUL4B
Dendritic cell	DC
Dendritic epidermal T cell	DETC
Dextran sodium sulfate	DSS
Dioxin response element	DRE
Enzyme-linked Immunosorbent Assay	ELISA
Follicle associated epithelium	FAE
Genome-wide significant	GWS
Granulocyte macrophage colony-stimulating factor	GM-CSF
Gut associated lymphoid tissue	GALT
Halogenated aromatic hydrocarbon	HAH
HBV X-associated protein,	XAP-2
Heat shock protein 90,	HSP
Immunoglobulin	Ig
Indole-3-carbinol	I3C
indolo[3,2-b]carbazol	ICZ
Inducible NO synthase	iNOS

Inflammatory bowel disease	IBD
Inhibitor of DNA binding 2	ID2
Innate lymphoid cell	ILC
Interferon	IFN
Interleukin	IL
Intestinal epithelial cell	IEC
Intraepithelial lymphocyte	IEL
Isolated lymphoid follicle	ILF
Lamina propria mononuclear cells	LPMC
Lymphoid tissue inducer	LTi
Lymphoid tissue organizer	LTo
Lymphotoxin α1β2	LTα1β2
Lymphotoxin β receptor	LTβR
Macrophage colony-stimulating factor	M-CSF
Mesenteric lymph node	mLN
Microfold cell	M cell
millimeter	mm
Natural cytotoxicity triggering receptor	NCR
Nuclear factor-κB	NF-κB
basic helix-loop-helix	bHLH
Pathogen-associated molecular pattern	PAMP
Pattern recognition receptor	PRR
Polychlorinated biphenyls	PCB
PER-ARNT-SIM	PAS)
Peyer's patches	PPs
Polycyclic aromatic hydrocarbon	PAH
Regulatory T cells	T_{reg}
Retinoic acid-related orphan receptor γt	RORγt
rounds per minute	rpm
Solitary isolated lymphoid tissue	SILT
Specific pathogen-free	SPF
T cell receptor	TCR
T helper	T_h

T-box transcription factor	T-bet
TCDD-inducible poly (ADP-ribose) polymerase	TiPARP
thymic stromal lymphopoietin	TSLP
TNF receptor	TNFR
Transforming growth factor	TGF
Tumor necrosis factor	TNF
Type 1 regulatory cell	Tr 1 cell
Ulcerative colitis	UC
Xenobiotic response element	XRE

Table of Figures

Table of Tables

1 Introduction

1.1 The immune system

All organisms are confronted with infectious agents or toxic substances throughout their life. A variety of organs, cells and molecules protect the body against infectious or harmful insults. The sum of these organs, cells and molecules form the immune system. The immune system is a complex and interactive network that fulfills four main tasks in order to equip an organism with effective protection. First, an infection needs to be detected and recognized in order to secondly instruct immune effector functions, which restrict and ideally eliminate an infection. Inactivity of the immune system can lead to chronic infections and immunodeficiency, whereas overshooting reactions may result in allergy and autoimmune diseases. In order to prevent these events, the third task of the immune system is to self-regulate its own actions. The fourth task is to prevent recurring disease due to infection with the same pathogen, by generating immunological memory[1,2].

With regard to speed and specificity of the response, the immune system can be divided into innate and adaptive immunity. These two parts consist of different cells types fulfilling distinct functions to achieve protection. Nonetheless, in practice none of the two systems works independently, as there is much interaction between innate and adaptive immunity.

1.1.1 Innate immunity

The innate immune system is the first line of defense, preventing pathogens from infiltrating the body. It is the evolutionary oldest part of the immune system and highly conserved even in the simplest organisms. Elements assigned to the innate immune system are physical barriers, inflammation-related serum proteins, antimicrobial peptides (AMPs), the complement system, cytokines and chemokines. Furthermore, cells phagocytozing invading pathogens and releasing cytokines or other inflammatory mediators are assigned to the innate immune system[3]. These are for instance neutrophils, monocytes and macrophages (MΦ). Together with other innate immune cells, such as innate lymphoid cells (ILCs) and mast cells, they endow the organism with immediate protection. In addition, the innate immune system is equipped with a variety of receptors to recognize pathogen-associated molecular patterns (PAMPs) present on many microorganisms. These pattern recognition receptors (PRRs) exist as membrane bound proteins on for example macrophages, neutrophils and dendritic cells (DCs), as cytoplasmic PRRs and as secreted molecules[4]. Activation of PRRs recruits signaling adaptors that control processes like the induction of local inflammation, recruitment

of further effector cells, restriction of a local infection and finally triggering of an adaptive immune response. However, the innate immune system lacks classical immunological memory, meaning its responses remain the same, irrespective of how many times a specific infectious agent is encountered. Interestingly, this concept has recently been challenged. Organisms lacking adaptive immunity have been shown to develop resistance to reinfections, a phenomenon termed “trained immunity”, that hereafter has also been demonstrated for more complex organisms[5]. Furthermore, the innate immune system cannot provide specificity against individual pathogens, which depends on activation of the adaptive immune system by antigen presenting cells[3].

1.1.2 Adaptive immunity

The adaptive immune response is of special importance when clearance of a pathogen by the innate immune system fails. Antigen presentation by antigen presenting cells accompanied by co-stimulation and changes in the cytokine microenvironment, trigger the adaptive immune response. Adaptive immunity involves selection and expansion of lymphocytes, bearing receptors with high specificity for foreign antigens. These receptors allow for a fine discrimination between self and non-self. Additional central features of the adaptive immune system are the elimination of pathogens and pathogen-infected cells and the creation of immunological memory that provides protection against re-infection[6]. Two central cells types of the immune system are T and B lymphocytes. T lymphocytes (T cells), which mature in the thymus are the effectors of the cellular immune response and can be functionally divided into subsets either assisting other cells in immunological processes ($CD4^+$ T cells) or directly destroying virus-infected cells or tumor cells ($CD8^+$ T cells)[7]. B lymphocytes (B cells), which arise in the bone marrow, develop into antibody producing plasma cells directed by signals from $CD4^+$ helper T cells. Antibodies form the humoral component of the adaptive immune system and are used to neutralize pathogens, precipitate antigens for phagocytosis and activate the complement system[1,7].

1.2 The mucosal immune system of the gut

Most pathogens enter the body through mucosal surfaces of the respiratory, urogenital and gastrointestinal tract. These mucosal surfaces represent an enormous area to be protected. For instance, the human small intestine has a surface area of almost $400m^2$, which is 200 times that of the skin[1]. Besides occasional incorporation of pathogens, the intestine is constantly exposed to antigens derived from the diet or the commensal microbiota. Under these

influences the gastrointestinal tract has developed into the largest compartment of the immune system with functional specialization in order to mount immune responses against pathogenic threats, while maintaining tolerance against non-harmful antigens. Distinctive anatomical features, specialized mechanisms for antigen uptake and unique effector and regulatory responses fulfill these challenges. Further, various mechanical mechanisms, including the epithelial cell barrier and extra-epithelial defenses at mucosal surfaces protect the underlying tissue from penetration by pathogens. Immune cells are organized in lymphoid tissues and are scattered across the surface epithelium of the mucosa and the underlying layer of connective tissue, termed lamina propria. Tissue compartments assigned to mucosa-associated lymphoid tissue (MALT) are principally divided into inductive sites, where antigens are sampled from mucosal surfaces and stimulate cognate naïve T and B cells, and effector sites, where effector cells perform their action[8].

1.2.1 Organized mucosa-associated lymphoid tissue

The gut associated lymphoid tissue (GALT), one of the best-studied mucosal inductive sites, is a network of highly organized lymphoid structures including mesenteric lymph nodes (mLNs), Peyer's patches (PPs), isolated lymphoid follicles (ILFs), cryptopatches (CPs) and fat-associated lymphoid tissue (Fig.1.1). The different tissues of the GALT differ from each other with regard to their location relative to the epithelium. CPs, ILFs and PPs are located closely to the gut lumen directly under the epithelial layer, while mLNs as well as fat-associated lymphoid tissue can be found more distant[9]. All structures of the GALT represent locations for priming of adaptive immune responses in the intestine[10].

1.2.2 Mesenteric lymph nodes

mLNs are the largest lymph nodes in the body. They are located alongside the anterior mesenteric artery in the mesentery and develop independent of PPs and peripheral lymph nodes. While development of PPs and peripheral lymph nodes is dependent on tumor necrosis factor (TNF), TNF receptor (TNFR), lymphotoxin α1β2 (LTα1β2) and lymphotoxin β receptor (LTβR), absence of these molecules does not affect mLN ontogeny[11,12]. Comparable to other lymph nodes, mLNs are encapsulated and drain the surrounding tissue. Migration of naïve lymphocytes to the mLNs via high endothelial venules (HEV) is dependent on L-selectin and α4β7 integrin adhesion molecules. mLNs are an important location of antigen processing and presentation. Intestinal DCs sample and process antigen, recirculate to the mLNs and in turn induce IgA^+ B cells to populate the intestinal lamina propria and become IgA^+ plasma cells. T cells responding to antigen presented by DCs leave the mLNs by the

afferent lymph, enter the bloodstream and finally reach the mucosa through vessels in the lamina propria. As a consequence of their pivotal anatomic position, mLNs can be regarded as the border between the mucosal immune system and the remainder of the immune system[9,10,12-15].

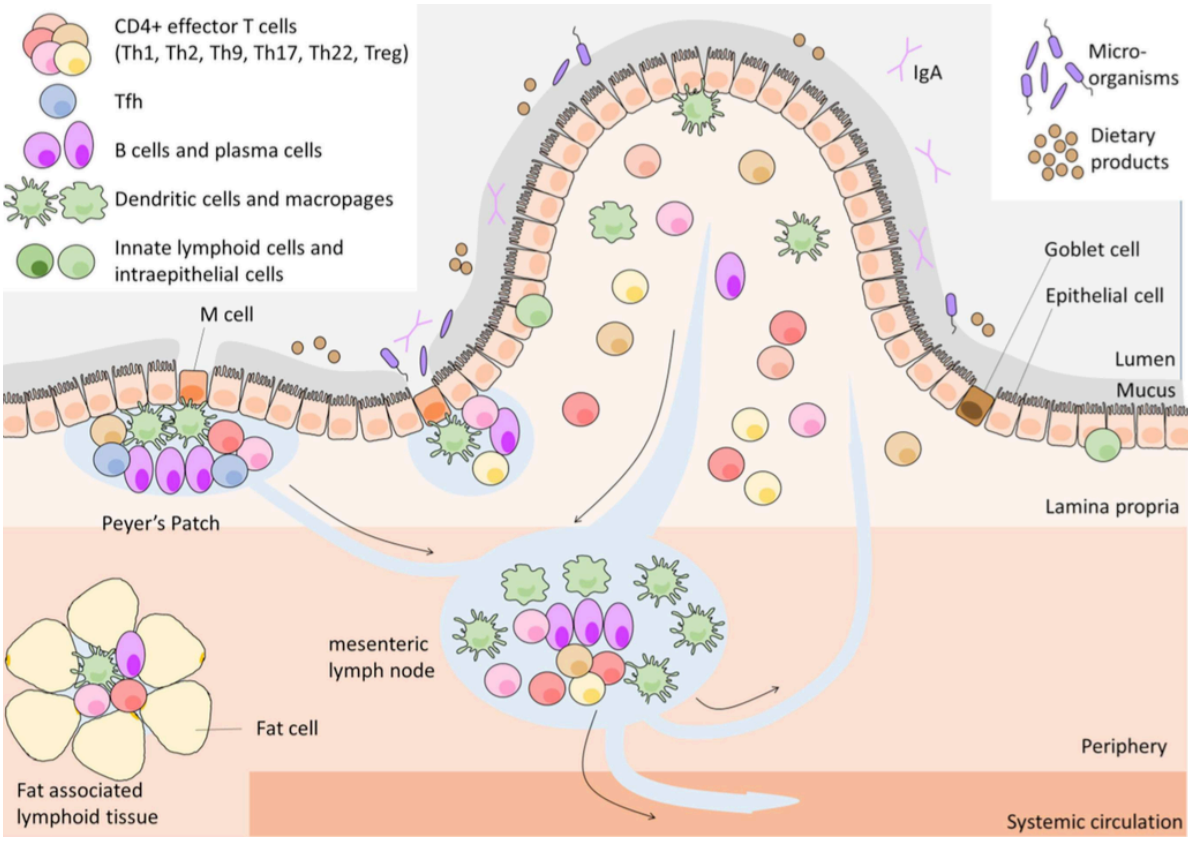

Figure 1.1: Architecture of gut-associated lymphoid tissue (GALT)
The GALT consits of a network of highly organized lymphoid structures that comprise mesenteric lymph nodes (mLNs), Peyer's patches (PPs), isolated lymphoid follicles (ILFs), cryptopatches (CPs) and fat associated lymphoid tissues. In addition, the lamina propria contains a lot of immune cells. CPs, ILFs and PPs are located directly under the epithelium, while mLNs and fat associated lymphoid tissue are located more distant. All structures of the GALT share certain similarities with regard to the structural organization and basic cellular architecture ensuring optimal interaction between antigen presenting cells (APCs) and other lymphocytes. Modified from Brucklacher-Waldert *et al.*, Frontiers in Immunology, 2014

1.2.3 Peyer's patches

PPs are macroscopic lymphoid structures located in the submucosa along the length of the small intestine. They consist of large B cell follicles and interjacent T cell areas. The PPs are separated from the intestinal lumen by the follicle associated epithelium (FAE) and the subepithelial dome, a diffuse area directly below the epithelium which is rich in DCs, T cells and B cells. The FAE differs from the normal epithelium by a reduced release of digestive

enzymes, a less pronounced brush border, absence of polymeric IgA-receptors and infiltration of a large number of immune cells. Specialized epithelial cells in the FAE, the so called microfold or M cells, are very potent in collecting and transcytosing antigen from epithelial surfaces of the gastrointestinal tract. These antigens can subsequently be taken up and sampled by DCs, located directly below the M cells in the PP dome region. As PPs have no afferent lymphatics, M cells represent the only route of antigen entering the PPs. Local DCs present the antigens to T cells, which then leave the PPs and migrate to the mLNs via the efferent lymphatics, where they further differentiate. Due to their ability to take up luminal antigens and bacteria, PPs are considered as immune sensors of the intestine. Several studies have indicated that PPs play an important role in the induction of immune tolerance as well as in the defense against pathogens. Intriguingly, malfunctions in PPs have been associated with inflammatory disorders of the digestive tract like Crohns disease and have also been shown to be involved in alloresponses, such as Graft versus Host Disease (GVHD)[1,12,14-16].

1.2.4 Solitary isolated lymphoid tissue (SILT)

Besides mLNs and PPs, the GALT includes smaller lymphoid aggregates that are collectively termed solitary isolated lymphoid tissue (SILT). These structures can only be detected microscopically and vary considerably in size from small cryptopatches (CPs) to mature isolated lymphoid follicles (ILFs). These different entities of the SILT likely represent different stages of maturation or development[17]. Mice have an estimated number of 1000-1500 evenly distributed SILT in the small intestine, while colonic SILT are concentrated in the distal colon[17-19]. CPs are aggregates of about 1000 cells composed of lymphoid tissue inducer (LTi) cells and lymphoid tissue organizer (LTo) cells, together with T cells and DCs[19,20]. By secretion of chemokines, CPs attract further lymphocytes and develop into ILFs, in response to signals from the commensal flora[21]. As opposed to PPs, ILFs nearly exclusively consist of B cells with no clear T cell zones. However, similar to PPs they contain germinal centers, indicating constant ongoing activation of humoral immunity. In this line, the FAE of ILFs also contains M cells, indicating constant antigen access to the follicle[22]. It has further been proposed that also ILFs have a central role in T cell-dependent IgA class switching and the subsequent IgA production by plasma cells[23,24].

1.2.5 Diffuse mucosa-associated lymphoid tissue

Diffuse mucosa-associated lymphoid tissue consists of leukocytes that are widely scattered throughout the intestinal epithelium and the lamina propria of the mucosa, collectively

forming the effector sites. These less organized lymphoid elements contain lamina propria mononuclear cells (LPMCs) and intraepithelial lymphocytes (IELs).

The lamina propria is a layer of connective tissue between the epithelium and the muscularis mucosae. This layer consists of lymphatics and small blood vessels embedded into smooth muscle cells and fibroblasts. The lamina propria comprises a huge number of lymphoid and myeloid cells including B cells, T cells and numerous innate immune cells such as DCs, MΦ, eosinophils and mast cells. $CD4^+$ and $CD8^+$ T cells are found in the lamina propria at a ratio of two to one. They are mostly classified as conventional T cells primed in secondary lymphoid organs displaying an effector memory phenotype ($CD45RO^+CCR7^-CD62L^-$). However, the $CD4^+$ T cell compartment is highly diverse with regional differences in distribution and function along the intestine[13]. These T cells might have regulatory functions and therefore be involved in maintenance of tolerance to environmental antigens. Lamina propria $CD8^+$ T cells can have potent cytolytic activity acting as antigen experienced true effector cells[12,15]. Large numbers of MΦ and DCs in the lamina propria suggest that antigens crossing the epithelium are directly processed and presented to $CD4^+$ T cells.

Besides the lamina propria, also the intestinal epithelium contains a large number of immune cells. These intraepithelial lymphocytes (IELs) are located at the basement membrane between the enterocytes. IELs comprise antigen-experienced T cells of both the T cell receptor (TCR)$\gamma\delta^+$ and TCR$\alpha\beta^+$ lineages. TCR$\gamma\delta^+$ cells can constitute up to 60% of small intestinal IELs[25]. Most of these cells express CD8, while only a minor fraction is $CD4^+$. A large fraction of the $CD8^+$ cells express a CD8αα homodimer as co-receptor, which is essentially not found in any other location[26].

The majority of the IELs possess cytotoxic activity and express effector cytokines like interferon gamma (IFNγ), interleukin-2 (IL-2), IL-4 or IL-17[27]. Further, all IELs express the αEβ7 integrin CD103, which interacts with E-cadherin possibly assisting in anchoring IELs in the epithelium[28,29]. Intestinal T cells can be subdivided into two subsets based on the mechanism by which they become activated. Induced IELs, also known as “type a” IELs, are the progeny of conventional T cells that are activated post-thymically in response to peripheral antigens. Natural IELs, also known as “type b” IELs, develop in the thymus from non-MHC restricted triple-positive thymocytes and subsequently migrate as $CD8\alpha^-CD8\beta^-CD4^-$ cells to the intestine where they undergo further differentiation[30]. Due to their position at the interface of the organism and the outside environment, IELs need to keep a tight balance between protecting the epithelial barrier while staying unresponsive to food antigens and other harmless substances. IELs can protect against inflammatory damage and guard the

epithelium in response to pathogen-induced stress antigens or pathogen-expressed antigens. On the other side IELs can also promote epithelial damage by recruiting inflammatory leukocytes or as a response to pathogen-induced stress antigens, microbial or dietary antigens[27]. Taken together IELs form the foremost line of defense at the biggest entry point for pathogens of the body. They protect the integrity of the mucosal border, however, can also mediate pathological responses driving detrimental inflammatory diseases.

1.2.6 Immune cells in the mucosal immune system of the gut

Intestinal **T cells** (Fig.1.2) play a critical role in sustaining intestinal homeostasis and protecting against environmental threats. As described in the previous section, IELs form an exclusive population of antigen-experienced T cells scattered throughout the epithelium. In addition, the lamina propria is largely populated by T cells, which express TCRαβ together with CD4 or CD8αβ co-receptors. These T cells are primed in mLNs or PPs by DCs. During priming they acquire gut homing properties, upregulate adhesion receptors including α4β7 and CCR9 and migrate to the lamina propria where they accumulate as long-lived effector memory cells over time. $CD4^+$ T cells in the lamina propria mainly provide help to plasma cells and $CD8\alpha\beta^+$ memory cells. However, besides the classical helper T cells, the lamina propria is enriched in in Foxp3-expressing regulatory T cells (Tregs) and proinflammatory IL-17-producing Th17 cells under steady state conditions. Tregs accumulating in the gut are crucial for keeping gut homeostasis by preventing excessive responses to harmless antigens[31]. Analysis of colonic T cells from mice bread under specific-pathogen-free (SPF) conditions revealed that about 30-40% of T cells produce the anti-inflammatory cytokine IL-10, with most of these cells also expressing Foxp3[32]. Intriguingly, a dominance of $IL\text{-}10^+CD4^+$ T cells not expressing Foxp3, referred to as Tr1 cells, has been described for the small intestine[33]. As opposed to Tregs, Th17 cells play an important role in the defense against a variety of fungal and bacterial infections. In steady state, Th17 cells can be mainly found in the lamina propria of the SI and to a lesser extent in the colon. They express the transcription factor retinoic acid-related orphan receptor γt (RORγt) and produce the cytokines IL-17A, IL-17F, IL-21, IL-22 and GM-CSF[34]. Development of Th17 cells in mice requires a combination of TCR signals, TGFβ, IL-1β and IL-6 or IL-21[35]. IL-23, which was originally thought to be necessary for Th17 cell generation, has been shown to be important for the modulation of Th17 effector functions and pathogenicity[36].

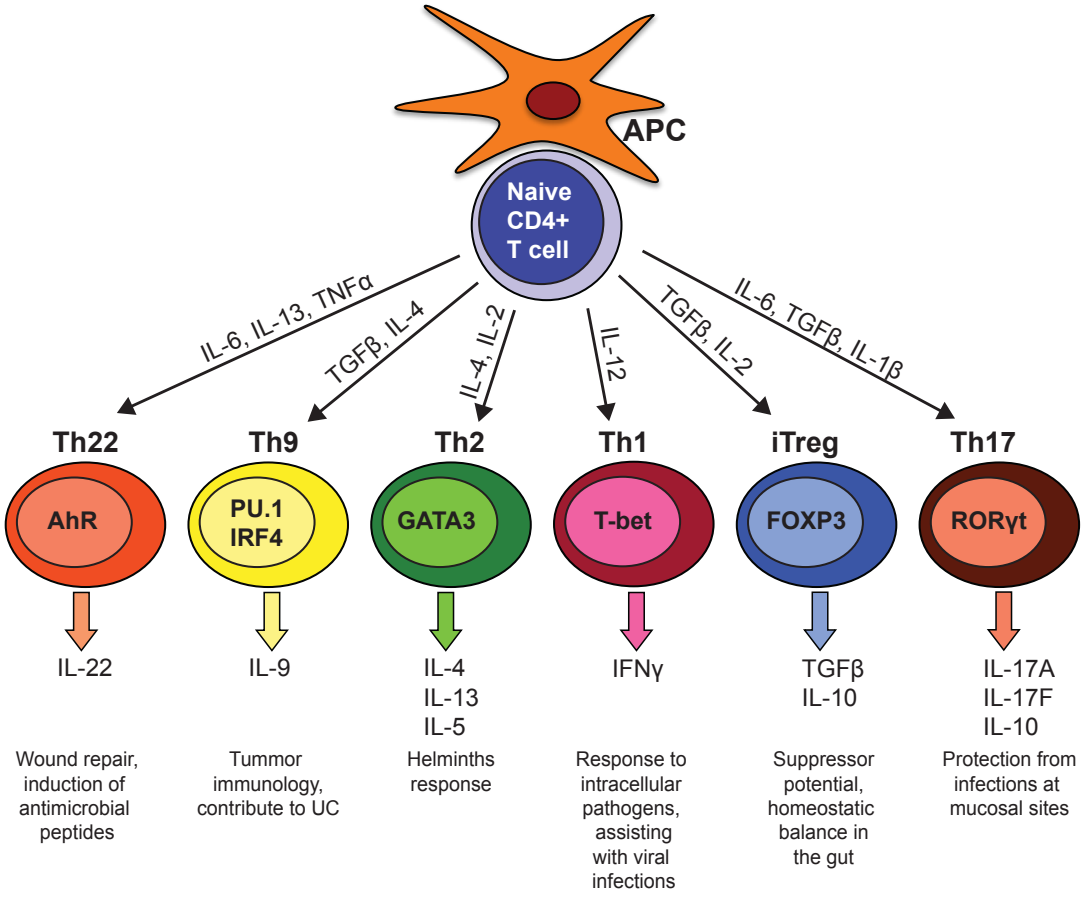

Figure 1.2: T helper cell subset differentiation and function in the intestine
Besides the strength of the T cell receptor (TCR) signal and the quality of co-stimulation, the cytokine environment mainly influences $CD4^+$ T cell polarization and differentiation. The cytokines driving the differentiation of naïve $CD4^+$ T cells into the respective Th cell fate, the master transcription factor of each Th cell subset, cytokines produced by the different subsets and specific functions associated with the various subsets are depicted.

Besides Th17 cells, Th1 cells are essential for the response to intracellular bacteria and viruses. Development of these T cells is critically dependent on induction of the transcription factor T-bet by STAT1 and STAT4 signaling. T-bet in turn drives upregulation of the IL-12Rβ2, thereby increasing responsiveness to IL-12, which induces optimal expression of the Th1 signature cytokine IFNγ[37]. Th1 and Th17 cells are important mediators of inflammation in Crohn's disease (CD), while Th1 cells also promote mucosal inflammation in celiac disease[38].

Th2 cells, expressing the master transcription factor GATA-3, differentiate upon IL-4 and IL-2 stimulation and produce the cytokines IL-4, IL-13 and IL-5. They predominate in response to gastrointestinal nematodes, however, are absent under homeostatic conditions[10]. Interestingly, Th2 responses and elevated levels of IL-5 and IL-15 have been associated with Ulcerative Colitis (UC), yet the underlying mechanism remains elusive[38].

Further, Th22 cells represent a distinct subset of T helper cells, whose differentiation is dependent on IL-6, IL-13 and TNFα. They express the aryl hydrocarbon receptor (AhR) as master transcriptional regulator and produce the cytokines IL-22, IFNγ and IL-17. These cells have been shown to be functionally important for wound repair and the induction of antimicrobial peptides, like β-defensin 2 and 3[10,39]. Increased levels of IL-22, likely produced by Th22 cells, have been found in patients with inflammatory bowel disease (IBD). Studies suggested that IL-22 might contribute to the inflammation, but also plays a beneficial role in promoting wound healing[40].

The most recently defined subset of T helper cells are Th9 cells, characterized by production of IL-9. However, the functional role of Th9 cells and IL-9 are not well understood yet. Th9 cells develop in response to a complex cytokine milieu including TGFβ and IL-4, generally promote inflammation, and are involved in tumor immunology. They further have been implicated in contributing to UC through IL-9 production, which can impair tissue repair, increase intestinal permeability and may enhance inflammatory T helper cell responses[10,41].

Innate lymphoid cells (ILCs) are a population of mucosal lymphocytes that were studied with increasing interest in recent years. These cells are enriched at barrier surfaces and lack antigen-specific receptors found on T and B cells. They further lack myeloid cell and DC phenotypical markers and display a lymphoid morphology[42]. Development of ILCs commonly depends on expression of the common cytokine receptor γ-chain (γ_c) and the transcriptional repressor inhibitor of DNA binding 2 (ID2). Further, all subsets rely on signaling via the IL-7 receptor subunit-α (IL-7Rα) for their development and maintenance. Similar to T helper cell subsets, ILCs are subdivided into different groups based on expression of specific transcription factors and effector cytokines (Fig.1.3).

Group 1 ILCs are primarily characterized by production and release of IFNγ upon stimulation with IL-12 and IL-18. They consist of NK cells and other ILC1s. NK cell development is regulated in close cooperation of the transcription factors T-bet and eomesodermin (Eomes). Murine NK cells can be identified by expression of the natural cytotoxicity triggering receptor (NCR) NKp46 (NCR1), although this is not an exclusive NK cell marker. NK cells are characterized by their cytotoxic function, and are therefore considered as the innate counterpart of $CD8^+$ cytotoxic T cells[43,44]. The residual ILC1s are developmentally dependent on expression of T-bet but not of Eomes and produce IFNγ but no Th2-, or Th17-cell-associated cytokines. Some ILC1s have been shown to develop from $NKp46^+$ILC3s that downregulate RORγt and upregulate T-bet. These cells have been reported to contribute to intestinal inflammation during colitis, presumably through their production of IFNγ[45,46].

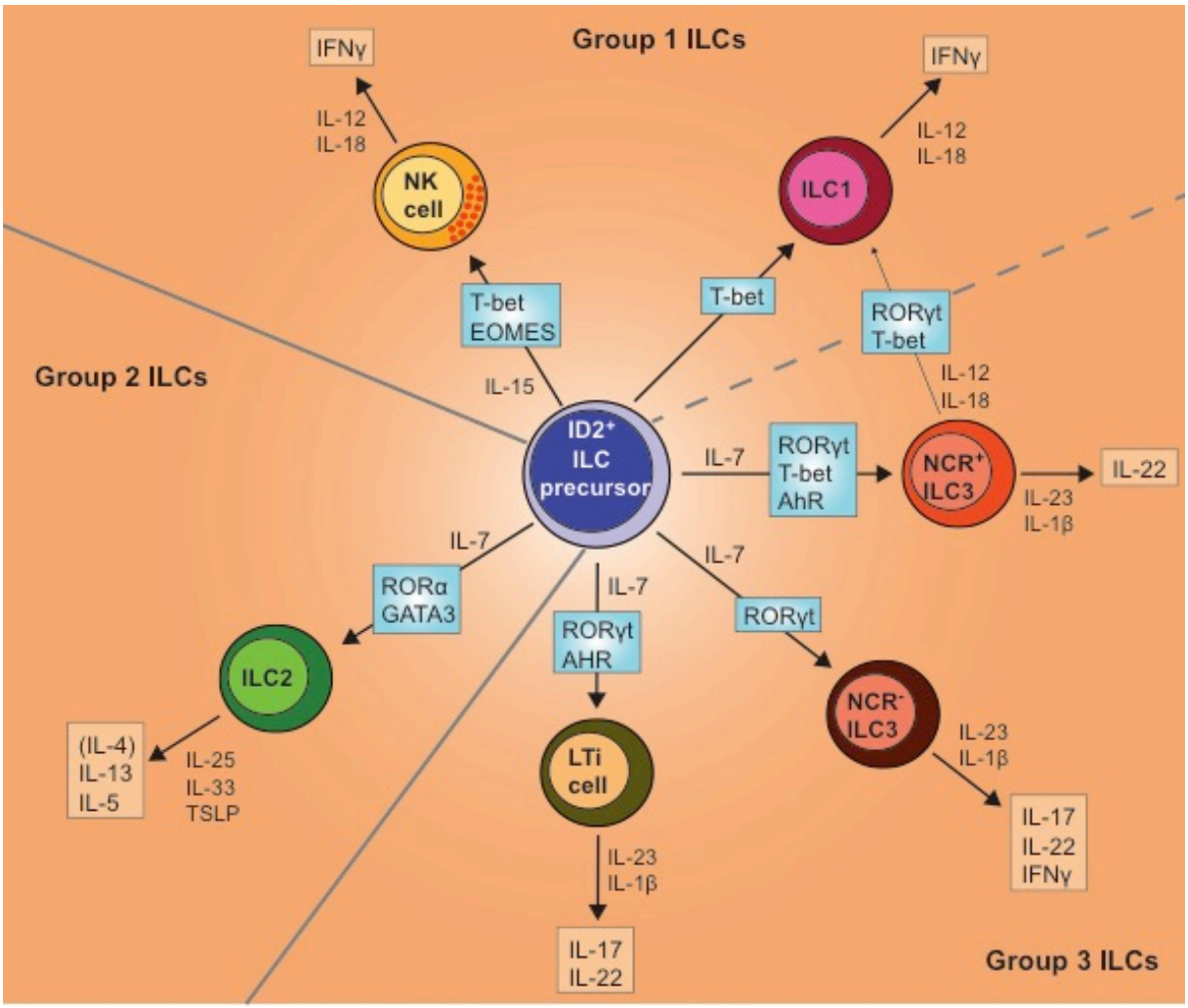

Figure 1.3: Classification of ILC subsets on the basis of their functional characteristics
Innate lymphoid cells (ILC) develop from a common precursor that depends on the expression of the transcriptional repressor inhibitor of DNA binding 2 (ID2). All ILCs depend on the common cytokine receptor γ-chain for their development and maintenance. Specific cytokines and several transcription factors regulate the differentiation of ILC precursors into distinct subsets. ILCs are classified into groups based on functional criteria. Group 1 ILCs are defined by their production of interferon-γ (IFNγ). Group 2 ILCs are able to produce T helper 2 (Th2) cell-associated cytokines, including IL-5 and IL-13. Group 3 ILCs produce the Th17 cell-associated cytokines IL-17 and IL-22. Figure is adapted from Spits *et al*., Nature reviews immunology, 2013.

Group 2 ILCs are distinguished from other ILCs by production of the Th2-associated cytokines IL-4, IL-13 and IL-5 upon stimulation with IL-25, IL-33 or thymic stromal lymphopoietin (TSLP). Like Th2 cells, ILC2s require expression of the transcription factor GATA3 for development and function. Moreover, their development is also dependent on the expression of the transcription factor RORα. Different studies have shown importance of ILC2s in mediating resistance to certain helminths and nematodes. Due to its broad cytokine production profile, including IL-9 and amphiregulin, ILC2s are also involved in metabolic

processes, tissue repair, alternative macrophage activation, thermoregulation and mucus production[46,47].

Group 3 ILCs are defined by their ability to produce the cytokines IL-17 and IL-22. They additionally release lymphotoxins and the granulocyte macrophage colony-stimulating factor (GM-CSF). Group 3 ILCs can be further sub-classified into three different categories. Lymphoid tissue inducer cells (LTi cells) are a prototypic ILC3 family member and are essential for the formation of secondary lymphoid organs. The remaining ILC3s are further phenotypically subdivided into NKp46^{+} and NKp46^{-} ILC3s. All subgroups consistently produce IL-22 and IL-17 upon stimulation with IL-23 and IL-1β, and their development and function depends on expression of RORγt. However, only NKp46^{-} ILC3 express the Th1 transcription factor T-bet and produce IFNγ, which is an important mediator of pathology in a mouse model of colitis[48]. In addition, LTi cells and NKp46^{+} ILC3s depend on expression of the aryl hydrocarbon receptor (AhR) for development and optimal maintenance. ILC3s promote tissue repair through their IL-22 production, while IL-17 and IFNγ producing ILC3s have been associated with intestinal pathology in colitis and infection with Salmonella enterica[44,45-47].

Induction of active immunity and maintenance of intestinal homeostasis is tightly controlled by intestinal mononuclear phagocytes (MPs) comprising **dendritic cells** (DCs) and macrophages (MΦ). DCs are able to sample antigens from the intestine, migrate to the mLNs and initiate adaptive immune responses by priming of naïve T cells. Although routinely identified as major histocompatibility complex II (MHCII) and CD11c co-expressing cells, this discrimination is insufficient to identify DCs in the intestinal tissue, as all intestinal macrophages also express CD11c[49]. However, intestinal MΦ have been identified to be F4/80^{+}CD64^{+}CX$_3$CR1$^{hi/int}$ phagocytes. Thus, DCs can conclusively be identified as CD11c^{+}MHCII^{+}CD64^{-} cells. In the GALT, DCs are located in PPs, mLNs, SILT and are diffusely scattered through the lamina propria. The majority of intestinal DCs express the integrin αEβ7 (CD103). These cells can be further subdivided by their CD11b expression into CD103^{+}CD11b^{+} and CD103^{+}CD11b^{-} DCs. Further, the murine lamina propria contains a poorly defined CD103^{-}CD11b^{+} subset. All three subsets can also be found in gut-draining afferent lymph and are all derived from a committed FMS-like tyrosine kinase 3 ligand (Flt3L)-dependent precursor. Intestinal DCs can fulfill several different functions. They can recieve luminal antigens from goblet cells[50]. DCs subsequently migrate to the mLNs in a CCR7-dependent process and have a central role in priming of naïve T cells, generating active immune responses and inducing Treg cells. The CD103^{+} DC subsets induce Treg

development, but can also prime Th17 or Th1 cells if readily activated. $CD103^-$ intestinal DCs are more immunogenic, inducing effector Th1 and Th17 cells[51,52].

Macrophages (MΦ) are the second cell type constituting the mononuclear phagocytes. These cells are resident in the lamina propria engulfing bacteria, secreting cytokines and maintaining intestinal homeostasis. Several studies could independently show that MΦ are $CD103^-$ but express the pan-MΦ marker F4/80, the MΦ-specific high affinity FcγRI (CD64) and high levels of the chemokine CX_3C receptor (CX_3CR)1[53-55]. Although these cells are present throughout the whole intestine, their abundance increases towards the colon. In most tissues, MΦ arise from yolk sac and fetal liver progenitors, which seed tissues during embryonic development. Subsequent self-renewal in situ ensures constant MΦ replenishment. Although this mechanism has been proven for microglia, lung alveolar MΦ, liver Kupffer cells and epidermal Langerhans cells, MΦ in the intestine need constant replenishment from circulating blood monocytes. $Ly6C^{hi}$ monocytes enter the intestinal mucosa, where they differentiate into CX_3CR1^{hi} MΦ. During this process, precursors upregulate MHCII, F4/80, CD64 and CX_3CR1 but downregulate Ly6C. This mechanism was first shown by Steffen Jung and colleagues and extended by the groups of Allan Mowat and Brian Kelsall[51,53,56-59]. Intestinal macrophages are not only essential for the elimination of invading bacteria or apoptotic cells. They may also sample luminal contents in a MyD88 and CX_3CR1-dependent process, although the *in vivo* relevance of this process is still controversial[60]. Macrophages in the intestine have very important homeostatic functions. They produce prostaglandins in a cyclooxygenase (COX)2-dependent process and thereby inhibit gastric acid secretion and protect the intestinal mucosa from inflammation and necrosis. Gut macrophages acquire a generally anti-inflammatory phenotype indicated by the constitutive high production of IL-10. This process likely involves signals from the microbiota and finally leads to secondary expansion of Treg cells[61]. Even during active colitis, macrophages keep this anti-inflammatory signature. Interestingly, steady state differentiation and proliferation of macrophages collapses during inflammation to some extent[57]. As a consequence, monocyte-derived CX_3CR1^{int} cells immigrate into in the lamina propria. These cells exhibit a more proinflammatory phenotype indicated by expression of TNFα and inducible NO synthase (iNOS). It has further been shown that during active immune responses, macrophages may produce IL-1β and thereby drive local differentiation or expansion of Th17 cells[62].

Neutrophils are a vital component of the innate immune system and are important first responders at sites of inflammation. They are equipped with several mechanisms to eliminate microbes and therefore maintain the intestinal homeostasis. Neutrophils produce vast amounts

of reactive oxygen species (ROS) and other toxic molecules that effectively destroy pathogens. They also carry different intracellular granules containing antimicrobial peptides like α-defensins and cathelicidins, myeloperoxidase (MPO), hydrolytic enzymes and metal chelators like Lipocalin-2 (LCN2). Moreover, neutrophils also form neutrophil extracellular traps (NETs) composed of chromatin mixed with toxic molecules to capture and kill invading microorganisms[63]. Of note, neutrophils can have beneficial, but also detrimental roles during intestinal inflammation. They are recruited to inflammatory sites within minutes, with the response peaking between 24 and 48 hours. IBD like UC and CD are characterized by massive inflammation and concomitant recruitment of neutrophils[64]. However, the exact contribution of neutrophils to the pathogenesis of the disease is not completely unraveled. Different studies have suggested a beneficial, a detrimental, or no role at all, suggesting that the contribution of neutrophils in regulating intestinal inflammation seems to be highly dependent on the conditions and models used[63].

The mucosal **B cell** system mainly provides a first line of defense through active production of secretory immunoglobulin A (SIgA) and the subsequent transport through intestinal epithelial cells. These antibodies are produced by plasma cells present at the mucosal wall. Naïve precursor B cells are activated in PPs and mLNs by presentation of antigens from follicular DCs and by CD40-mediated signals from primed helper T cells. Further, class switching to IgA producing B cells or formation of memory B cells is induced in the GALT inductive sites (PPs, mLNs), driven by the substances TGFβ, RA, IL-6 and iNOS. IgA^+ B cells then upregulate gut homing receptors ($\alpha_4\beta_7$) and migrate to the lamina propria, where they differentiate into plasmablasts and finally plasma cells, secreting large amounts of IgA[65,66]. The continuous production of large amounts of IgA is almost exclusively driven by the resident microbiota. IgA, secreted into the gut lumen by transcytosis through gut epithelial cells, inhibits microbial adherence to the epithelium and neutralizes microbial toxins or enzymes. In contrast to humans, mice can additionally produce intestinal IgA after T cell independent B cell activation, possibly as a result of B cell-DC interaction in solitary lymphoid follicles. This pathway involves B-1 cells derived from peritoneal B cell precursors and results in IgA antibodies with limited diversity and low antigen affinity[1].

1.3 The gut microbiota

The sum of microorganisms that live within and on an organism is generally referred to as the microbiota. Microbial communities are immensely active and provide crucial signals for development and function of the immune system. Especially the gastrointestinal tract harbors

an enormous number of commensal bacteria that have co-evolved with its host over millennia. The resulting dynamic crosstalk between host and its microbiota is important for maintaining homeostasis of immune tissues and the regulation of immune responses[67]. The human microbiota is mainly composed of the dominant phyla *Firmicutes* (50-75%) and *Bacteroidetes* (15-25%), followed by the much less frequent *Proteobacteria* and Actinobacteria[68]. *Firmicutes* and *Bacteroidetes* also dominate the gut microbiota of mice, although when exploring deeper taxonomic classifications, 85% of bacterial genera found in the mouse gut microbiota are not present in human[69]. Due to the technical advances in sequencing technologies it has become possible to perform culture-independent microbial analysis, revealing microbial complexity and composition by bacterial 16S ribosomal RNA amplicon sequencing[70]. Using mass spectrometry-based and chromatography-based techniques it is furthermore possible to target the chemical diversity and also biochemical capacity of substances produced by the microbial communities. The systemic study of the unique chemical and biochemical metabolite composition that specific microbial communities produce is termed metabolomics. Even more sophisticated approaches, like the combination of flow cytometry with tandem mass spectrometry are now used to characterize and quantify individual microbial cells and in addition measure their metabolic activity[71].

Approaches to understand the importance of the microbiota in shaping the innate and adaptive immunity include the use of germ-free mice and the manipulation of the microbiota with antibiotic treatment or microbiota reconstitution. These experiments offer valuable insights into the regulation of gut immune homeostasis by the microbiota. Intestinal MΦ located in close proximity to the microbiota keep a non-inflammatory profile upon encountering microbial stimuli[72]. In addition, a reduced number of intestinal DCs could be observed in germ-free animals, although colonization with *Escherichia coli* was sufficient to recruit DCs to the intestine[73]. In a similar fashion, IL-22 producing NKp46$^+$ ILCs are missing in germ-free mice, indicating importance of the gut microbiota in the development or maintainance of these cells[74]. Commensal bacteria have also been shown to be essential for CD4$^+$ T cell differentiation. *Bacteroides fragilis* induce a systemic Th1 response, while *segmented filamentous bacteria* (SFB) were found to be potent inducers of lamina propria Th17 cells[75,76]. In addition, single metabolites derived from the gut microbiota have the ability to influence immunes responses through interaction with host cells. One of the most abundant metabolic end products from bacterial fermentation are short-chain fatty acids (SCFAs), including acetic acid, butyric acid and propionic acid. SCFAs act as potent signaling molecules and can therefore influence expansion and function of cells. They are inhibitors of histone

deacetylases and they promote a tolerogenic cell phenotype that is very important to maintain immune homeostasis. They inactivate nuclear factor-κB (NF-κB) and they inhibit production of TNF[67]. Furthermore they act as ligands for G-protein coupled receptors.

Another group of substances derived from the metabolism of the gut microbiota are AhR ligands. Turnover of dietary components generates metabolites with the ability to bind and activate the AhR. In general, activation of the AhR is influenced by composition of the diet but also by the composition of the microbiota. Only certain commensal strains of the *Lactobacilli spp.* can metabolize dietary tryptophan and thereby generate AhR ligands that are important for conferring protection from inflammation at mucosal surfaces[77].

Polyamines are polycationic molecules that influence a wide range of biological functions, such as transcription, translation, cell growth and cell death. The intestinal tract contains a high concentration of polyamines derived from the diet and from de novo synthesis from host and microbial cells. Studies have demonstrated great importance of polyamines for production of intracellular junction proteins and consequently for regulation of the epithelial barrier function[78]. Further, dietary supplementation of polyamines induces production of mucus and secretory IgA in the small intestine, underlining an important role for microbiota- and diet-derived polyamines in regulating important immune functions.

The pathogenesis of IBD involves genetic predispositions and environmental factors and is often associated with a dysbiosis in the gut microbiota. Several studies have revealed a reduced diversity of the gut microbiota in IBD patients, the most consistent one being a reduction in *Firmicutes* and an increase in *Proteobacteria*[79-83]. It remains however controversial whether the dysbiosis is cause or consequence of IBD pathology and if the formation of a "dysbiosis index" can be used as a clinical marker to predict disease severity, prognosis and response to treatment.

In addition, the composition of the microbiota is highly dependent on the dietary lifestyle. Dietary patterns, specific foods as well as certain food constituents have the ability to influence the composition of the microbiota and hence the host immune system and metabolism[84]. Graf *et al.* summarized effects of western diet, vegetarian diet, whole grain, fruit, fiber, fat and much more substances on the composition of the microbiota[84]. Although an important influence of diet on the microbiota composition is obvious, the interpretation of long term effects is highly dependent on the methodology. Further, it seems to be increasingly complicated to find an agreement on what a healthy microbial composition means and if this might not be very different for every individual[85].

In summary, it is undoubtful that the complex crosstalk between the immune system and microbiota has consequences and is likely necessary for an optimal functioning of the host's immune system and metabolism.

1.4 The immune cells of the skin

Next to the intestine and the lung, the skin is an important interface between the body and the environment. Besides being a very stable mechanical barrier, the skin forms an active barrier that provides a strong line of immunological defense against infections. The human skin consists of the epidermis, which is mainly formed by several epithelial cell layers, and the connective tissue-rich dermis. The most frequent cell type of the epidermis is the keratinocyte, however, a lot of immune cells, such as Langerhans cells and dendritic epidermal T cells (DETCs), which can only be found in mice, are located in this tissue. The dermis contains a lot of extracellular matrix, in which fibroblast are embedded, and is additionally rich in blood and lymph vessels. Further a multitude of myeloid and lymphoid immune cells like MΦ, mast cells, conventional αβ T cells, γδ T cells and ILCs are distributed through the dermis.

Both resident and trafficking myeloid cells populate the skin. Langerhans cells (LC), a DC population seeding the epidermis pre-birth, are of embryonic origin and mainly fetal liver- and, to a minor extent, yolk sac-derived[86]. They are locally maintained, but repopulation from circulating monocytes occurs under inflammatory conditions in a macrophage colony-stimulating factor (M-CSF)- and IL-34-regulated process[87]. In the murine dermis either CD103 or CD11b expressing DCs and double-negative DCs have been identified[88]. All DC subsets perform T cell priming either inducing Th17 (LCs) or Th1 ($CD103^+$DCs) responses, or alternatively executing regulatory functions[89]. Skin resident MΦ originate from the yolk sac. They can have a proinflammatory or regulatory character. Moreover, they can promote wound healing and support tissue repair by enhancing epithelialization[90]. In addition, circulating monocytes trafficking through the skin give functional support to DCs[91]. Mast cells store preformed proinflammatory mediators within cytoplasmic granules that can be quickly released upon antigen contact. They play a role in contributing to the innate immune response and have diverse functions in skin pathology[92]. Different studies have shown the presence of epidermis-resident memory $CD8^+$ T cells and a population of recirculating memory $CD4^+$ T cells, mainly located in the dermis[93]. DETCs in mice form a network to monitor the integrity of the epidermal layer and further contribute to inflammation and assist in wound healing processes[94]. Persistence of both DETCs and tissue resident memory T cells

has been shown to depend on signals via the AhR[95]. In addition to these, dermal γδ T cells are important for the cutaneous immune surveillance, while Tregs in the skin orchestrate hair follicle regeneration, augment wound healing and promote tolerance to skin commensals[89,94,96]. Last but not least also ILCs and in particularly ILC3s have been shown to contribute to skin inflammation[97].

1.5 The Aryl hydrocarbon receptor (AhR)

The aryl hydrocarbon receptor (AhR) is a protein that has been identified as a ligand activated transcription factor and has been first cloned in the early 90's[98]. The AhR belongs to the family of basic helix-loop-helix (bHLH)-PER-ARNT-SIM (PAS) proteins, which are all heterodimeric transcription factors involved in the response to environmental or physiological signals[99]. The AhR is one of the oldest and best-studied members of the bHLH-PAS family and the only ligand-activated member of the family[100]. Historically the AhR has been studied by toxicologists for its response to xenobiotics, which are substances that are not naturally produced by an organism. However, several studies also identified the AhR as an important regulator for mucosal barrier function[101]. All members of the bHLH-PAS family are structurally similar. They contain a bHLH motif that consist of 4-6 DNA-binding, basic amino acids, attached to a HLH dimerization domain and PAS domains, which consist of a five-stranded antiparallel β-sheet flanked by α-helices, which can bind a wide array of chemically diverse ligands[102]. The AhR in particular consists of the bHLH domain, two PAS domains (PAS-A and PAS-B) and a Q-rich (glutamine-rich) region (Fig.1.4). The bHLH domain is involved in DNA-binding, the PAS-B domain forms the ligand-binding pocket and the amino-terminal Q-rich region is essential for transcriptional activation. The bHLH domain and the PAS-A domain have been shown to be involved in dimerization with the AhR nuclear translocator (ARNT), forming a transcriptional active heterodimer. Regions in the bHLH domain and the PAS-B domain are involved in binding to the chaperone Hsp90, keeping the AhR inactively stabilized in the cytosol[103].

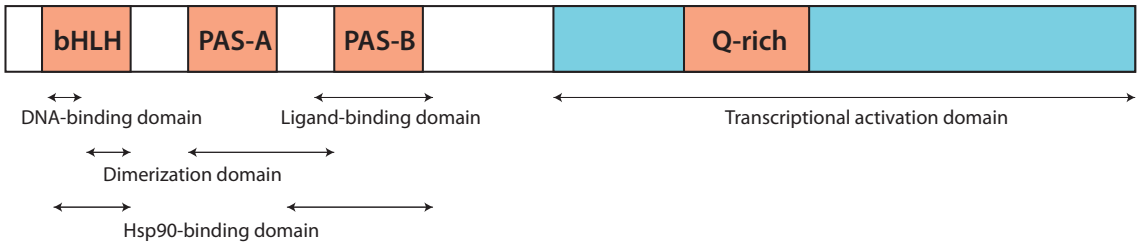

Figure 1.4: Aryl hydrocarbon receptor functional domains
The AhR is a member of the basic helix-loop-helix/Per-Arnt-Sim (bHLH/PAS) family of transcription factors. The N-terminal basic part of the bHLH domain conveys DNA binding, while the HLH region facilitates protein interactions. Two 200-350 amino acid PAS domains mediate interactions with other PAS domain containing proteins, like the AhR nuclear translocator (ARNT). PAS-B contains the ligand-binding domain. Regions in the bHLH and PAS domains are involved in Hsp-90 binding. The C-terminal located Q-rich domain is involved in transactivation.

1.5.1 The AhR pathway

In the absence of any ligand, the AhR is located in the cytosol, stabilized in a complex with the chaperon proteins Hsp90, aryl hydrocarbon receptor interacting protein (AIP) and p23 (Fig.1.5). AhR ligands diffuse into the cell and bind the cytosolic AhR complex, thereby inducing a conformational change that in turn leads to nuclear translocation. Upon dimerization with ARNT the AhR is released from its chaperons and the AhR-ARNT complex binds to its cognate DNA binding motif, named dioxin response element (DRE) or xenobiotic response element (XRE). To date the number of genes influenced by AhR activation through AhR ligands is in the order of about 600[104]. Genes that contain DRE/XRE sites in their promoter region and are therefore directly regulated by the AhR are for example the xenobiotic metabolism genes *cyp1a1*, *cyp1a2* and *cyp1b1*. The arising gene products are critically involved in the feedback metabolism of xenobiotics that initially activate the AhR. The AhR-induced AhR repressor (AHRR), one of the most strongly upregulated genes upon AhR activation, can similarly form dimers with ARNT, forming a transcription-repressing complex that competes with the AhR/ARNT complex for binding to DRE/XRE sites. The TCDD (2,3,7,8-Tetrachlorodibenzo-*p*-dioxin)-inducible poly-ADP-ribose polymerase (TiPARP) is a strongly AhR induced gene, acting as an inhibitor of AhR activity by increasing the proteolytic degradation of AhR[105,106]. More indirect transcriptional effects have been shown for genes required for development or reproductive physiology[99,103]. Besides metabolism of ligands and inhibition through the AhRR or TiPARP, AhR protein levels are controlled via ubiquitin-mediated proteasomal degradation. AIP inhibits ubiquitination of the

AhR in its inactive state, however, ligand binding and release from the chaperon complex induces AhR ubiquitination and degradation by the proteasome[107,108].

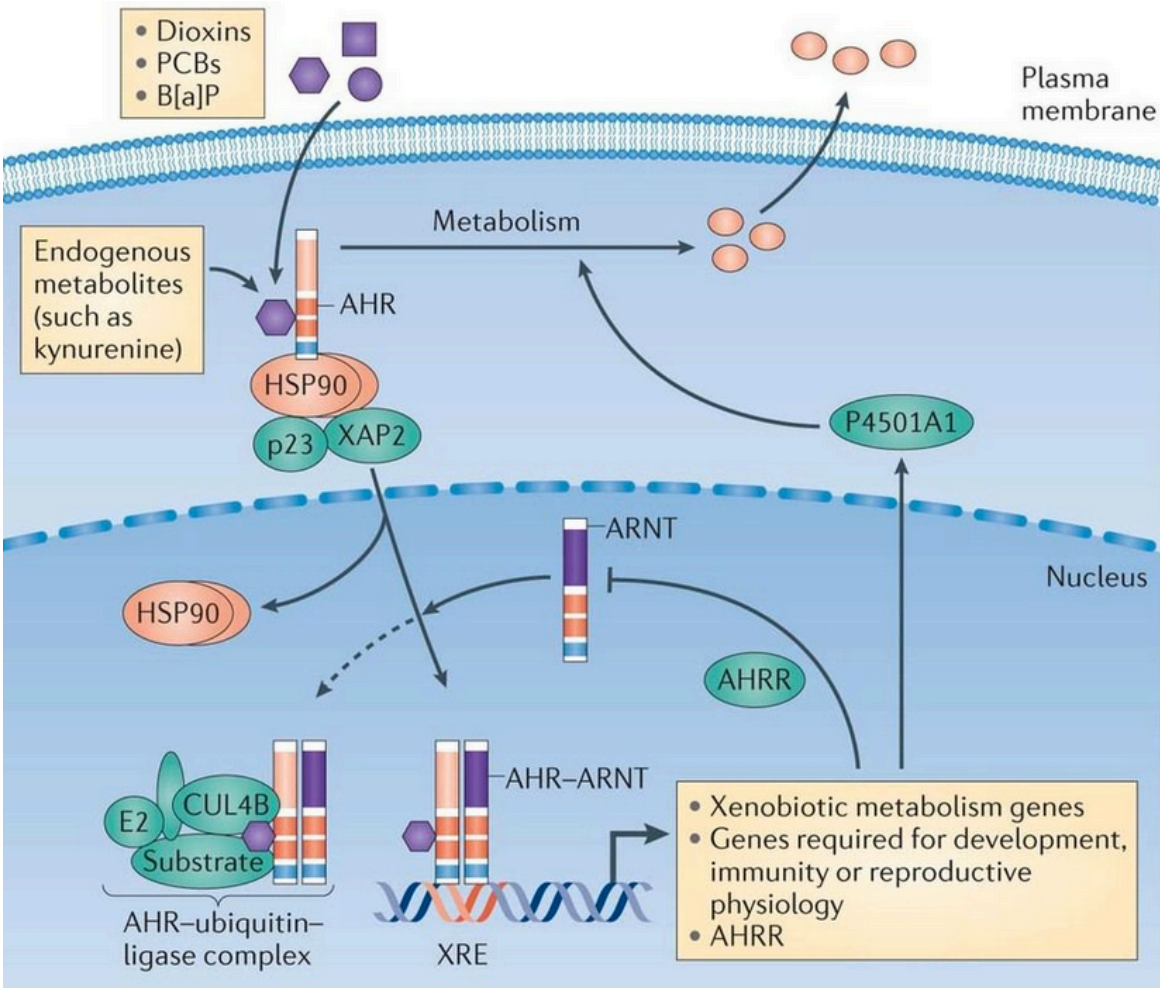

Figure 1.5: Ligand-dependent AhR activation and negative feedback control mechanism
Exogenous substances and endogenous metabolites bind the chaperon associated AhR in the cytoplasm inducing translocation into the nucleus. There, the AhR forms a heterodimer with the AhR nuclear translocator (ARNT) and binds to its genetic target sequence, the DRE (dioxin response element) and XRE (xenobiotic response element) sites and induces transcription of target genes. These belong to the xenobiotic metabolism and include genes required for development, immunity, reproductive physiology and the AhR repressor (AhRR). The AhRR competes with the AhR for binding to ARNT, forming a second heterodimer competing with the AhR-ARNT complex without activating target gene transcription. Additionally AhR activity is regulated through ubiquitylation and proteasome-mediated degradation. PCBs: polychlorinated biphenyls, B[a]P: benzo[a]pyrene, HSP90: heat shock protein 90, XAP-2: HBV X-associated protein, cullin 4B:CUL4B;
Adapted from Murray L. Whitelaw, Nature Reviews Cancer, 2013

Besides the canonical AhR pathway, cross-talk between the AhR and other signaling pathways can lead to activation of the AhR and subsequent induction of AhR target genes. Several types of cross-talk have been described. For example, the AhR has been shown to bind to the transcription factor c-Maf, which plays an important role for type 1 regulatory T

cell (Tr1) differentiation[109]. Moreover, the AhR is able to bind STAT1, influencing NF-κB promoter activity, and interacts with the estrogen receptor, β-catenin, Nrf2, RelA and RelB[110].

1.5.2 AhR ligands

The AhR can be activated by a variety of structurally diverse synthetic or naturally occurring ligands. The best-characterized ligands include a variety of environmental toxins like the halogenated aromatic hydrocarbons (HAHs) and non-halogenated polycyclic aromatic hydrocarbons (PAHs). 2,3,7,8-tetrachlordibenzo-ρ-dioxin (TCDD, dioxin), the prototypical and most potent HAH, is highly toxic and biologically persistent[111]. Dioxin is found in industrial byproducts and as a toxic contaminant of some herbicides. Immune and liver defects in AhR-deficient mice suggested that in addition to xenobiotics, physiological and natural occurring AhR ligands might play an important role under homeostatic conditions[112]. The perhaps greatest exposure to physiological AhR ligands comes from the diet, particularly flavonoids in vegetables and fruits have agonistic effects on AhR activation[113]. An example for a physiological AhR ligand precursor is indole-3-carbinol (I3C), which is produced by the breakdown of glucobrassicin, a glucosinolate that can be found in high concentrations in cruciferous vegetable such as broccoli[114]. By exposure to the stomach acid, I3C is converted into the high affinity AhR ligand indolo[3,2-b]carbazol (ICZ). Other naturally occurring AhR ligands are derived from the degradation of tryptophan. L-Kynurenine is an endogenous molecule, formed by catalytic breakdown of tryptophan, with low AhR affinity but potential physiological relevance[110]. The indoles 6-formylindolo[3,2-b]carbazol (FICZ) and 2-(1′H-indole-3′-carbonyl)-thiazole-4-carboxylic acid methylester (ITE) have been shown to strongly induce AhR activity[115,116]. Molecules that do not bind the AhR ligand-binding pocket, but activate the AhR via changing molecular levels of FICZ or modulating chaperon activity, have been termed AhR activators. This group includes inflammatory mediators, organic solvents and metals[117]. Kaufmann *et al.* identified a bacterial virulence factor as AhR ligand, suggesting the AhR might be a new form of an intracellular PRR that can sense microbial insults[118].

1.5.3 AhR in gut immunity

Expression and consequently functional significance of the AhR strongly varies between different tissues. While muscle tissue, testes, kidney and brain show only weak expression of the AhR, constitutive high expression can be found in the liver and in barrier tissues such as the skin, the lung and the gut. Moreover, the AhR expression differs among cells of the

hematopoietic lineage. Cells expressing the AhR at the highest levels are Th17 cells, γδ T cells, ILC3s, macrophages, DCs and plasma cells[110].

An organ with particularly high expression of the AhR and of central interest in this thesis is the gut. Different groups have described the importance of AhR expression in various cell-types for maintaining gut barrier integrity and immunological functionality. RORγt^{+} ILC3s, which are a major source of intestinal IL-22, show reduced expression of IL-22 in AhR$^{-/-}$ mice as well as a defect in ILC3 maintenance in the intestine[119]. This was attributed to lack of transcription of the cell-specific proliferation factor c-kit that is expressed in an AhR-dependent fashion[120]. As a consequence of reduced LTi cell frequency, neither CPs nor ILFs are formed in the intestine. AhR-deficient mice also exhibit highly reduced frequency of IELs, which is accompanied by low IL-22 levels, reduction in antimicrobial peptide production (RegIIIβ, RegIIIγ) and higher microbial load[121]. These defects render mice more susceptible for infections with *Citrobacter rodentium* and also more sensitive to dextran sodium sulfate (DSS)[122]. In addition, AhR signaling impacts CD4^{+} T cell immunity. AhR signaling in Foxp3^{+} Tregs triggers Foxp3 demethylation and transactivation, which finally leads to expansion of the Treg cell compartment. AhR signaling in Th17 cells promotes IL-22 expression and limits inhibitory effects on Th17 cell differentiation through IFNγ and IL-2[112]. Further, AhR signaling has been shown to positively influence proliferation of colonic crypt stem cells[123]. Especially dietary AhR ligands strongly impact the gut immunity and immune cell homeostasis. Mice colonies fed with experimental diets containing low levels of AhR ligands exhibited similar phenotypes as AhR-deficient animals, indicating the importance of these micronutrients[120]. Other studies also showed beneficial effects of dietary AhR ligands on oral tolerance[124,125].

Taken together, several independent studies have established a role for AhR activation in regulating intestinal homeostasis and barrier integrity.

1.5.4 The Aryl hydrocarbon receptor repressor (AhRR)

Although AhR activation and its functional consequences are well-studied, negative regulation of the AhR signaling pathway is not that well-understood. A protein that has been identified and proposed to negatively regulate AhR actions is the AhR repressor (AhRR). Expression of the AhRR is induced by a variety of AhR agonists. The AhRR in turn competes with AhR for binding to ARNT and therefore reduces the binding of the AhR-ARNT complex to DRE/XRE sites by a negative feedback loop. The AhRR protein shares great structural similarities to AhR and ARNT. It contains a bHLH DNA-binding domain and a dimerization

domain (PAS-A). However, neither a PAS-B nor a Q-rich domain and ligand-binding pocket are present. Due to the structural similarity, the AhRR is able to form a dimer with ARNT. The AhRR-ARNT complex can also bind to the genomic target sequences of the AhR, however no transcriptional transactivation and consequently no target gene expression is induced. It is also further speculated that negative regulation of the AhR might involve transrepression through protein-protein interactions instead of inhibiting DNA binding of the AhR-ARNT complex[126,127].

Recent studies in our group using AhRR-reporter and knockout mice revealed that the AhRR is mainly expressed in immune cells of barrier organs and does not strictly mimic the expression profile of the AhR. Thus, the AhRR might be important to regulate AhR controlled processes in immune cells. It was further shown that the interplay between the AhR and AhRR is highly complex and that differential effects of AhRR-deficiency might be explained by tissue and cell-type restricted expression patterns. Investigations of the AhRR in inflammatory responses in the intestine revealed that lack of the AhRR results in increased susceptibility to colitis, similar to AhR-deficient mice[128]. How this elevated susceptibility in AhRR-deficient mice is mediated, will be elaborated in this thesis.

1.6 Chronic inflammatory bowel disease

Chronic inflammatory bowel diseases (IBDs) are a group of diseases, characterized by a chronic inflammation of the gastrointestinal tract, associated with an imbalanced microbiota. Crohn's disease (CD) and ulcerative colitis (UC) are the most common types of IBD. In the US over 1.4 million people are affected, creating a significant burden on the health system[129]. It is well accepted that the development of IBD has a genetic predisposition, involves the immune system and is influenced by environmental factors.

CD and UC generally develop as polygenic disorders that in most cases arise spontaneously. However, 5-10% of IBDs are familial and humans with a family history of IBD have an up to 5 times higher risk of developing these diseases[130]. Previous studies have identified over 200 genome-wide significant (GWS) IBD susceptibility loci in a European population[131]. Genetic risk factors for CD and UC interestingly show a significant overlap. Molecules and pathways involved in disease development are highly diverse. For example, components of the immune system, like IL-23 and Th17 cells[132] but also the autophagy pathway are involved in development of IBD[133]. The autophagy genes *ATG16L1* and *IRGM,* the NOD-like receptor *NOD2* and the intelectin *ITLN1* are highly specific susceptibility genes for CD, while genes of

regulatory pathways like *IL10* and *ARPC2*, intestinal epithelial cell (IEC) function (e.g., *ECM1*), and an E3 ubiquitin ligase (e.g., *HERC2*) appear to be specific for UC[134].

Intestinal homeostasis depends on complex interactions between microbiota, intestinal epithelium and host immune system. A breakdown of regulatory pathways that cooperate to maintain intestinal homeostasis may critically precipitate the chronic pathology found in IBD. Further, an immunological imbalance leads to hyper-responsiveness to self-antigens resulting in chronic inflammatory conditions in the intestine[135]. Thus, it was shown that T cells restricted to antigens from microbiota induce intestinal inflammation, whereas non-specifically activated T cells do not mount an immune response[136]. UC is often described as a Th2-mediated disease, while CD is characterized by Th1 activation. However, this simple classification has been challenged as individual cytokines can have diverse and even opposing functions in some clinical and immunological settings[137,138]. Different studies and experimental models indicated that TNFα, TGFβ and IFNγ are related with establishment and onset of IBD[139]. More recently, it has been shown that Th17 cell-derived cytokines might have opposing effects in IBD. While some Th17-type cytokines (IL-17F/Il-21) may trigger inflammatory pathways, other Th17-related cytokines like IL-17A and IL-22 also promote counter regulative mechanism that support the recovery of the intestinal epithelium[140].

Development of both common forms of IBD, CD and UC, involve environmental factors. One of these environmental drivers is the intestinal microbiota. 16S rRNA sequencing identified changes in the composition of the intestinal microbiota in CD and UC patients. A significantly lower bacterial diversity especially affecting the two major classes of commensal phyla, the *Firmicutes* and *Bacteroidetes*, were detected[79]. The profound influence of the microbiota on IBD-like disorders could be particularly shown in murine intestinal inflammation models. Several genetic mouse models for inflammatory intestinal disorders do not establish the disease when they are maintained under germfree conditions, indicating the necessity for commensals in disease development. This could be shown for IL-10-deficient mice as well as for HLA-B27 transgenic rats[141,142]. Further, it could be shown more specifically that adequate development of Treg responses is impaired in germfree mice, which might have an influence on the development of inflammation in IBD[134]. Recently, GWAS studies identified mutations in the AhR as risk factor for IBD[143]. Association of the AhR with Th17 cell expansion, production of IL-22, maintenance of intestinal homeostasis and controll of the microbial load highlight why the AhR might have a pivotal role in IBD pathogenesis[121,143].

In summary, the cumulative findings about IBD suggest that chronic intestinal inflammation requires genetic predispositions, perturbations of the host immune system and changes in environmental components such as the microbiota.

2 Aim of the Thesis

The AhR has been extensively studied in the field of toxicology for its role in the detoxification of xenobiotic substances. It is a ligand activated transcription factor that is probably most widely known for binding 2,3,7,8-Tetrachlorodibenzo-*p*-dioxin (TCDD) and inducing enzymes that are involved in detoxifying dioxin. However, investigations of the physiological functions and importance of the AhR as an immune regulator have come into the focus of immunologists more recently. The AhR has emerged as a regulator of the gastrointestinal immune system modulating inflammatory cytokine and chemokine responses, enhancing certain T helper cell subset differentiation and mediating interactions between the commensal flora and the gut luminal wall.

This thesis focuses on the AhR repressor (AhRR), a direct target gene and a negative regulator of the AhR. Recent studies in our laboratory have shown very strong expression of the AhRR in immune cells of barrier organs, like the gastrointestinal tract. Additionally, it could be shown that AhRR-deficient mice display similarly enhanced sensitivity to DSS-induced colitis than AhR knockout mice. The aim of this thesis is hence to understand which cells and molecules mediate the enhanced susceptibility and if this mechanism is distinct or similar to what has already been found for the AhR. In addition to previously investigated AhRR/EGFP reporter and knockout mice, $AhRR^{fl/fl}$LysM-Cre mice were utilized to investigate the role of the AhRR in myeloid lysozyme M positive ($LysM^{+}$) cells in colitis induction.

In the second part of the thesis, the reason for the physiologically high AhRR expression in immune cells will be investigated. As a direct AhR target gene, AhRR expression is AhR ligand driven. Whether these ligands are derived endogenously, provided by the microbiota or from dietary origin, will be investigated in this thesis. Moreover, this study will additionally investigate, whether different amounts or types of AhR ligands in certain diets influence the intestinal barrier integrity.

This thesis aims at gaining a better understanding of the role of dietary AhR ligands for AhR-signaling in the intestinal immune system and what role the AhRR plays in regulating AhR signaling processes.

3 Materials

3.1 Equipment

Table 3.1: Equipment

Equipment	Article/ Company
Automatic tissue processor	Leica TP1020 (Leica Microsystems, Wetzlar, Germany)
Balances	440-35A (Kern & Sohn, Balingen, Germany) ABJ-NM (Kern & Sohn, Balingen, Germany) EW-N (Kern & Sohn, Balingen, Germany)
Beaker glass	100ml (Simax Bohemia Cristal, Selb, Germany)
Cell counting chamber	Neubauer improved (La Fontaine via Labotec, Göttingen, Germany)
Centrifuges	MicroStar17 (VWR, Wayne, USA), 5415R (Eppendorf, Hamburg, Germany) 5424R (Eppendorf, Hamburg, Germany) 5810R (Eppendorf, Hamburg, Germany) Allegra X-15R (Beckman Coulter, Pasadena, USA)
Cryostat	CM3050S (Leica, Wetzlar, Germany)
ELISA washer	CAPP wash 12 (CAPP, Odense, Germany)
Flow Cytometer	BD LSR II Flow (BD Biosciences, Heidelberg, Germany) BD FACSCanto II (BD Biosciences, Heidelberg, Germany)
Freezer (-20°C)	Comfort (Liebherr, Biberach, Germany) Bosch GSD12A20 (Bosch, Gerlingen, Germany) Profi Line GG4310 (Liebherr, Biberach, Germany)
Freezer (-80°C)	New Brunswick Ultra-Low Temperature Freezer (Eppendorf, Hamburg, Germany)

Fridge (+4°C)	KTR16A21/02 (Bosch, Gerlingen, Germany) MediLine LKUexv1610 (Liebherr, Biberach, Germany)
Gel electrophoresis	PerfectBlue Gel System (Peqlab, Erlangen, Deutschland)
Heating devices	TS1 ThermoShaker (Biometra, Göttingen, Germany) Heatingblock Thermostat TH21 (HLC BioTech, Bovenden, Germany) Waterbath WNB 22 (Memmert, Schwabach, Germany)
Homogenizer	Precellys®24 (Peqlab, Erlangen, Germany)
Hydrophobic barrier pen	ImmEdge pen (Vector Lab Inc., Burlingame, USA)
Ice machine	Scotsman Flockeneisbereiter AF200 (Hubbard Systems, Birmingham, USA)
Incubator	CB 150 (Binder, Tuttlingen, Germany)
Incubator shaker	Innova 44 (Eppendorf, Hamburg, Germany)
Laminar flowWorkbench	BDK Laminar Flow (BDK, Sonnenbühl, Genkingen, Germany)
Magnetic stirrer	IKA RCT basic (IKA-Werke GmbH & Co. KG, Staufen, Germany)
Measuring cylinder	250ml, 500ml, 1000ml, 2000ml (VWR, Wayne, USA)
Microscopes	BZ-9000 (Keyence, Montabaur, Germany) Leica DM2500 (Leica Microsystems, Wetzlar, Germany) Nikon Eclipse TS100 (Nikon, Amsterdam, Netherlands)
Microtome	Leica RM2255 (Leica Microsystems, Wetzlar, Germany) Leica HI1210 (Leica Microsystems, Wetzlar, Germany)

Microwave	NN-E235M (Panasonic, Osaka, Japan)
Pipette Controller, cordless	MATRIX CellMate II (Thermo Scientific, Waltham, USA)
Pipettes	10µl, 20µl, 200µl, 1000µl (Eppendorf, Hamburg, Germany) 2,5µl ErgoOne (StarLab, Hamburg, Germany) Multichannel DV8-10, DV12-50, DV8-300 (HTL Lab Solutions, Warszawa, Poland)
Power supply	PowerPac™ (BioRad, Hercules, USA)
Real-Time PCR Detection System	CFX96 TouchReal-Time PCR Detection (Bio-Rad, Munich, Germany)
Spectrophotometer	NanoDrop™ ND-1000 (NanoDrop Products, Wilmington, USA) EL 800 (BioTek, Winooski, USA) infinite M200 (Group Ltd., Männedorf, Switzerland)
Thermal cycler	T100™ (BioRad, Hercules, USA), TProfessional Thermocycler (Biometra, Göttingen, Germany) T1 Thermocycler (Biometra, Göttingen, Germany)
Threaded bottles	100ml, 250ml, 500ml, 1000ml (Schott, Mainz, Germany)
Transilluminator	Transilluminator UST-30M-8R (BioView, Rehovot, Israel) Biostep Dark Hood DH-40/50 (biostep, Burkhaltsdorf, Germany)
Vortex shaker	Vortex Genie 2 (Scientific Industries, New York, USA)

3.2 Consumables

Table 3.2: Consumables and plastic ware

Item	Company
BD Plastipak 1ml Sub-Q	BD Medical, Le Pont de Claix Cedex, France
Biopsy punch	Kai Europe, Solingen, Germany
Cell strainer nylon (40µm, 70µm, 100µm)	VWR, Radnor, USA
CellTrics®	Partec, Meckenheim, Germany
Cover slips	Roth, Karlsruhe, Germany
Culture plates (6-well/ 24-well/ 48-well/ 96-well, flat bottom)	Greiner, Frickenhausen, Germany
Disposal bags	Roth, Kalsruhe, Germany
ELISA plate (half-area, 96 K)	Greiner, Kremsmünster, Austria
Eppendorf Tubes® 5ml	Eppendorf, Hamburg, Germany
Filter tips	Sarstedt, Nümbrecht, Germany
Flow cytometry tubes	Sarstedt, Nümbrecht, Germany
Glass beads	Roth, Kalsruhe, Germany
Gloves	Semperit Technische Produkte GmbH, Wien, Austria
Hard-shell PCR plates	Bio-Rad, München, Germany
Measuring pipettes (5ml, 10ml, 25ml)	Greiner, Kremsmünster, Austria
Micro tube 1.1ml Z-Gel	Sarstedt, Nümbrecht, Germany
Micro tube 2ml + screw cap	Sarstedt, Nümbrecht, Germany
Microplate, 96well (F/U)	Greiner, Frickenhausen, Germany
Microscope slides (Superfrost plus)	Thermo Scientific, Waltham, USA
Multiply®µStrip Pro mix.colour	Sarstedt, Nümbrecht, Germany
Parafilm®	American National Cam, Greenwich, USA
PCR tubes	Sarstedt, Nümbrecht, Germany
Petri dishes	Greiner, Kremsmünster, Austria

Precision wipes	Kimberly-Clark, Reigate, United Kingdom
Reaction tubes (15ml, 50ml)	Greiner, Frickenhausen, Germany
Reagent reservoirs	Thermo Scientific, Waltham, USA
Safe seal reaction tubes (0,5, 1.5ml, 2.0ml)	Sarstedt, Nümbrecht, Germany
Sterican needles (0.90x40mm, 20G x 1½)	Braun, Melsungen, Germany
Sterile filters (Filtopur S 0.45)	Braun, Melsungen, Germany
Surgical disposable scalpel	Braun, Tuttlingen, Germany
Syringe filtration unit (Filtropur S0.2/0.45)	Sarstedt, Nümbrecht, Germany
Syringes Inject-F Tuberkulin (1ml)	Braun, Melsungen, Germany
Syringes Inject® (2ml, 5ml, 10ml, 20ml)	Braun, Melsungen, Germany
Tissue freezing medium	Leica, Nussloch, Germany
Tissue-Tek® Cryomold (15x15mm, 25x20mm)	Sakura Finetek, Torrance, USA
Weighing pans	Roth, Karlsruhe, Germany

3.3 Chemicals and reagents

Table 3.3: Chemicals and reagents

Chemical/ reagent	Company
100bp DNA Ladder	New England BioLabs, Ipswich, USA
10x TAE buffer	Invitrogen, Carlsbad, USA
2-Propanol >99.5%	Roth, Karlsruhe, Germany
3-Methylchloranthren	Sigma-Aldrich, St. Louis, USA
Acetic acid 100%	Roth, Karlsruhe, Germany
Acetone	VWR, Darmstadt, Germany
Albumin Bovine Fraction V, pH=7.0	SERVA Electrophoresis GmBH, Heidelberg, Germany
Ampicillin-ratiopharm 1g/l	Ratiopharm, Ulm, Germany
Ampuwa	Fresenius Kabi, Bad Homburg, Germany

Brefeldin A solution (1000x)	eBioscience, San Diego, USA
Ciprofloxacin Kabi 200mg/100ml	Fresenius Kabi Deutschland GmbH, Langenhagen, Germany
CountBright™ absolute counting beads	Life technologies, Carlsbad, USA
Dextran Sulfate Sodium Salt, Colitis Grade	MP Biomedicals, Solon, USA
Dithiothreitol (DTT) Molecular Grade	Promega, Fitchburg, USA
DNase/RNase-Free Water	Zymo Research, Irvine, USA
Dulbecco's PBS	Sigma-Aldrich, Steinheim, Germany
Entellan	Merck, Darmstadt, Germany
Ethanol 70% (methylated)	Roth, Karlsruhe, Germany
Ethanol absolute for molecular biology	ApliChem, Darmstadt, Germany
Ethanol Rotipuran >99.8%	Roth, Karlsruhe, Germany
Ethylenediaminetetraacetic acid (EDTA)	Sigma-Aldrich, St. Louis, USA
FACS Clean Solution	BD Bioscience, Franklin Lakes, USA
FACS Rinse Solution	BD Bioscience, Franklin Lakes, USA
Fetal Bovine Serum	ThermoFischer, Waltham, USA
FICZ	Abcam, Cambridge, UK
Fixable Viability Dye eFluor 450/ 780	eBioscience, San Diego, USA
Hank's Balanced Salt Solution (HBSS) (10x)	gibco by Life Technologies, Carlsbad, USA
HEPES	Sigma-Aldrich, St. Louis, USA
Hydrochloric acid 37%	Roth, Karlsruhe, Germany
Imipenem/Cilastatin Kabi 500mg/500mg (powder)	Fresenius Kabi Deutschland GmbH, Langenhagen, Germany
Indole-3-carbinol	Sigma-Aldrich, St. Louis, USA
Ionomycin	Sigma-Aldrich, St. Louis, USA
Metronidazol B. Braun 5 mg/ml (infusion)	Braun, Tuttlingen, Germany

Monensin Solution (1000x)	eBioscience, San Diego, USA
Myeloperoxidase from human leukocytes	Sigma-Aldrich, St. Louis, USA
OneComp/ UltraComp ebeads	eBioscience, San Diego, USA
Paraformaldehyde (PFA)	Merck, Darmstadt, Germany
Penicillin-Streptomycin	gibco by Life Technologies, Carlsbad, USA
peqGOLD Universal Agarose	peqlab, Erlangen, Germany
Phorbol myristate acetate (PMA)	Sigma-Aldrich, St. Louis, USA
Phosphate Buffered Saline Dulbecco	Merck, Darmstadt, Germany
Protease Inhibitor cOmplete Tablets, Mini	Roche, Indianapolis, USA
QIAzol Lysis Reagent	Qiagen, Hilden, Germany
RPMI 1640	ThermoFisher, Waltham, USA
Saponin	Sigma-Aldrich, St. Louis, USA
Sodium hydroxide solution	Roth, Karlsruhe, Germany
Sulfuric acid (H_2SO_4)	Roth, Karlsruhe, Germany
SYBR® DNA Gel Stain	Invitrogen, Carlsbad, USA
Tissue Freezing Medium	Leica Biosystems, Nussloch, Germany
TruStain fcX™ (anti-mouse CD16/32) (Clone: 93)	BioLegend, San Diego, USA
Trypan Blue	Sigma-Aldrich, St. Louis, USA
Tween-20	Roth, Karlsruhe, Germany
Vancomycin HEXAL 1.0g (dry solid)	Hexal, Holzkirchen, Germany
Xylol	Roth, Karlsruhe, Germany

3.4 Solutions and buffers

Table 3.4: Solutions and buffers

Solution/buffer	Content
Complete RPMI 1640	RPMI Medium 8% FCS 1% L-Glutamine 1% Penicillin-Streptomycin 50µM β-Mercaptoethanol
EDTA (0.5M)	186.g EDTA approx. 20g NaOH 1000ml H_2O pH 7.8-8.0
ELISA stopping solution	25% H_2SO_4 in H_2O
ELISA wash buffer	0.05% Tween-20 in PBS
HATAB buffer	Aqua dest. 50mM potassium phosphate 5mg/ml Hexadecyltrimethylammonium bromide
Histology blocking buffer	PBS 1% FCS 1% mouse serum 1% rat serum
IEL isolation buffer	PBS 10% FCS 15mM HEPES 5mM EDTA
Intestinal digestion solution #1	5mM DTT in HBSS 2% FCS Penicillin: 100U/ml Streptomycin: 100µg/ml

Intestinal digestion solution #2	5mM EDTA in HBSS 2% FCS Penicillin: 100U/ml Streptomycin: 100µg/ml
Intestinal digestion solution #3	HBSS 10mM HEPES Penicillin: 100U/ml Streptomycin: 100µg/ml
Lysis buffer (tail lysis)	A. dest 5 mM EDTA, pH 8,0 0,2 % SDS 200 mM NaCl 0,1 mg/ml Proteinase K
MACS buffer	PBS 0.5% BSA 2mM EDTA
PERM buffer	PBS 0.5% Saponin 0.5% BSA
PFA (4%)	4g PFA 100ml PBS
Skin digestion buffer	PBS DNase I (200 U/ml) Liberase™ (0.8 U/ml)

3.5 Elisa

Table 3.5: Elisa Kits

Target molecule/protein	Company
IFNγ	R&D Systems, Mineapolis, USA

IL-10	R&D Systems, Mineapolis, USA
IL-17	R&D Systems, Mineapolis, USA
IL-1β	R&D Systems, Mineapolis, USA
IL-22	R&D Systems, Mineapolis, USA
IL-6	R&D Systems, Mineapolis, USA
KC/CXCL1	R&D Systems, Mineapolis, USA
Lipocalin 2	R&D Systems, Mineapolis, USA
TNFα	R&D Systems, Mineapolis, USA

3.6 Antibodies

3.6.1 Antibodies for flow cytometry

Table 3.6: Flow cytometry antibodies

Antigen	Isotype	Clone	Conjugate	Company
B220	Rat IgG2a, κ	RA3-6B2	APC/Cy7	BioLegend
CD103	Rat IgG2a, κ	M290	BV421	BD Biosciences
CD11b	Rat IgG2a, κ	M1/70	APC, PE, BV605	BioLegend
CD11c	Armenian Hamster IgG	N418	APC/Cy7	BioLegend
CD127	Rat IgG2a, κ	A7R34	PerCp/Cy5.5	ebioscience
CD19	Rat IgG2a, κ	6D5	PerCP, PerCp-Cy5.5	BioLegend
CD207 (Langerin)	Mouse IgG2a, κ	4C7	APC	BioLegend
CD25	Rat IgG1, λ	PC61	APC/Cy7, APC	BioLegend
CD326 (Ep-CAM)	Rat IgG2a, κ	G8.8	APC	BioLegend
CD3ε	Armenian Hamster IgG	145-2C11	APC/Cy7, PE, PE/Cy7, PerCP-Cy5.5	BioLegend

CD4	Rat IgG2a, κ	RM4-5	APC, APC/Cy7, BV605, PerCP	BioLegend
CD45	Rat IgG2b, κ	30-F11	PE/Cy7, PE, BV510	BioLegend
CD64	Mouse IgG1, κ	X54-5/7.1	PerCp-Cy5.5	BioLegend
CD86	Rat IgG2a, κ	GL-1	PE	BioLegend
CD8β	Rat IgG2b, κ	YTS156.7.7	PerCP-Cy5.5	BioLegend
CD8α	Rat IgG2a, κ	53-6.7	PE/Cy7	BioLegend
F4/80	Rat IgG2a, κ	BM8	APC	ebioscience
FoxP3	Rat IgG2a, κ	FJK-16s	PE	ebioscience
I-A/I-E (MHCII)	Rat IgG2b, κ	M5/114.15.2	APC	BioLegend
IFNγ	Rat IgG1, κ	XMG1.2	APC	BD Biosciences
IL-17A	Rat IgG2a, κ	eBio17B7	PE	ebioscience
Isotype ctrl	Rat IgG1, κ	RTK2071	APC, PE	BioLegend
Isotype ctrl	Rat IgG2a, κ	eBR2a	APC, PE	BioLegend
NK1.1	Mouse IgG2a, κ	PK136	PE	BD Biosciences
NKp46	Rat IgG2a, κ	29A1.4	PE, PE/Cy7	ebioscience
RORγt	Rat IgG1, κ	B2D	APC	ebioscience
TCR β chain	Armenian Hamster IgG	H57-597	PE	BioLegend
TCR γ/δ	Armenian Hamster IgG	GL3	APC	BioLegend

3.6.2 Antibodies for Immunohistology

Table 3.7: Immunohistology antibodies

Antigen	Isotype	Clone	Conjugate	Company
GFP	Rabbit IgG	Polyclonal	purified	Life Technologies
Rabbit IgG	Rabbit IgG (H+L)	Polyclonal	Alexa Fluor 488	Life Technologies

3.7 Kits

Table 3.8: Kits

Name	Company
ABsolute qPCR SYBR Green ROX Mix	Thermo Scientific, Waltham, USA
Direct-zol™ RNA MiniPrep Kit	Zymo research, Irvine, USA
LIVE/DEAD® Fixable Violet Dead Cell Stain Kit, for 405 nm excitation	Life Technologies, Carlsbad, USA
MyTaq HS Red DNA Polymerase	Bioline, London, UK
QIAamp® DNA Stool Mini Kit	Qiagen, Hilden, Germany
Quick-RNA™ MiniPrep	Zymo research, Irvine, USA

3.8 PCR primers

Table 3.9: PCR primers

Target		Sequence
CYP1A1	fwd	5'-CCTCATGTACCTGGTAACCA-3'
	rev	5'-AAGGATGAATGCCGGAAGGT-3'
GAPDH	fwd	5'-GAGCCAAACGGGTCATCA-3'
	rev	5'-CATATTTCTCGTGGTTCACACC-3'
RPS6	fwd	5'-ATTCCTGGACTGACAGACAC-3'
	rev	5'-GTTCTTCTTAGTGCGTTGCT-3'

3.9 Software

Table 3.10: Software

Software	Company
Adobe Illustrator CS5	Adobe Systems, Dublin, Republic of Ireland
Argus X1	biostep, Burkhardtsdorf, Germany
BZ-II Analyzer	Keyence, Montabaur, Germany

CFX Manager™ Software	Bio-Rad, Munich, Germany
FACS Diva	BD, Franklin Lakes, USA
Fiji (Image J)	Open source scientific analysis program
FlowJo 9.9.7/10.4.1	TreeStar, Inc., Ashland, USA
Gen 5 2.03	BioTek, Winooski, USA
GraphPad Prism 6	GraphPad, La Jolla, USA
Microsoft Office 2011 for Mac	Microsoft, Redmond, USA
NanoDrop™ ND-1000	NanoDrop Products, Wilmington, USA
Papers 2	Papers, Dordrecht, The Netherlands

3.10 Enzymes

Table 3.11: Enzymes

Enzyme	Company
DNase I	Roche, Basel, Switzerland
Horseradish Peroxidase	Sigma-Aldrich, St. Louis, USA
Liberase™	Roche, Basel, Switzerland
Proteinase K	Sigma-Aldrich, St. Louis, USA

3.11 Mouse diets

Table 3.12: Mouse diets

Mouse diet	Producer
LASQCdiet® Rod16-A	LASvendi, Soest, Germany
ssniff® EF R/M acc. AIN 93G	ssniff Spezialdiäten GmbH, Soest, Germany
ssniff® EF acc. D12492 (I) mod.	ssniff Spezialdiäten GmbH, Soest, Germany
ssniff® EF acc. D12450B (I) mod.	ssniff Spezialdiäten GmbH, Soest, Germany

3.12 Animals for research

All mice used during the experiments were kept under SPF (specific pathogen free) conditions in the Life & Medical Sciences Institute (LIMES) Genetic Resources Center (GRC). All experiments were performed in accordance with institutional, state and federal guidelines and with permission of the state government of North Rhine-Westphalia (Germany).

Table 3.13: Genetically modified mouse lines

Mouse line	Strain	Description
AhR$^{-/-}$	C57BL/6	Mouse line deficient for the AhR[144]
AhRR$^{+/+}$	C57BL/6	Mouse line expressing the functional AhRR
AhRR$^{E/+}$	C57BL/6	Mouse line expressing eGFP under the control of the *ahrr* promoter on one allele and the functional AhRR on the other allele[128]
AhRR$^{E/E}$	C57BL/6	Mouse line expressing eGFP under the control of the *ahrr* promoter instead of functional AhRR[128]
AhRR$^{fl/fl}$	C57BL/6	These mice are described separately (3.13).
AhRR$^{fl/fl}$ LysM-Cre	C57BL/6	AhRR$^{fl/fl}$ mice are crossed to LysM-Cre mice that express the Cre recombinase under the control of the LysM promoter[145].

3.13 Generation of AhRR$^{fl/fl}$ mice

AhRR$^{fl/fl}$ is a transgenic mouse line generated in our group at the Leibniz Research Institute for Environmental Medicine (IUF) Düsseldorf by Heike Weighardt and Markus Korkowski. Mice were generated by homologous recombination and subsequent blastocyst injection of a targeting vector. LoxP sites were inserted upstream and downstream of exon 3 of the *ahrr* gene, which encodes for the basic helix-loo-helix (bHLH) domain (Fig.3.1). Between the 5' loxP site and exon 3 a flippase recognition target (FRT) site-flanked neomycin selection cassette was inserted, facilitating selection of successfully transfected embryonic stem cells. After having created mutant mice the neomycin cassette was removed through crossing with a transgenic mouse line expressing the flippase (Flp) ubiquitously (Flp-Deleter-strain). The resulting AhRR$^{fl/fl}$ mice can be crossed to mice that express the cre recombinase in a cell-type specific manner. This results in a cell-type specific excision of the loxP site flanked exon 3 and as a consequence in a cell-type specific AhRR-deficient mouse.

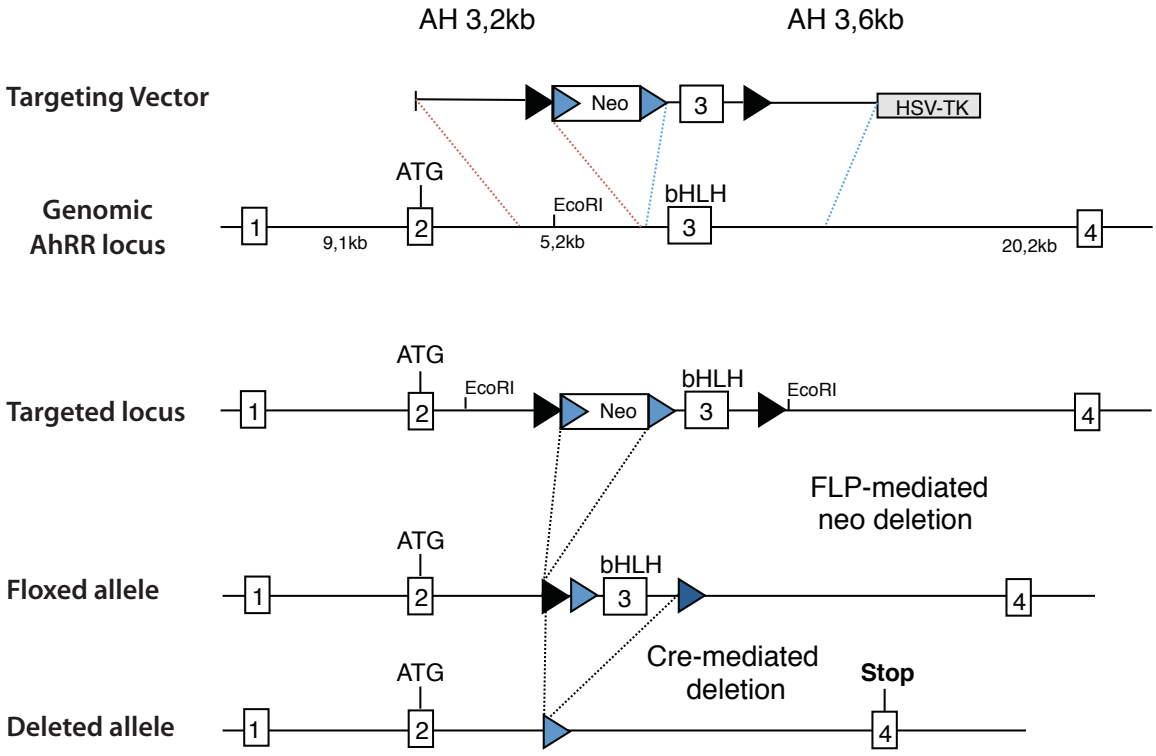

Figure 3.1: AhRR$^{fl/fl}$ mice targeting strategy
AhRR$^{fl/fl}$ mice were generated by insertion of the targeting vector into the genomic AhRR locus via homologous recombination. The neomycin cassette was removed by Flp-mediated deletion before excision of exon three by Cre-mediated deletion. This figure was kindly provided by Heike Weighardt.

4 Methods

4.1 DSS-induced colitis

Dextran sodium sulfate (DSS) colitis was induced in aged-matched female mice by adding 2%, 3% or 5% DSS (w/vol) to the drinking water. Mice were kept on DSS-containing water for 5 to 7 days. In some experiments DSS water was replaced after 7 days with normal drinking water. The general state of health, behavior, posture, stool consistency, rectal bleeding and body weight were monitored every other day. At the end of the experiment blood was drawn from the facial vein and serum was separated for analysis of inflammatory cytokines or markers. Moreover, colons were removed and the colon length was determined. Small intestine, colon, PPs, mLNs and spleen were removed and either transferred into 4% Paraformaldehyde (PFA) or stored in PBS on ice until further use.

4.2 Histology

Directly after removal organs were transferred to 4% PFA in order to preserve tissue structures. Organs were kept in PFA-solution either for 4 hours at room temperature or up to several weeks at 4°C.

4.2.1 Preparation of tissue for cryosectioning

The tissue was dehydrated with sucrose in PBS at rising concentrations (5%, 10%, 20%). Therefore, organs were kept for 1 hour in each solution or alternatively in the 20% sucrose solution overnight. Afterwards, tissue samples were embedded in cryomedium and frozen using dry ice. Subsequently, samples were stored at -80°C until cryosectioning. Using a cryostat, tissue sections of 7 to 10µm were produced and mounted on a microscope slide. Sections were air dried for 45 minutes and then fixed with acetone for 10 minutes. Slides were stored at -80°C.

4.2.2 Preparation of tissue for paraffin sections

PFA-fixed tissue samples were transferred into plastic cassettes and further processed with the Leica Benchtop Tissue Processor that incubates tissue samples in a series of ascending alcohol concentrations for dehydration. Then, tissue samples were embedded into paraffin, cooled down and stored at room temperature. Paraffin embedded tissue samples were subsequently processed with a rotary microtome to obtain 5µm sections. These sections were transferred to a warm water bath (40°C) and afterwards dragged onto microscope slides. After

drying in a heating cabinet (2 hours), slides were stored at room temperature until further processing.

4.2.3 Immunofluorescence staining

Frozen sections were thawed and encircled with a water-repellent pen (ImmEdge Pen), creating a hydrophobic barrier around the sample. Specimens were then rehydrated in PBS for 5 minutes and then placed into a humid chamber. To prevent unspecific binding, sections were blocked with self-made histoblock containing 1% murine serum, 1% rat serum and 1% FCS for 1 hour at room temperature. Slides were washed three times for 5 minutes in PBS before adding antibodies in PBS onto the tissue sections. Antibodies were incubated 2 hours at room temperature or overnight at 4°C. Slides were then washed three times for 5 minutes in PBS. If necessary, secondary antibodies in PBS were added to the tissue specimens and incubated for 2 hours at room temperature before washing the slides three times for 5 minutes in PBS. Next, nuclei were stained with 4',6-diamidino-2-phenylindole (DAPI) diluted 1:5000 in PBS for 10 minutes. Slides were washed three times in PBS for 5 minutes and afterwards 1 minute in distilled water. After air-drying, slides were mounted with Mowiol-DABCO. Afterwards the slides were dried overnight at room temperature and then stored at 4°C in the dark.

4.2.4 Hematoxylin and Eosin staining

Hematoxylin and eosin stain (H&E stain) was performed in order to analyze tissue morphology. The protocol is outlined in the table below (Table 4.1). In brief, paraffin sections were treated with xylol, alcohol and water to remove the paraffin from the tissue. Afterwards, the nuclei of cells were stained with hemalaun. Hemalaun acts as a basic dye and reacts with negatively charged cell components, such as nucleic acids in the nucleus, resulting in a blue stain. Eosin Y is an acidic, negatively charged dye that reacts with positively charged components, such as amino groups in proteins in the cytoplasm, resulting in a pink stain.

Table 4.1: H&E staining protocol

Treatment	Time
Xylol	10 [min]
Xylol	10 [min]
100% Ethanol	5 [min]
100% Ethanol	5 [min]
95% Ethanol	2 [min]
70% Ethanol	2 [min]
Aqua dest.	1 [min]
Mayer's hemalaun solution	3 [min]
0.1% Hydrochloric acid	2 [sec]
Tab water	3 [min]
Alcoholic Eosin Y solution	3 [min]
Tab water	30 [sec]
95% Ethanol	10 [sec]
95% Ethanol	10 [sec]
100% Ethanol	10 [sec]
100% Ethanol	10 [sec]
Xylol	5 [min]
Xylol	5 [min]

4.2.5 Microscopy

Microscopic analysis of immunoflourescently or H&E stained sections was performed using the Keyence BZ-9000 microscope. Afterwards, images were edited and analyzed with the BZ-II Analyzer or Fiji (ImageJ) software. To determine colitis severity H&E stained samples of murine colon sections were scored according to Dieleman *et al* (Table 4.2)[146].

Table 4.2: DSS colitis severity scoring

Feature graded	Grade	Description
Inflammation	0	none
	1	slight
	2	moderate
	3	severe
Extend	0	none
	1	mucosa
	2	mucosa and submucosa
	3	transmural
Regeneration	4	no tissue repair
	3	surface epithelium not intact
	2	regeneration with crypt depletion
	1	almost complete regeneration
	0	complete regeneration or normal tissue
Crypt damage	0	none
	1	basal 1/3 damaged
	2	basal 2/3 damaged
	3	only surface epithelium intact
	4	entire crypt and epithelium lost
Percent involvement	1	1-25%
	2	26-50%
	3	51-75%
	4	76-100%

4.3 Isolation of intestinal immune cell subsets

Mice were sacrificed either by cervical dislocation or by asphyxiation with 100% carbon dioxide (CO_2). The murine abdomen was opened and colon, SI and mLNs were transferred into PBS filled tubes and stored on ice until further processing. Colon and SI were cleaned from residual fat tissue using small forceps and flushed with cold PBS in order to remove

intestinal content. PPs were removed from the colon with scissors and stored on ice until cell isolation. Colon and SI were opened longitudinal and cut into 1-2 cm long pieces. From these tissue pieces IELs or lamina propria lymphocytes were isolated.

4.3.1 Intraepithelial lymphocytes (IELs)

SI or colon tissue pieces were transferred into 50ml tubes filled with 25ml of IEL isolation buffer (3.4) and shaken at 37°C for 45 minutes at 150 rounds per minute (rpm) in a shaking incubator. After that the content of the tube was filtered through a 70 µm cell strainer. The flow through containing intestinal epithelial cells (IECs) and IELs was further analyzed via flow cytometry.

4.3.2 Lamina propria lymphocytes

Intestinal tissue pieces were transferred into a 50ml tube containing intestinal digestion solution 1 (SI: 20ml, colon: 10ml) and incubated at 37° for 20 minutes while shaking (150 rpm). Afterwards, the tissue was transferred into a second 50ml tube with solution 2 (SI: 15ml, colon: 7,5ml) and incubated for 15 minutes in the shacking incubator. Incubation in solution 2 was repeated twice. Tissue pieces were subsequently incubated in 10ml intestinal digestion solution 3 for 10 minutes at 37°C while shaking. Then, intestinal tissue was transferred into a 6 well plate, minced with scissors into small pieces and mixed with 7ml of intestinal digestion solution 3. DNase I (200 U/ml) and Liberase™ (0.2 U/ml) were added and the 6 well plate was incubated for 45 minutes at 37°C with gentle shaking (60 rpm). After that, the tissue was further homogenized by pipetting up and down several times with a 10ml serological pipette. The cell suspension was filtered through a 70 µm cell strainer to receive a clean single cell suspension and retain undigested tissue. Moreover, an equal volume of MACS buffer was added in order to stop the enzymatic activity of DNase I and Liberase. The cells were washed twice and then further processed.

4.3.3 mLNs/ PPs

Residual fat and connective tissue were removed from mLNs using small forceps and scissors. Afterwards mLNs or PPs were mashed through a 100µm cell strainer with the plunger of a 2ml syringe. The single cell suspension was washed with PBS and further processed as required.

4.4 Isolation of dermal and epidermal immune cells

Ears and tails were harvested and stored in PBS on ice. Dorsal and ventral ear sides were separated with forceps. Tail skin was mechanically detached from the spine. 3ml of Trypsin-EDTA (0.25%) was pipetted into a 6 well plate and tail and ears were floated epidermal side-up on the Trypsin-EDTA. After 90 minutes incubation period at 37°C epidermis and dermis were separated with forceps and processed independently.

The **dermis** was transferred into a 12 well plate and minced with scissors and was digested in 500 µl of digestion buffer at 37°C for 60 to 90 minutes in a shaking incubator at 100 rpm. For further separation the cell suspension was resuspended with a blunted tip of a 1000 µl pipette and then filtered through a 100 µm cell strainer and subsequently through a 70 µm cell strainer in order to separate cells from undigested residual tissue. Lastly, the suspension was centrifuged at 4000 rpm for 10 minutes and the cell pellet was suspended in 1ml PBS. Cells were afterwards stained for analysis via flow cytometry.

Epidermal tissue was mashed through a 100 µm cell strainer in a 6 well plate containing 5ml PBS. The obtained cell suspension was then filtered through a 70 µm and a 40 µm cell strainer, centrifuged at 4000 rpm for 10 minutes, suspended in 1ml PBS and further stained for flow cytometric analysis.

4.5 Flow Cytometry

Flow cytometry is a laser-based technique to analyze several thousand cells per second with regard to multiple parameters simultaneously. Further, this technology can be used to sort certain cell populations according to their expression profile of defined biomarkers. Usually fluorophore-coupled antibodies or fluorescent dyes are used as labels in flow cytometry. Using different laser wavelength, certain bandpass filters and different fluorophores, modern flow cytometers allow for analysis of up to 50 different characteristics of one cell.

4.5.1 Staining of cell surface antigens

For staining of cell surface antigens, a certain number of cells that have been produced by one of the previously described protocols were transferred into FACS tubes. The tubes were filled up with PBS and centrifuged at 1400 rpm for 5 minutes. After discarding the supernatant, cells were resuspended in 100 or 200 µl PBS or MACS buffer containing a mixture of fluorophore-coupled antibodies directed against the antigens of interest. Cells were incubated for 15 minutes one ice, protected from direct light. Afterwards, cells were washed with 300 to

500 µl cold PBS or MACS buffer (1400 rpm, 5min) and resuspended in 300 µl MACS buffer for flow cytometric analysis.

4.5.2 LIVE/DEAD® Fixable Dead Cell Stain Kit

The LIVE/DEAD® fixable dead cell stain kit was used to discriminate between living and dead cells. Cells were incubated in 100 or 200 µl PBS containing the fixable dye at a dilution of 1:1000 for 30 minutes on ice. The staining was typically performed in combination with the surface antibody staining. Afterwards, cells were washed with 300 to 500 µl PBS (1400 rpm, 5min) and then further processed.

4.5.3 Fixation of cells for flow cytometric analysis or intracellular staining

After surface staining and optional LIVE/DEAD® staining, cells were fixed with 2% Paraformaldehyde (PFA), if required, for 20 minutes at room temperature. Afterwards, cells were washed with 300 to 500 µl PBS (1400 rpm, 5min) and resuspended in 300 µl MACS buffer.

4.5.4 Intracellular cytokine and transcription factor staining

Staining of intracellular proteins was performed following fixation of cells as described in the previous section. After PFA fixation, cells were washed with PBS and resuspended in 100 to 200 µl PERM buffer containing fluorophore-coupled antibodies directed against intracellular antigens. Afterwards, cells were incubated for 1 hour at 4°C or alternatively over night if anti-GFP staining was performed. As the anti-GFP antibody is not directly labeled with a fluorochrome, cells were washed with 300 µl PERM buffer on the next day (1400 rpm, 5min) and then resuspended in 100 to 200 µl PERM buffer containing a fluorophore-coupled secondary antibody directed against the species of the primary anti-GFP antibody. After 45 minutes cells were washed with 300 µl PERM buffer (1400 rpm, 5min), 300 µl MACS buffer (1400 rpm, 5min) and finally resuspended in 300 µl MACS buffer for flow cytometric analysis.

4.6 Colon explant cultures

To culture colon explants, colons were explanted and intestinal content was removed. Colons were opened longitudinal and tissue was cleaned in ice-cold PBS. A biopsy punch was used to obtain a 6mm diameter tissue sample. The biopsy was transferred into a 48 well plate with 300 µl complete RPMI (cRPMI). The plate was incubated at 37°C and 5% CO_2 for 6 hours.

Afterwards, the concentration of cytokines released from the biopsy was determined in the supernatant by Enzyme-linked Immunosorbent Assay (ELISA).

4.7 Myeloperoxidase (MPO) activity assay

Measurement of the enzymatic activity of the oxidative enzyme myeloperoxidase (MPO), which is the most abundant proinflammatory enzyme stored in granules of neutrophil granulocytes, is widely used to evaluate the degree of inflammation in biological samples. After DSS colitis, colon tissue samples were snap frozen in liquid nitrogen and subsequently stored at -80°C until further processing. After thawing on ice, 350 µl of HATAB buffer were added to the tissue in glass bead tubes. The tissue was homogenized using the Precellys®24 tissue homogenizer (6000 rpm, 3x30seconds) and afterwards snap frozen again. Then, the samples were thawed at 55°C using a heating block. The lysate was subsequently cleared by centrifugation at 13000 rpm for 15 minutes and the supernatant was transferred into a new tube and stored on ice. The protein concentration was determined with the NanoDrop spectrophotometer. The cleared lysate was diluted 1 to 5 with HATAB buffer and 50µl were transferred into a 96 well flat bottom microtiter plate. Human MPO was diluted in HATAB buffer to prepare a standard curve with a top activity of 1 U/ml. An 8-point serial dilution of the top standard and three blank wells containing just HATAB buffer were prepared. Then, 50 µl of TMBplus2 substrate was added to the wells and incubated for approximately 10 minutes. Substrate reaction was stopped by addition of 50 µl of 2N H_2SO_4. Absorption was determined at 450 nm using a microtiter plate reader.

4.8 ELISA (Enzyme-linked Immunosorbent Assay)

The sandwich Enzyme-linked Immunosorbent Assay (ELISA) detects antigens in a fluid sample by the application of antibodies and an enzyme-catalyzed color reaction. All ELISAs were purchased from R&D Systems and conducted according to the manufacturer's instruction. In brief, antigen capture antibodies were immobilized in a 96-well ELISA plate by incubation for 2 hours at room temperature in PBS. After washing once with ELISA wash buffer, plates were blocked with blocking buffer (1% BSA in PBS) for 1 hour at room temperature. Following three more washing steps, antigen-containing samples were incubated for 2 hours at room temperature. To quantify the amount of antigen in the samples, a serial dilution of a protein standard in reagent diluent was also applied to antibody-coated wells. After three more washing steps, the diluted biotinylated-detection antibody was applied to the plate and incubated for 2 hours at room temperature or at 4°C overnight. Subsequently, the

plate was washed three more times. Streptavidin-coupled Horseradish Peroxidase in reagent diluent was incubated for 20 minutes at room temperature. Following three final washing steps 50 µl of TMB PLUS2 was added to the plate and incubated until appearance of blue color indicates turnover of added substrate. To stop the reaction, the same volume of 0.5M sulfuric acid was added, leading to a yellow color development. Absorption was measured at 450nm/630nm using a microtiter plate reader.

4.9 Real Time Quantitative PCR (qPCR)

4.9.1 RNA isolation

In order to isolate whole RNA from SI, colon or any other tissue, small tissue samples were explanted, cleaned from intestinal content or fat and transferred into glass bead tubes. These tubes were snap frozen in liquid nitrogen and subsequently stored at -80°C until further usage. 600µl of QIAzol Lysis Reagent were added to the tissue samples immediately before thawing. Tissue lysis and homogenization was performed with the Precellys®24 homogenizer at 6000rpm (3x20 seconds). RNA was isolated using the Zymo Research Direct-zol MiniPrep kit according to the manufacturer's instructions. RNA was eluted with 50µl of DNase/RNase free water and RNA concentration was determined using the NanoDrop1000 Photospectrometer. The RNA was stored at -80°C for further procedures.

4.9.2 cDNA synthesis

Isolated whole RNA was transcribed into complementary DNA (cDNA) by the enzyme reverse transcriptase. The employment of Oligo(dT) primers ensures the transcription of in particular messenger RNA (mRNA), which is protected against degradation by exonucleases by modification with a 3' poly(A) tail. For all experiments between 0.5 and 1 µg of RNA was used for the transcription. The RNA was diluted to the desired concentration in DNase/RNase free water. A maximum volume of 10 µl RNA was used. RNA was mixed with 3 µl $Oligo(dT)_{12-18}$ primer, which hybridize to the poly(A) tail of mRNA. The mixture was incubated for 10 minutes at 70°C in order to unfold and denature the RNA and allow the primers to anneal to the RNA. Afterwards the samples were cooled down on ice. Then, a master mix consisting of other reagents needed (Table 4.3) were added and the cDNA reaction mix was incubated for 1 hour at 40°C. A final 5 minute incubation at 95°C inactivated the reverse transcriptase and stopped the reaction.

Table 4.3: cDNA synthesis Master Mix

	Volume (1 reaction)
DEPC water	9.4 µl
5x RT buffer	8.0 µl
dNTP (10mM)	4.0 µl
DTT (100mM)	4.0 µl
RiboLock (40U/µl)	0.8 µl
RT (200U/µl)	0.8 µl
	27 µl

4.9.3 RPS6 PCR

In order to control the efficiency of cDNA synthesis, a polymerase chain reaction (PCR) for the ribosomal protein S6 (RPS6) was performed. RPS6 is a constitutively expressed gene and can therefore be used to evaluate the cDNA quality. A PCR mix containing 1.5 µl cDNA, 13.05 µl water, 4 µl 5x MyTaq reaction buffer and 0.05 µl MyTaq DNA polymerase was prepared and run in a thermocycler according to the program in table 4.4. The PCR product was analyzed on an agarose gel, and the band strength was compared between samples as a measure of comparable cDNA synthesis efficiency.

Table 4.4: RPS6 PCR program

	Incubation time	**Temperature**
1x	5 [min]	95°C
35x	1 [min]	95°C
	1 [min]	55°C
	1 [min]	72°C
1x	10 [min]	72°C

4.9.4 qPCR

The real-time polymerase chain reaction (qPCR) is a technique that is commonly used to monitor amplification of targeted DNA in real-time in order to quantify an amount of DNA molecules, which has been transcribed from mRNA previously. After conversion of RNA in cDNA (4.9.2) the cDNA was used as a template for amplification via PCR. The 2x ABsolute qPCR SYBR Green Mix contains all components for the quantitative PCR reaction, except primer and template. The mix contains appropriate amounts of SYBR Green I dye and Thermo-Start DNA Polymerase. SYBR Green preferentially intercalates into newly synthesized double-stranded DNA and subsequently emits green light at a wavelength of 520nm. The CFX96 Touch™ Real-Time PCR Detection System detects the signal that increases with advancing DNA amplification. One PCR reaction had a volume of 15 µl and included 7,5 µl 2x ABsolute qPCR SYBR Green Mix, 0,3 µl forward primer, 0,3 µl reverse primer, 1,9 µl water and 5 µl cDNA. The cDNA, synthesized according to section 4.9.2, was diluted 1:5 with water prior to the qPCR reaction. The CFX96 thermocycler program is listed in the table below (Table 4.5).

Table 4.5: qPCR thermocycler program

	Incubation time	**Temperature**
1x	15 [min]	95°C
44x	20 [min]	95°C
	40 [min]	60°C
	60 [min]	40°C

Following the amplification, a melting curve analysis of the synthesized double stranded DNA fragments was performed in order to check if the PCR primers produce one specific PCR product or potential unwanted unspecific products or primer dimers. For this purpose the thermo cycler raises the temperature in steps of 0.5°C from 65 to 95°C. The melting temperature was determined by a strong reduction of SYBR Green fluorescence signal as a consequence of its dissociation from the DNA.

4.9.5 Comparative Ct Method Quantification

The comparative Ct Method of quantification is a relative quantification method based on an internal reference gene that is used to determine fold-difference expression of a target gene.

The quality of this method largely depends on the selection of a good reference or housekeeping gene that is stably expressed and largely independent of any experimental conditions. A housekeeping gene corrects for differences in the quality and quantity of the RNA that was initially utilized, which can affect the whole PCR process. During the PCR the accumulation of the SYBR Green fluorescence signal was measured. A threshold cycle (Ct) was determined at the time-point where the amount of SYBR green fluorescence exceeds the background fluorescence. Ct values are inversely correlated to the amount of nucleic acid within the sample. Ct values of the target gene were corrected for the Ct values of the reference gene forming the ΔCt value in treated and control samples ($\Delta Ct1=Ct_{Target\ treated}-Ct_{Reference\ treated}$, $\Delta Ct2=Ct_{Target\ control}-Ct_{Reference\ control}$). In a second step control Ct values were subtracted from the Ct values of treated samples ($\Delta\Delta Ct=\Delta Ct1-\Delta Ct2$). Normalized target gene expression as fold change of treated over control samples was finally determined by the formula "$Fold\ Change=2^{-\Delta\Delta Ct}$".

4.10 Determination of intestinal permeability

Intestinal barrier function and intestinal barrier permeability can be determined by oral application of the FITC-coupled anhydroglucose polymer dextran and subsequent measurement of the amount of FITC that is transmitted to the circulation. As the intestinal barrier is normally not permeable for FITC-dextran, high FITC fluorescence in the murine serum indicates a defect and leakiness of the intestinal barrier. Thus, FITC-dextran was orally applied and subsequently FITC fluorescence was determined in serum. Mice were fasted 4 hours prior to FITC-dextran administration to facilitate absorption from the intestinal lumen. Then, mice were orally gavaged with 600mg per kg body weight with FITC-dextran in PBS using a gavage needle. Mice were left without food for 4 more hours and then blood was taken from the facial vein and serum was separated using 1.1ml Serum Gel with Clotting Activator Micro tubes. In order to quantify the amount of FITC-dextran transmitted over the intestinal barrier into the blood, FITC fluorescence of 40µl serum, pipetted into a 96 well flat bottom microtiter plate, was determined with the Tecan infinite M200 plate spectrophotometer at an excitation wavelength of 492nm and an emission wavelength of 525nm. Fluorescence intensity was plotted as arbitrary units (AU).

4.11 Statistical analysis

Statistical analysis was performed using the unpaired students t-test, if just two independent groups or two conditions on one experimental group were compared. For the determination of

any statistical difference between three or more independent experimental groups the one-way ANOVA was used. The two-way ANOVA was used when analyzing the mean differences between groups that have been split on two independent variables. All data are presented as mean plus standard error of the mean (SEM) if not stated otherwise in the figure legend. Significance was defined by reaching certain p-values in the statistical tests (* $p<0.05$, ** $p<0.01$, *** $p<0.001$). All statistical analysis was conducted with the software GraphPad Prism.

5 Results

5.1 AhRR-deficient mice are highly susceptible to DSS colitis

The AhR pathway has been shown to be very important for the intestinal immune system in health and disease. Recent studies have identified the genetic locus of the AhR as a susceptibility locus in inflammatory bowel disease (IBD)[143]. In line with mediation of several anti-inflammatory effects[147], activation of the AhR leads to protection from DSS-induced colitis, whereas mice deficient for the AhR are highly susceptible to IBD[148]. In this context, the AhR has been shown to be important for the maintenance of intraepithelial lymphocytes (IELs)[121] and for the production of the barrier protective cytokine IL-22 by ILC3s in the intestine[119,120]. Actions of the AhR are regulated through the AhRR by negative feedback inhibition. Previous studies performed in our group by Dr. O. Brandstätter could show that mice deficient for the AhRR show, similar to AhR knockout mice, high susceptibility to DSS colitis[128,149]. These mice showed greater tissue damage, more weight loss and higher production of proinflammatory cytokines early in the disease. However, neither higher intestinal barrier permeability nor changed frequencies of myeloid cells or lamina propria T cells could be observed in AhRR-deficient mice compared to wild-type littermates. Similar to AhR-deficient mice, a reduced frequency of $CD8\alpha^{+}TCR\gamma\delta^{+}$ IELs could be shown. However, IEL frequency was not affected as strong as in AhR-deficient mice. Furthermore, reduced fecal and higher serum IgA titers of AhRR-knockout mice indicated a potential migration defect of IgA producing B1-cells from the peritoneal cavity to the gut[149].

The aim of this study was to understand, if the susceptibility of AhRR-deficient mice to DSS colitis is mechanistically linked to the same cells and molecular drivers as in AhR-deficient mice or if different pathways, possibly independent of the AhR, are of additional importance.

5.1.1 Innate lymphoid cell frequency is unchanged in AhRR-deficient mice

Colitis susceptibility of $AhR^{-/-}$ mice can be largely attributed to the lack of IL-22-producing ILC3s in the intestinal lamina propria[119,150]. Therefore the presence of ILC3s in the small intestinal lamina propria of untreated WT, $AhR^{-/-}$ and $AhRR^{E/E}$ mice was compared. Lamina propria lymphocytes were isolated and ILC3s were identified by flow cytometry as $CD45^{+}CD3^{-}$ non-T cells expressing the transcription factor $ROR\gamma t$[151]. Furthermore, two different subsets of ILC3s were discriminated by their expression of NKp46/NCR1 (Natural cytotoxicity triggering receptor 1). In addition to the overall ILC3 frequency, presence of

AhRR-expressing ILC3s was determined in AhRR$^{E/E}$ mice using the EGFP reporter (Fig.5.1a).

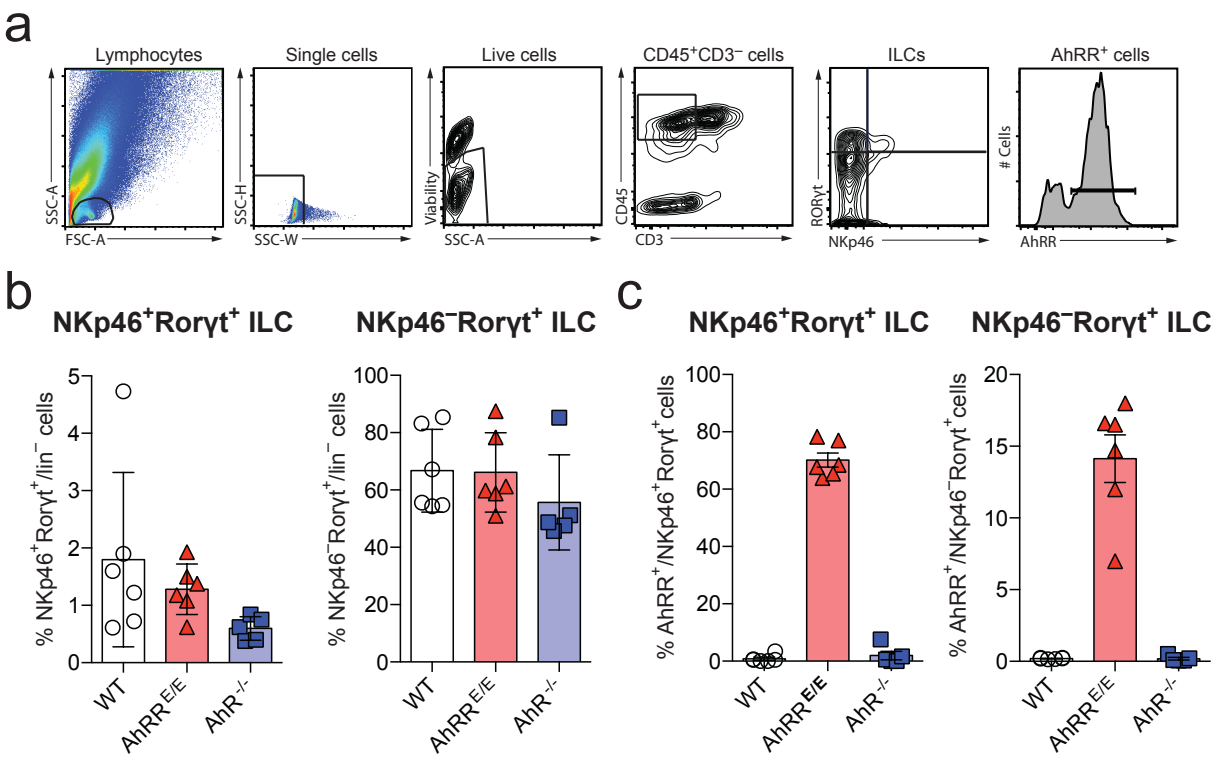

Figure 5.1: The intestinal ILC3 frequency is reduced in AhR$^{-/-}$, but not in AhRR$^{E/E}$ mice.
The frequency of ILC3s was determined in the small intestinal lamina propria of untreated WT, AhRR$^{E/E}$ and AhR$^{-/-}$ mice. (a) Gating strategy for group 3 ILCs. Lymphocytes and singles cells were gated from the FSC/SSC and SSC-W/SSC-H signals. Living cells were selected as viability dye negative events. ILC3s were identified as CD45^{+}CD3^{-} cells expressing RORγt and NKp46 (b) Frequencies of NKp46 positive and negative subsets were determined. (c) ILC3s were further analyzed for the frequency of AhRR expressing cells. Data in b and c is pooled from three independent experiments (n=5-7 mice). Results are given as mean +/– SD. This data has been published in Brandstätter *et al.*, Sci Rep, 2016[128].

Similar to previous studies, the frequency of NKp46^{+} and NKp46^{-} ILC3s was reduced in the intestinal lamina propria of AhR$^{-/-}$ mice (Fig.5.1b). NKp46^{+}RORγt^{+} ILC3s were about 50% reduced, while NKp46^{-}RORγt^{+} ILC3s were about 20% reduced in AhR$^{-/-}$ mice compared to WT animals. Although the reduction was visible, the effect was not statistical significant. In contrast, a reduction of both ILC3 subsets could not be observed in AhRR$^{E/E}$ mice. Interestingly, 70% of the NKp46^{+} and 15% of the NKp46^{-} ILC3s were positive for the AhRR/EGFP reporter (Fig.5.1c).

Taken together, these experiments confirm previous studies observing reduced frequency of ILC3s in AhR$^{-/-}$ mice although the reduction was not as pronounced. However, no such reduction could be observed in AhRR-deficient mice, likely excluding an involvement of this cell type in the colitis susceptibility of AhRR$^{E/E}$ mice.

5.1.2 AhR- and AhRR-deficiency alter T helper cell differentiation in DSS colitis

Besides ILCs also T cells have been shown to be important for the pathogenesis of IBD. Enhanced retention in the tissue as well as production and release of proinflammatory cytokines by T cells contribute to the pathogenesis of the disease. Chronic IBD in humans and also DSS colitis in mice are predominantly Th1- and Th17-mediated diseases. Further, the AhR was shown to balance Treg and Th17 cell differentiation[152] and is therefore linked to the inflammatory processes in colitis[153]. In order to find out if AhRR-deficiency might likewise be involved in the differentiation of effector T cells in colonic and small intestinal lamina propria as well as in the mLNs during colitis, frequencies of the aforementioned cell types were investigated in $AhRR^{E/E}$ mice treated with 5% DSS for 6 days, in order to induce an acute colitis. Frequencies of effector T cells in AhRR-deficient mice were compared to WT and AhR-deficient mice.

$CD45^{+}Live/Dead^{-}$ cells were gated based on their expression of CD3 and CD4 or CD3 and CD8, respectively (Fig.5.2a/b). Th17, Th1, Tc17 and Tc1 cells were identified by the expression of their signature cytokines IL-17 or IFNγ. $AhRR^{E/E}$ mice showed elevated frequencies of Th17 cells from 10% to 17% and Tc17 cells from 2% to 8% in the small intestinal lamina propria compared to WT animals (Fig.5.2c/d). Frequency of Th1 cells was significantly reduced from 20% to under 5% IFNγ positive cells in the SI lamina propria and also slightly reduced in the colon (Fig.5.2c). Tc1 cell frequencies were comparable in WT and $AhRR^{E/E}$ mice in SI and colon (Fig.5.2d). All effector T cell subsets showed similar frequencies in the mLNs when comparing WT and $AhRR^{E/E}$ mice. $AhR^{-/-}$ mice showed significantly elevated frequencies of Th17 cells in SI, colon and mLNs. Th1 cell frequencies were elevated from 10% to 30% $IFN\gamma^{+}$ cells in the colon but not in SI and mLNs compared to WT mice (Fig.5.2c). AhR knockout mice displayed similar numbers of Tc17 cells as WT mice and significantly elevated frequencies of Tc1 cells in SI, colon and mLNs (Fig.5.2d).

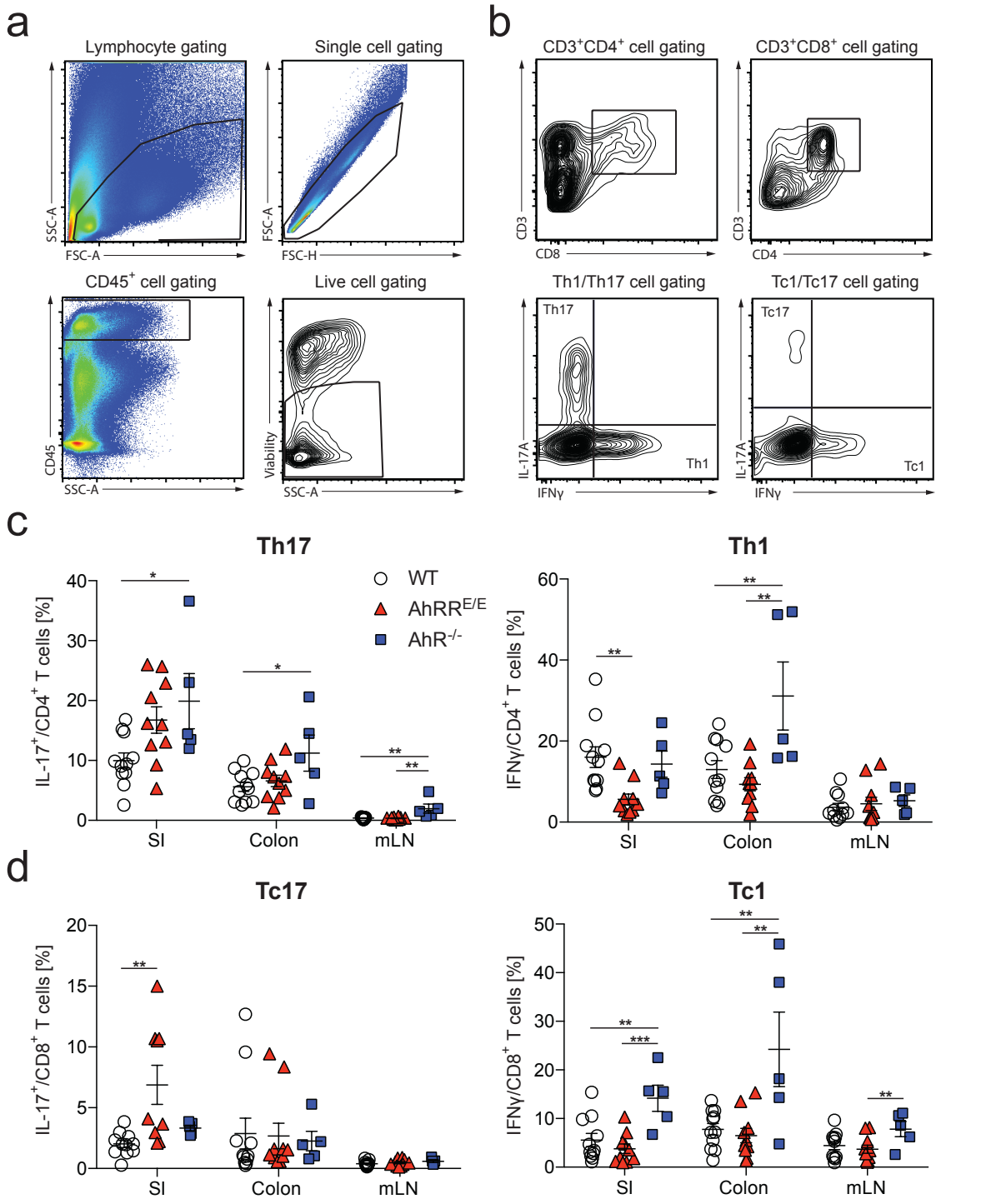

Figure 5.2: Analysis of IL-17- and IFNγ-producing T cells in the intestinal tissue after 6 days of DSS colitis

(a) Intestinal immune cells were identified by flow cytometry, gating on lymphocytes, single cells and $CD45^+$ living cells. (b) T cells subsets were discriminated by the expression of CD3 and of CD4 or CD8. Th17, Tc17, Th1 and Tc1 cells were identified by production of their signature cytokine. Frequencies of Th17 and Th1 (c) and Tc17 and Tc1 (d) cells were determined in single cell suspension of SI and colon lamina propria as well as mLNs. Data is pooled of two to five independent experiments (n=5-10). Results are given as mean +/– SEM and significance was determined by ordinary one-way ANOVA corrected for multiple comparisons by the Bonferroni's method (*$p<0.05$, **$p<0.01$, ***$p<0.001$). (c)/(d) This data has been published in Brandstätter *et al.*, Sci Rep, 2016[128]. T_h= helper T cell, T_c=cytotoxic T cell

In summary AhRR$^{E/E}$ mice showed higher frequencies of IL-17-producing T cells and reduced frequencies of IFNγ-producing T cells indicating a more Th17/Tc17 directed effector T cell differentiation in the SI during DSS colitis. AhR$^{-/-}$ mice show elevated frequencies of IL-17- and IFNγ-producing T cells, however, no higher numbers of Tc17 cells, which was exclusively observed in AhRR$^{E/E}$ mice. Thus, there appear to be clear differences in the phenotype of AhR$^{-/-}$ and AhRR$^{E/E}$ mice regarding T cell differentiation in the cause of colitis.

5.1.3 Intestinal IL-1β production is altered in AhRR$^{E/E}$ mice

Differentiation of Th17 cells is generally described to be dependent on the presence of the cytokines IL-6 and TGFβ[154-156]. However, it has also been shown that the combination of IL-23 and IL-1β[157] or a combination of TGFβ and IL-1β[158,159] is able to induce Th17 differentiation. Similar conditions for the differentiation of Tc17 cells in mouse and humans have been described[160]. In order to find out, if the cytokine microenvironment might be responsible for the enhanced Th/Tc17 differentiation in AhRR$^{E/E}$ mice, cytokines released by colonic tissue were determined under homeostatic and inflammatory conditions.

Cytokine levels in colonic tissue protein lysates were measured and normalized to the whole protein concentration of these lysates. No differences in IL-22, IL-10, TNFα, IL-6 and IFNγ levels could be observed in colons of untreated mice under homeostatic conditions, comparing WT and AhRR$^{E/E}$ mice. After 6 days of 5% DSS application in the drinking water, cytokine levels were generally elevated two to four times (Fig.5.3a). However, the increase was similar in WT and AhRR$^{E/E}$ mice. As IL-1β could not be detected in colon protein lysates (data not shown), colonic punch biopsies were taken and incubated in complete cell culture medium for 6 hours at 37°C. IL-1β released into the medium was measured by ELISA (Fig.5.3b). Interestingly, the amount of IL-1β released from the biopsies of untreated AhRR$^{E/E}$ mice was significantly higher than from WT mice. Punch biopsies taken from both WT and AhRR-deficient mice after DSS application released more IL-1β than those of naïve mice. Under inflammatory conditions however, there was no difference in IL-1β release from punch biopsies of AhRR-deficient and WT mice.

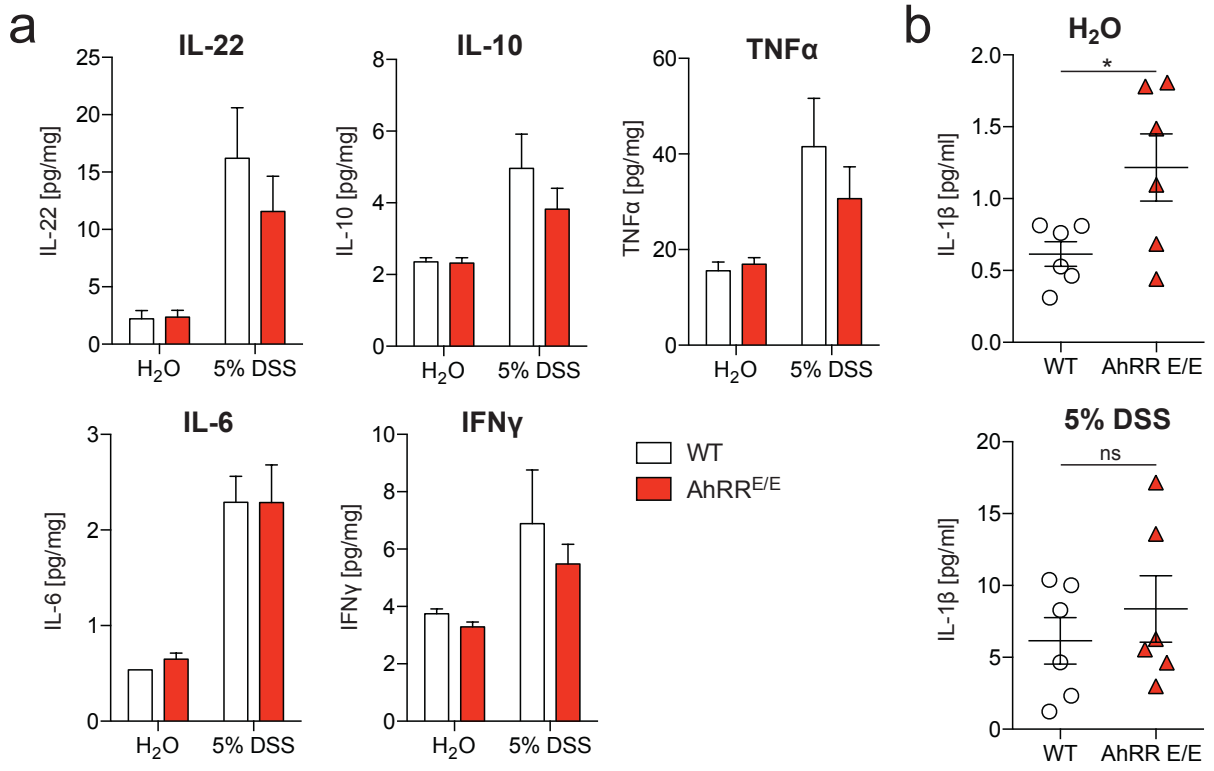

Figure 5.3: IL-1β levels are increased in colon tissue of AhRR$^{E/E}$ mice
Cytokines in the colonic tissue or released from colonic biopsies from untreated WT and AhRR$^{E/E}$ mice and after six days of 5% DSS treatment were measured. (a) IL-22, IL-10, TNFα, IL-6 and IFNγ levels were measured in protein lysates of colon tissue by ELISA and normalized to total protein levels. (b) IL-1β was measured in the supernatant of colon biopsies that were incubated in complete RPMI for six hours at 37°C. Data is pooled of at least two independent experiments (n=5-6 mice). Results are given as mean +/– SEM and significance was determined by two-tailed students t test (*p<0,05). The data in (b) has been published in Brandstätter *et al.*, Sci Rep, 2016[128].

Overall, colonic cytokine composition was unchanged comparing WT and AhRR$^{E/E}$ mice. However, significantly elevated IL-1β levels released from cultured colon biopsies of untreated AhRR$^{E/E}$ mice might hint to IL-1β as a potential driver of Th/Tc17 biased effector cell differentiation.

5.1.4 Myeloid cell frequency is normal in AhRR$^{E/E}$ mice under inflammatory conditions in DSS colitis

IL-1β is a proinflammatory cytokine with systemic and local effects on immune cell and non-immune cell function[161]. It is produced by innate leukocytes, such as intestinal DCs and macrophages. Changes in specific DC or macrophage subsets might be partially responsible for elevated IL-1β levels and therefore indirectly influence differentiation of IL-17-producing effector T cells. Further, changed myeloid cell frequencies might also directly affect effector T cell differentiation or the colitis susceptibility of AhRR$^{E/E}$ mice.

In order to analyze the frequency of intestinal myeloid cells, leukocytes were isolated from organs of the gastrointestinal tract and analyzed by flow cytometry. Cell gating was performed as shown in Fig.5.2a and Fig.5.4. DCs were identified by expression of the surface marker profile $CD64^{-}MHCII^{+}CD11c^{+}$ (Fig.5.4a). Using the surface markers CD11b and CD103 three different DC subsets, $CD11b^{-}CD103^{+}$, $CD11b^{+}CD103^{+}$ and $CD11b^{+}CD103^{-}$, were discriminated[51]. Macrophages were identified as $CD64^{+}F4/80^{+}$ cells (Fig.5.4b).

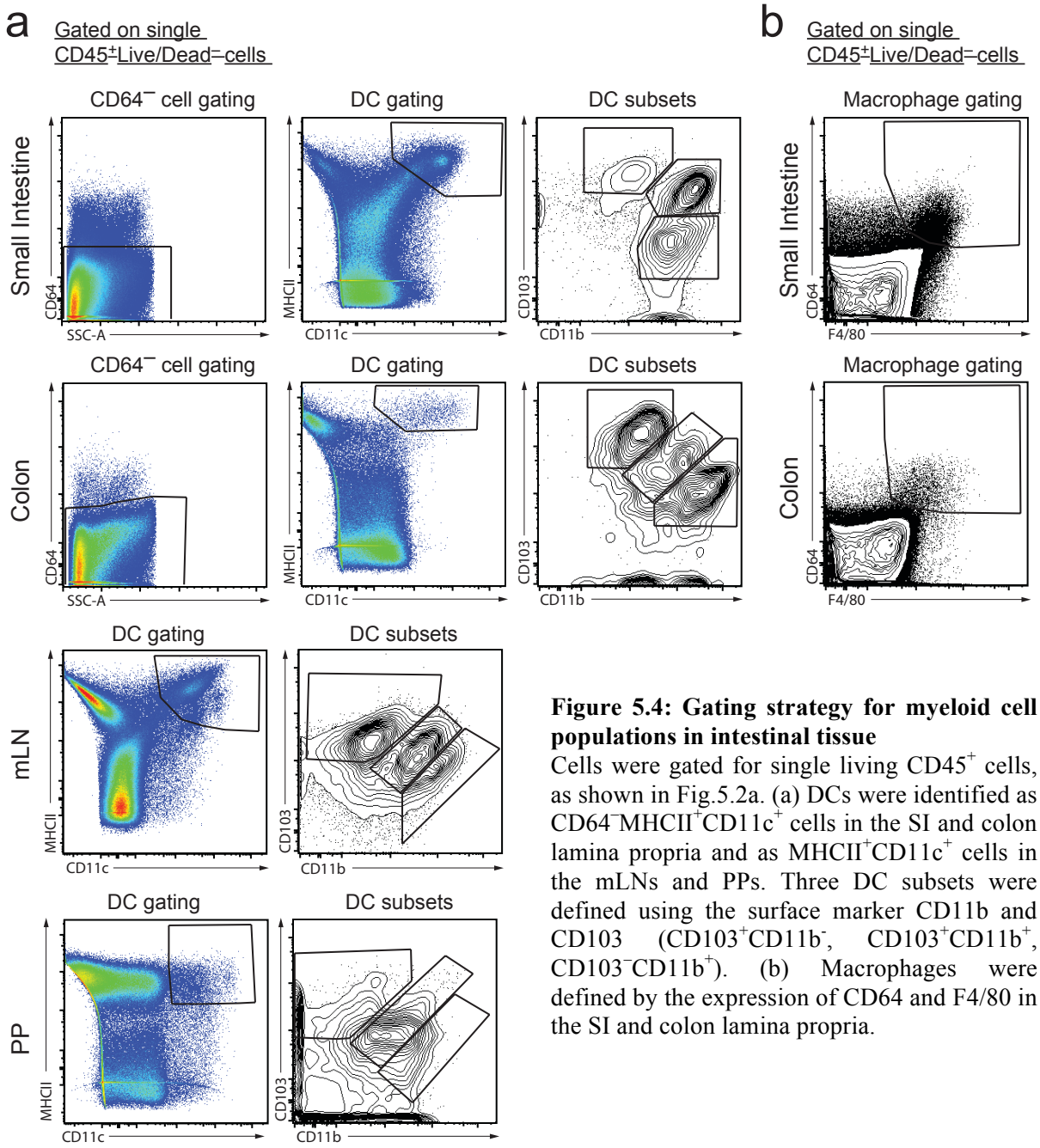

Figure 5.4: Gating strategy for myeloid cell populations in intestinal tissue
Cells were gated for single living $CD45^{+}$ cells, as shown in Fig.5.2a. (a) DCs were identified as $CD64^{-}MHCII^{+}CD11c^{+}$ cells in the SI and colon lamina propria and as $MHCII^{+}CD11c^{+}$ cells in the mLNs and PPs. Three DC subsets were defined using the surface marker CD11b and CD103 ($CD103^{+}CD11b^{-}$, $CD103^{+}CD11b^{+}$, $CD103^{-}CD11b^{+}$). (b) Macrophages were defined by the expression of CD64 and F4/80 in the SI and colon lamina propria.

The macrophage numbers in the lamina propria of the SI and the colon were unchanged comparing WT and AhRR$^{E/E}$ mice (Fig.5.5a). Insufficient macrophage numbers in mLNs and PPs did not allow for quantification of this cell-type in these organs (data not shown). This might be a result of the relinquishment of collagenase in the cell isolation of mLNs and PPs. DCs were detected in the mLNs, the PPs and the lamina propria of SI and colon. While similar DC frequencies were detected in PPs and colon, AhRR$^{E/E}$ mice had reduced DC frequencies in the mLNs and elevated frequencies in the SI (Fig.5.5a).

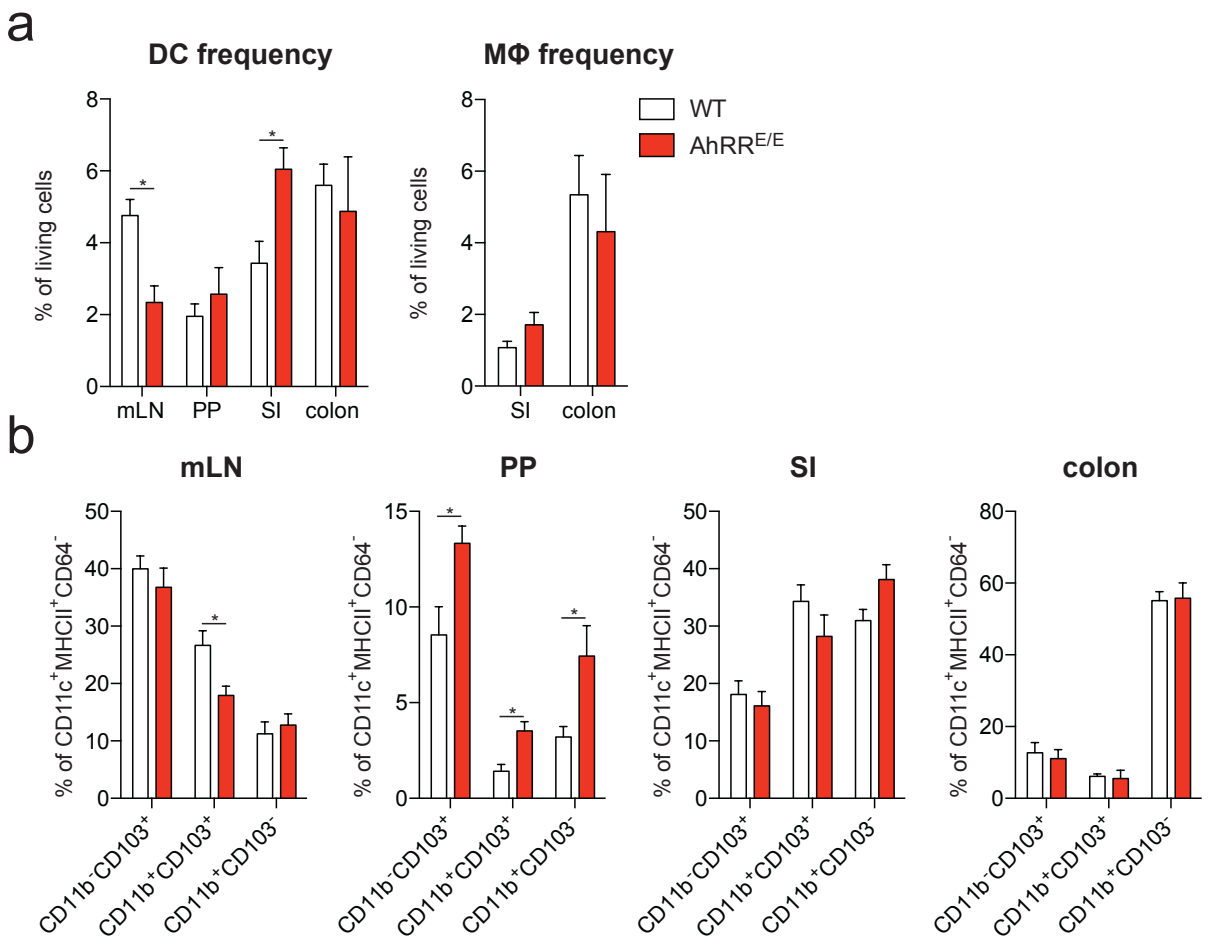

Figure 5.5: Frequency of DCs and macrophages in intestinal tissue of wild-type and AhRR$^{E/E}$ mice after 6 days 5% DSS treatment
(a) Frequency of DCs was determined in mLNs, PPs and the lamina propria of SI and colon. MΦ frequency was determined in SI and colon lamina propria. (d) Frequencies of intestinal DC subsets of total CD11c^{+}MHCII^{+} were determined in mLNs, PPs, SI and colon using the markers CD11b and CD103. Data is pooled of two independent experiments (n=3-6 mice total). Results are given as mean +/– SEM and significance is determined by two-tailed students t-test corrected for multiple comparisons by the Holm-Sidak method (*p<0.05). This data has been published in Brandstätter *et al.*, Sci Rep, 2016[128].

As DC subsets are functionally diverse with regard to priming or expansion of different T cell subsets, frequencies of all three DC subsets were investigated. However, frequencies of

$CD11b^{-}CD103^{+}$, $CD11b^{+}CD103^{+}$, $CD11b^{+}CD103^{-}$ DCs did not differ in the lamina propria of SI and colon (Fig.5.5b). The experiments identified the $CD11b^{+}CD103^{-}$ DCs as the major subset in the colon, while equally high frequencies of $CD11b^{+}CD103^{+}$and $CD11b^{+}CD103^{-}$ DC could be detected in the SI. In PPs, $AhRR^{E/E}$ mice showed elevated frequencies of all three mentioned DC subsets compared to WT mice, but no differences in total DC frequency, suggesting changes in the $CD11b^{-}CD103^{-}$ DC subset (data not shown). The latter population was even slightly bigger in the WT mice. In mLNs a reduction of $CD11b^{+}CD103^{+}$ DCs in $AhRR^{E/E}$ mice compared to WT mice was apparent (Fig.5.5b).

In summary, the frequencies of myeloid cells within the organs of the gastrointestinal tract were relatively similar. However, slight differences in the total DC frequency in mLNs and SI and some differences with regard to subset distribution in PPs an mLNs could be observed comparing WT and $AhRR^{E/E}$ mice.

5.1.5 Macrophage- and neutrophil-specific AhRR-deficiency does not convey elevated susceptibility to DSS colitis

In order to investigate which cells specifically mediate increased colitis susceptibility in AhRR-deficient mice, $AhRR^{fl/fl}$ mice were created, in which the third exon was flanked by loxP sites (Fig.3.1). Crossing mice expressing the Cre recombinase under the control of a cell type-specific promoter, results in a cell type-specific AhRR-knockout. Crossing the $AhRR^{fl/fl}$ mice with LysM-Cre mice, which express the Cre recombinase under the control of the lysozyme M promoter[145], results in a mouse line deficient for the AhRR in macrophages and neutrophils. This line allows investigating the contribution of the AhRR in macrophages and neutrophils to enhanced susceptibility to colitis observed in the full AhRR knockout.

$AhRR^{fl/fl}$LysM-Cre, $AhRR^{E/E}$ and WT mice were treated with 3% DSS in the drinking water for 7 days in order to induce colitis, followed by 5 days of normal drinking water to analyze the ability to recover from inflammation (Fig.5.6a). Over the course of the experiment the body weight of the mice was monitored. All mice showed weight loss from day four (100 hours) onwards. Weight loss stopped in WT and $AhRR^{fl/fl}$LysM-Cre after changing to normal drinking water, demonstrating their ability to recover from the disease. However, $AhRR^{E/E}$ mice lost more weight and did not recover (Fig.5.6b). Determination of colon length after the 12 days revealed a significant shortening of colons from all DSS-treated mice, compared to control WT mice just receiving water. However, no apparent genotype specific differences could be observed (Fig.5.6c).

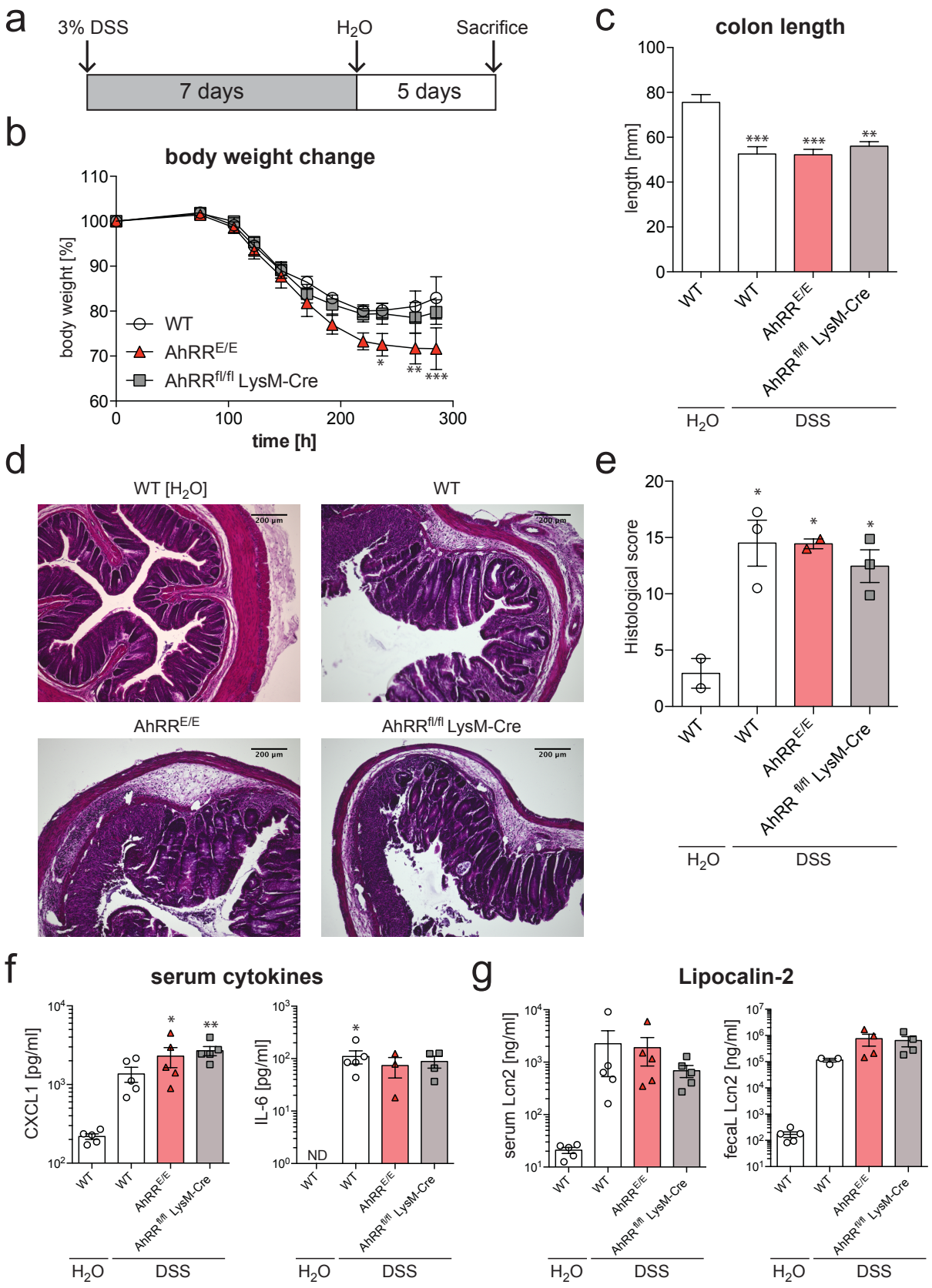
a
3% DSS
H2O
Sacrifice
7 days
5 days
b
body weight change
body weight [%]
time [h]
WT
AhRRE/E
AhRRfl/fl LysM-Cre
c
colon length
length [mm]
d
WT [H2O]
WT
AhRRE/E
AhRRfl/fl LysM-Cre
200 µm
e
Histological score
f
serum cytokines
CXCL1 [pg/ml]
IL-6 [pg/ml]
ND
g
Lipocalin-2
serum Lcn2 [ng/ml]
fecaL Lcn2 [ng/ml]
H2O
DSS

Figure 5.6: Macrophage- and neutrophil-specific AhRR-deficiency does not convey elevated susceptibility to DSS colitis
(a) WT, $AhRR^{E/E}$ and $AhRR^{fl/fl}$ LysM-Cre mice were treated with 3% DSS in the drinking water for seven days before returning to normal drinking water for five days. (b) Body weight changes were monitored over the course of the experiment. (c) Colon length was determined at the end of the experiment (day12). (d)/(e) Paraffin sections of colon tissue were stained with hematoxylin and eosin and the Histological score was determined as described in the Methods section. (f) CXCL1 and IL-6 levels in serum were measured by ELISA. (g) LCN2 levels were determined in serum and stool lysate. Data is representative of at least three independent experiments, of which one is shown here (n=2-5 mice). Results are given as mean +/– SEM and significance is determined by two-way ANOVA (b) corrected for multiple testing by the Dunnett's method or ordinary one-way ANOVA corrected for multiple comparisons by the Bonferroni's method (*$p<0.05$, **$p<0.01$, ***$p<0.001$). Significance is calculated in comparison to WT/H_2O (c/e/f/g). These experiments were performed together L.Schlautmann.

Paraffin sections of distal colon tissue of DSS-treated mice and WT mice just receiving water were stained with hematoxylin and eosin to visualize tissue morphology (Fig.5.6d). Colitis severity and tissue destruction was histologically scored as described in the methods section (4.2.5). All DSS-treated mice showed significantly elevated histological scores compared to untreated mice, but no differences between the different genotypes could be observed (Fig.5.6e).

The cytokine profile in IBD is very complex and might have an important influence on disease severity. The cytokine IL-6, which is among others macrophage derived, as well as the chemokine CXCL1 have been shown to be highly upregulated in serum of DSS-treated mice[162]. IL-6 and CXCL1 were upregulated in DSS-treated mice, but there was no difference between WT, $AhRR^{E/E}$ and $AhRR^{fl/fl}$LysM-Cre mice (Fig.5.6f). Recent reports identified the small, mainly neutrophil-secreted protein Lipocalin-2 (LCN2) as a non-invasive biomarker for intestinal inflammation[163]. Concordantly, LCN2 was highly upregulated in serum and stool of mice treated with DSS (Fig.5.6g). About 1000-fold higher levels of LCN2 in serum and stool samples were detected compared to WT mice just receiving water, however, LCN2 levels in WT, $AhRR^{E/E}$ and $AhRR^{fl/fl}$LysM-Cre mice treated with DSS were not different.

In summary, AhRR-knockout mice showed signs of enhanced colitis susceptibility, indicated by increased weight loss. $AhRR^{fl/fl}$LysM-Cre mice did not show elevated susceptibility, as weight loss was similar to WT mice over the course of the experiment. Interestingly, apart from elevated weight loss, $AhRR^{E/E}$ mice did not show any signs of stronger disease development with regard to the examined parameters in this experimental setup.

Overall, the data shown in section 5.1 indicated that the mechanism of disease in $AhRR^{E/E}$ mice is different from $AhR^{-/-}$ mice. $AhRR^{E/E}$ showed no defect in intestinal ILC3s and only minor differences with regard to IEL frequency[149]. Instead, these mice seemed to have more IL-17-producing T cells under inflammatory conditions while the frequency of IFNγ producing cells was reduced. Further, AhRR-knockout mice showed elevated colonic IL-1β levels under homeostatic conditions and only minor differences in myeloid cell frequency. It was moreover shown that the cell type-specific deletion of the AhRR in $LysM^{+}$ cells was not sufficient to recapitulate the colitis susceptibility of the full AhRR knockout.

5.2 Dietary AhR ligands drive AhRR expression in immune cells of barrier organs

The AhRR is a protein with AhR suppressing functions that is strongly induced by the AhR as part of a negative feedback regulation mechanism[105,164]. AhR activation and target gene induction is dependent on binding of various AhR ligands, such as xenobiotics, environmental toxins, endogenous ligands derived from the tryptophan metabolism, bacterial pigments, or diet-derived substances[118,123,165]. Previous studies revealed a cell-type specific expression of the AhRR that is basically absent in AhR-deficient animals[128]. Hence, measurement of AhRR expression can be used to detect AhR activation. However, it is still elusive, which type of AhR ligands drives the high expression of the AhRR in barrier organs under physiological conditions.

5.2.1 Oral antibiotic treatment does not influence intestinal AhRR expression

Intestinal commensals or their metabolites are potential AhR ligands. In order to investigate the influence of these bacterial components on AhRR expression following AhR activation, $AhRR^{E/+}$ mice were treated with antibiotic in the drinking water for 6 weeks. Oral antibiotic treatment reduces the commensal load and also changes the composition of intestinal microbes[166,167]. This was confirmed, since no bacteria could be cultured from fecal samples in thioglycolate culture medium or on Columbia blood agar plates (data not shown). T cells and myeloid cells were isolated from the colonic and small intestinal lamina propria and from the mLNs. Frequencies of AhRR-expressing cells were determined by flow cytometry as described previously (Fig.5.2/5.4). Furthermore, the AhRR mean fluorescent intensity (MFI) was determined for the analyzed immune cell subsets. Similar frequencies of $CD4^+$ T cells, $CD8^+$ T cells, DCs and macrophages expressed the AhRR in the SI (Fig.5.7a), colon (Fig.5.7b) and mLNs (Fig.5.7c) of antibiotic-treated mice and control mice receiving water only. Only the DC frequency in the colon was slightly increased in antibiotic-treated mice (Fig.5.7b). Likewise, no differences in MFI of the AhRR in intestinal T cells, DCs and macrophages could be observed comparing antibiotic-treated and control mice in one representative experiment (Fig.5.7a/b/c).

Histological analysis of DAPI-stained cryosections from the colon and mLNs of $AhRR^{E/+}$ mice treated with antibiotic revealed high numbers of AhRR expressing cells in these organs (Fig.5.7d/e). In line with the data obtained from flow cytometry, no differences in comparison to untreated mice were apparent.

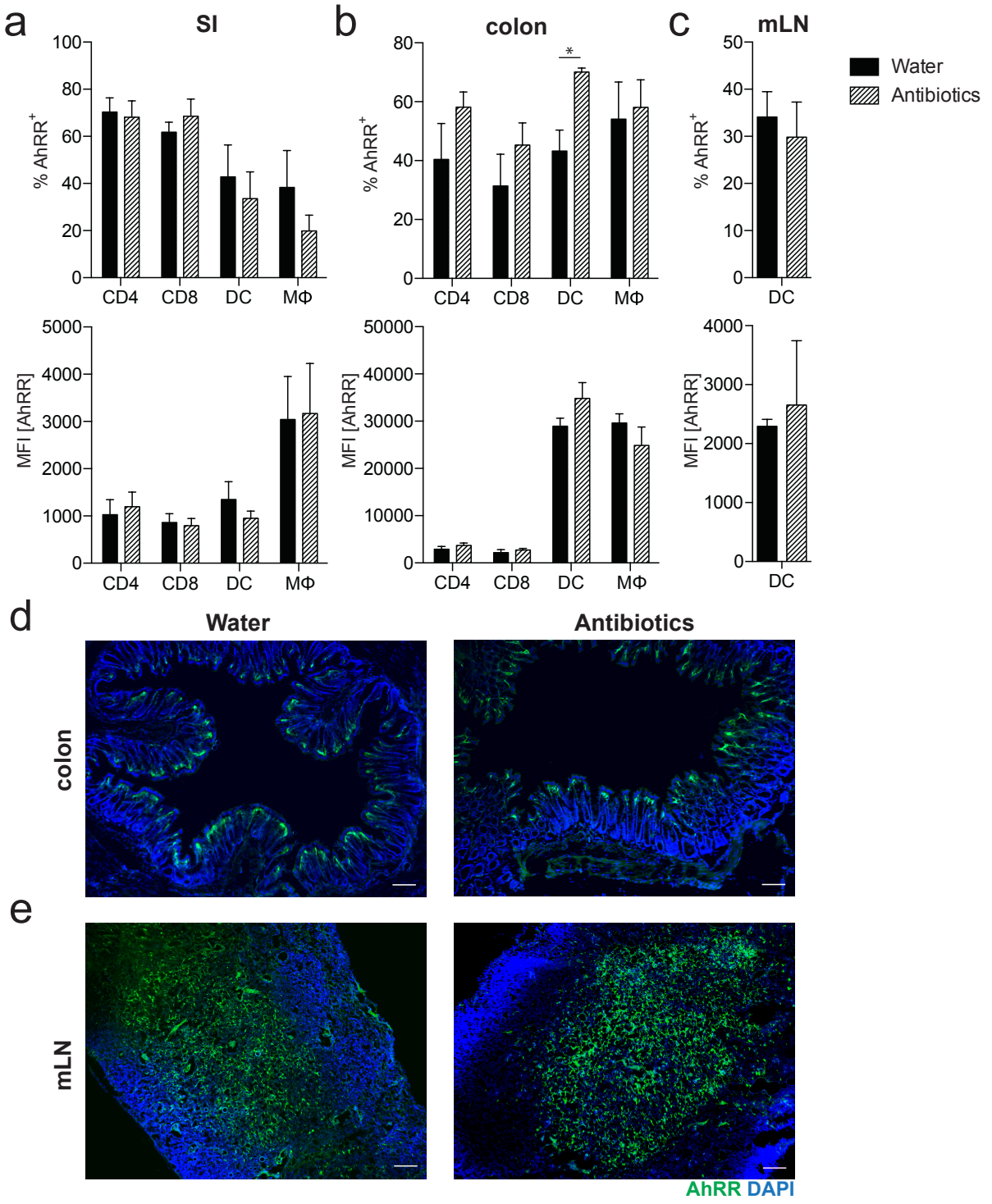

Figure 5.7: Antibiotic treatment does not influence AhRR expression in intestinal tissue
$CD4^+$ T cells, $CD8^+$ T cells, DC and MΦ were analyzed for frequency of $AhRR^+$ cells and AhRR MFI in SI (a) and colon (b) of $AhRR^{E/+}$ mice after four weeks of antibiotic treatment (Ampicillin 1g/l, Vancomycin 500mg/l, Ciprofloxacin 200mg/l, Imipenem 250mg/l, Metronidazole 1g/l in drinking water). (c) Frequency of $AhRR^+$ DCs and mean AhRR expression in mLN of antibiotic-treated and control mice. AhRR expression was analyzed by histology in colon (d) and mLN (e) [scale bar = 100µm]. Data is pooled from two independent experiments (n=4 mice) or exemplary shown for one of at least two independent experiments (MFI). Results are shown as mean +/– SEM and significance was determined by two-tailed student's t-test corrected for multiple comparisons by the Holm-Sidak method (*$p<0.05$).

Overall, antibiotic treatment and the resultant changes of the intestinal commensals did not alter AhRR expression indicating that microbiota-derived AhR ligands did not influence AhRR expression in immune cells of the intestine.

5.2.2 Food-derived AhR ligands enhance AhR target gene expression in the intestine

Small lipophilic components in the diet can also be responsible for AhR activation in the intestine. The phytochemical indole-3-carbinol (I3C) has been shown to increase the expression of AhR target genes in the gastrointestinal tract[165]. Further, dietary tryptophan and tryptophan metabolites can be converted into the high affinity AhR ligand 6-formylindolo[3,2-b]carbazole (FICZ), which has been shown to activate the AhR transcriptional program[168].

In order to investigate the role of diet-derived AhR ligands for AhR target gene expression and especially for AhRR expression, $AhRR^{E/+}$ mice were fed with different diets either containing or lacking AhR ligands. Therefore, mice were fed with a purified diet (AIN-93G) that is formulated with a refined and restricted set of ingredients such as isolated proteins, sugar, vegetable oil and crude cellulose. Due to the lack of plant derived phytochemicals activating the AhR, this diet was termed ligand-reduced diet (LRD). The latter was additionally supplemented with the single AhR ligand precursor I3C, which is converted to the high affinity AhR ligands ICZ and DIM by the stomach acid, and fed to a second group of mice. Control mice received normal chow, a grain-based diet containing plant-derived phytochemicals and therefore potent AhR activators.

Immune cells of the gastrointestinal tract were isolated and analyzed for expression of the AhRR by flow cytometry. Previous work in our group already showed[128,149] that intestinal T cells, DCs and macrophages of mice fed with normal chow comprise a large proportion of AhRR-positive cells (Fig.5.8a). The highest frequencies of AhRR expressing cells could be detected in the lamina propria of the SI and colon. Further, DCs in the mLNs showed a high frequency of $AhRR^{+}$ cells, while lower frequencies were observed in the PPs. Interestingly, mice that were fed with LRD for four weeks showed significantly lower frequencies of AhRR-positive immune cells in all organs. This effect could be observed in $CD4^{+}$ and $CD8^{+}$ T cells, DCs and macrophages. However, the reduction of $AhRR^{+}$ cells was strongest for T cells in the colon and DCs in the mLNs (Fig.5.8a). Analysis of the MFI of the AhRR in the intestinal immune cell subsets revealed a clear reduction of AhRR expression in T cells, DCs and macrophages in all analyzed intestinal organs (Fig.5.8b). This reduction in AhRR expression was strongest in DCs of the colon and mLNs and macrophages of the colon

whereas decrease of AhRR expression was lower in $CD4^+$ and $CD8^+$ T cells, except for $CD8^+$ T cells in the PPs.

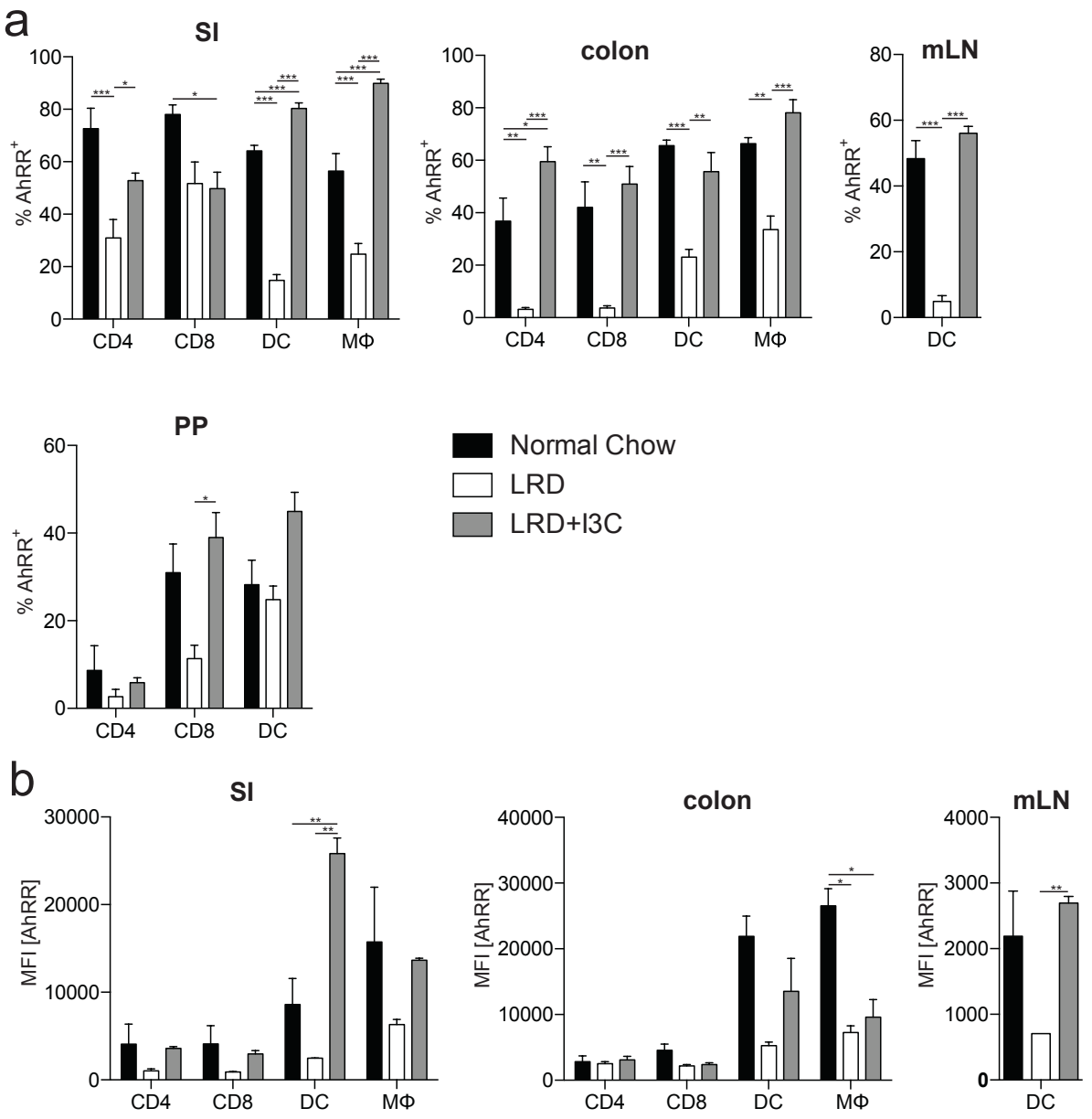

Figure 5.8: Dietary AhR ligands drive expression of AhRR in intestinal immune cells

$AhRR^{E/+}$ mice were fed for four weeks from weaning onwards with normal chow, AhR ligand reduced diet (LRD) or LRD supplemented with indole-3-carbinol (LRD+I3C)(2g/kg). (a) Frequencies of AhRR expressing $CD4^+$ T cells, $CD8^+$ T cells, DCs and MΦ were determined in the lamina propria of SI and colon, in the PPs and in the mLNs. (b) AhRR MFI is shown for the same organs and cells as in (a). Data is pooled from at least two independent experiments (a) or shown from one representative experiment (b) (n=2-9 mice). Results are shown as mean +/– SEM and significance was determined by one-way ANOVA corrected for multiple comparisons by the Bonferroni's method (*p<0.05, **p<0.01, ***p<0.001).

Interestingly, AhRR$^{E/+}$ mice, which were fed with LRD supplemented with 2g/kg I3C (LRD+I3C), showed similar frequencies of AhRR-expressing immune cells as mice fed with normal chow (Fig.5.8a). DCs and macrophages in the SI lamina propria, CD8$^+$ T cells in the PPs and CD4$^+$ T cells in the colonic lamina propria showed even higher numbers of AhRR-expressing cells as observed in normal chow fed animals. Only frequencies of CD8$^+$ T cells in the SI were not restored by I3C supplementation. The MFI of the AhRR was similar in mice receiving the I3C supplemented diet compare to normal chow fed mice (Fig.5.8b). AhRR expression was even higher in DCs of the small intestinal lamina propria and mLNs, while slightly lower MFI values could be measured for DCs and macrophages in the colon.

As a second AhR target gene, expression of *cyp1a1* was analyzed by qPCR in the SI of WT and AhRR$^{E/E}$ mice either fed with LRD or LRD+I3C (Fig.5.9). *cyp1a1* expression was low in mice fed with LRD, but was about 100fold upregulated in mice fed with LRD+I3C. This effect could be observed in WT animals as well as in mice deficient for AhRR (Fig.5.9).

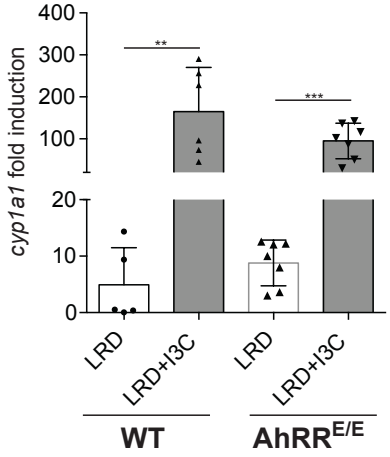

Figure 5.9: Dietary AhR ligands drive expression of c*yp1a1* in intestinal tissue
Relative expression of *cyp1a1* was determined by RT-PCR in SI tissue samples of WT and AhRR$^{E/E}$ mice fed with LRD or LRD+I3C for four weeks after weaning. Data is pooled from at least two independent experiments (n=2-9 mice). Results are shown as mean +/– SEM and significance was determined by two-tailed student's t-test (**p<0.01, ***p<0.001).

In summary, these experiments revealed that AhRR expression in gastrointestinal immune cells is highly dependent on dietary AhR ligands. Noteworthy, AhRR expression can be driven by a variety of ligands contained in the normal chow or by one discrete ligand precursor in LRD+I3C. Further, this effect could also be confirmed for a second AhR target gene *cyp1a1*, encoding a member of the cytochrome P450 superfamily of enzymes.

5.2.3 AhRR expression of dermal and epidermal immune cells is influenced by diet-derived AhR ligands

In addition to the gut, AhR activation by AhR ligands is also of great importance for homeostasis of skin cells and skin immunity[95]. Keratinocytes, fibroblasts, melanocytes, endothelial cells and immune cells like Langerhans cells and γδ T cells show expression of the AhR[169]. Recent experiments in our institute highlighted that especially Langerhans cells and γδ T cells of the epidermis and dermis show high expression of the AhRR (unpuplished data, P. Jäger). Therefore it was investigated, whether dietary AhR ligands are also capable to influence AhRR expression in the skin.

As shown for the gastrointestinal immune cells, AhRR expression in mice on normal chow diet, LRD and LRD+I3C was investigated. In order to test the influence of dietary AhR ligands on AhRR expression in the skin, leukocytes were isolated from the epidermis and dermis of $AhRR^{E/+}$ mice separately and analyzed by flow cytometry. Leukocytes were gated for single, $CD45^{+}$, living cells (Fig.5.10a). γδ T cells in the epidermis were identified by high expression of the γδ T cell receptor (TCR), while Langerhans cells showed expression of MHCII and CD207 (langerin) (Fig.5.10b). Dermal γδ T cells were identified similar to the epidermis by high expression of the γδ TCR (Fig.5.10c). Epidermal and dermal immune cells were subsequently analyzed for the frequency of AhRR expressing cells (Fig.5.10d) as well as for the MFI of the AhRR.

Analysis of AhRR expression on γδ T cells in epidermis and dermis showed that independent of the diet between 95% and 100% of these cells expressed the AhRR (Fig.5.10e). The MFI of the AhRR in γδ T cells was high in mice fed with normal chow, but was significantly reduced in mice fed with LRD for four weeks, although a residual AhRR expression could still be detected. In mice fed with LRD+I3C the MFI of the AhRR in γδ T cells was stronger than in mice fed with LRD and even significantly increased compared to control mice receiving normal chow (Fig.5.10f). This effect was similarly observed in epidermis and dermis of $AhRR^{E/+}$ mice.

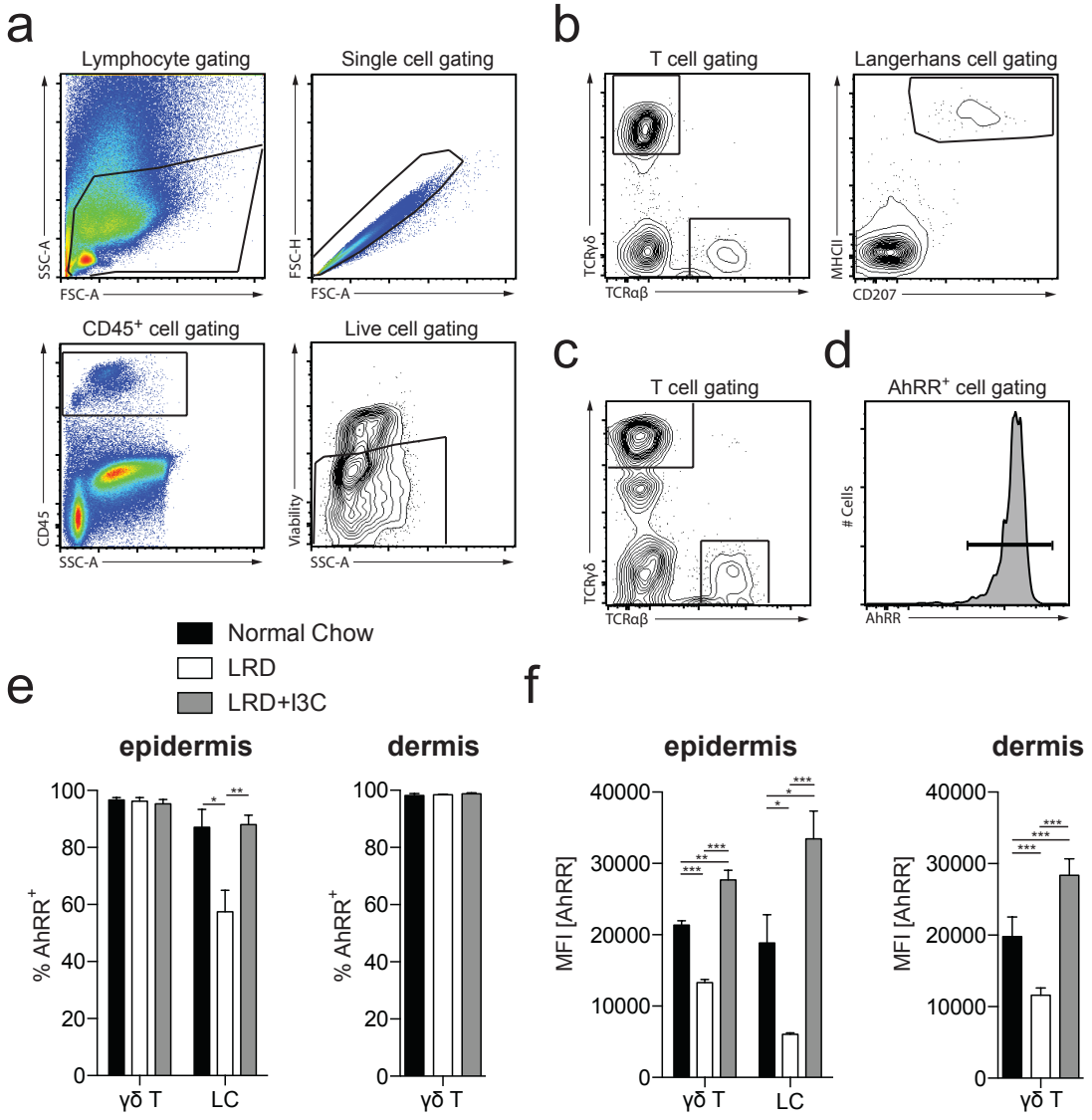

Figure 5.10: AhRR expression in the skin is influenced by dietary AhR ligands
AhRR$^{E/+}$ mice were fed with different diets (Normal chow, LRD, LRD+I3C) for four weeks from weaning onwards. Afterwards, single cell suspensions of epidermis and dermis were produced and analyzed for AhRR-expressing cells by flow cytometry. (a) Cells were gated for single CD45$^+$ and living cells. In the epidermis (b) γδ T cells were distinguished from conventional T cells by expression of the γδ T cell receptor (TCR). LCs were identified by expression of MHCII and CD206 (langerin). (c) Dermal γδ T cells were identified similarly by high expression of the γδ TCR. (d) AhRR-expressing cells were identified by expression of the EGFP reporter, exemplary shown for γδ T cells of the epidermis. (e) Frequency of AhRR-expressing epidermal γδ T cells and Langerhans cells as well as dermal γδ T cells was quantified. (f) Mean fluorescent intensity (MFI) of the AhRR in the analyzed cell subsets was determined. Data is pooled from two independent experiments (n=3-6 mice). Results are shown as mean +/– SEM and significance was determined by one-way ANOVA corrected for multiple comparisons by the Bonferroni's method (*p<0.05, **p<0.01, ***p<0.001).

About 90% of the Langerhans cells in normal chow fed mice were found to be AhRR-positive. The frequency was reduced to about 60% in LRD fed mice and restored to 90% in mice receiving LRD+I3C (Fig.5.10e). Analysis of the AhRR MFI on Langerhans cells

revealed reduced AhRR expression under the influence of LRD and higher levels when feeding LRD+I3C compared to normal chow fed control mice (Fig.5.10f).

Overall these experiments revealed that dietary AhR ligands also influence AhR target gene expression in immune cells of the skin, here demonstrated for the AhRR. However, changes in frequency and MFI were not as pronounced as in the gastrointestinal tract (Fig.5.8), suggesting that other sources of AhR ligands, next to the diet, drive AhR target gene expression in the skin.

5.2.4 LRD, high fat diet and matched control diet reduce AhRR expression in lamina propria lymphocytes, mLN DCs and IELs

Experimental and purified diets for laboratory rodents are extensively used to study all kinds of topics. Especially metabolic studies using high fat diets or western diets have gained interest over the last years, addressing common problems of the western society. Similar to the LRD these purified diets are composed of isolated proteins, carbohydrates, fats and fiber. Therefore, it is of common interest to investigate if high fat diet (HFD) and a matched control diet with reduced fat content (HFD ctrl) are similarly reduced in the content of AhR ligands, as shown for AIN 93G, and hence will alter AhR/AhRR signaling in the body.

To answer the question whether these diets also lead to reduced AhR activation, immune cells of the intestine of $AhRR^{E/+}$ mice were investigated for their frequency of $AhRR^{+}$ cells and, additionally, the MFI of AhRR. Experiments were performed after feeding HFD and HFD ctrl for four weeks in direct comparison to the LRD and LRD+I3C used in the experiments of sections 5.2.2 and 5.2.3 (Fig.5.11). First, immune cells of the lamina propria were investigated, as previous experiments showed a huge influence of LRD on these cells (Fig.5.8). Overall the immune cells (T cells, DCs, macrophages) of SI and colon were similarly influenced by LRD and LRD+I3C as observed before. Frequency of $AhRR^{+}$ cells and the MFI of AhRR were reduced under influence of LRD in SI (Fig.5.11a) and colon (Fig.5.11b). Furthermore, a strong enhancement of the expression of AhRR in LRD+I3C fed mice could be demonstrated here (Fig.5.11). However, frequencies of $CD4^{+}$ and $CD8^{+}$ T cells expressing the AhRR in the SI were similar in mice on normal chow and LRD. $CD4^{+}$ and $CD8^{+}$ T cells previously comprised 70 to 80% $AhRR^{+}$ cells in normal chow fed mice, whereas only 10 to 20% expressed the AhRR after feeding LRD (Fig.5.11/Fig.5.8). While the proportion of $AhRR^{+}$ cells was similar in LRD fed mice in these experiments, normal chow fed mice showed clearly reduced frequency of $AhRR^{+}$ immune cells as previously observed.

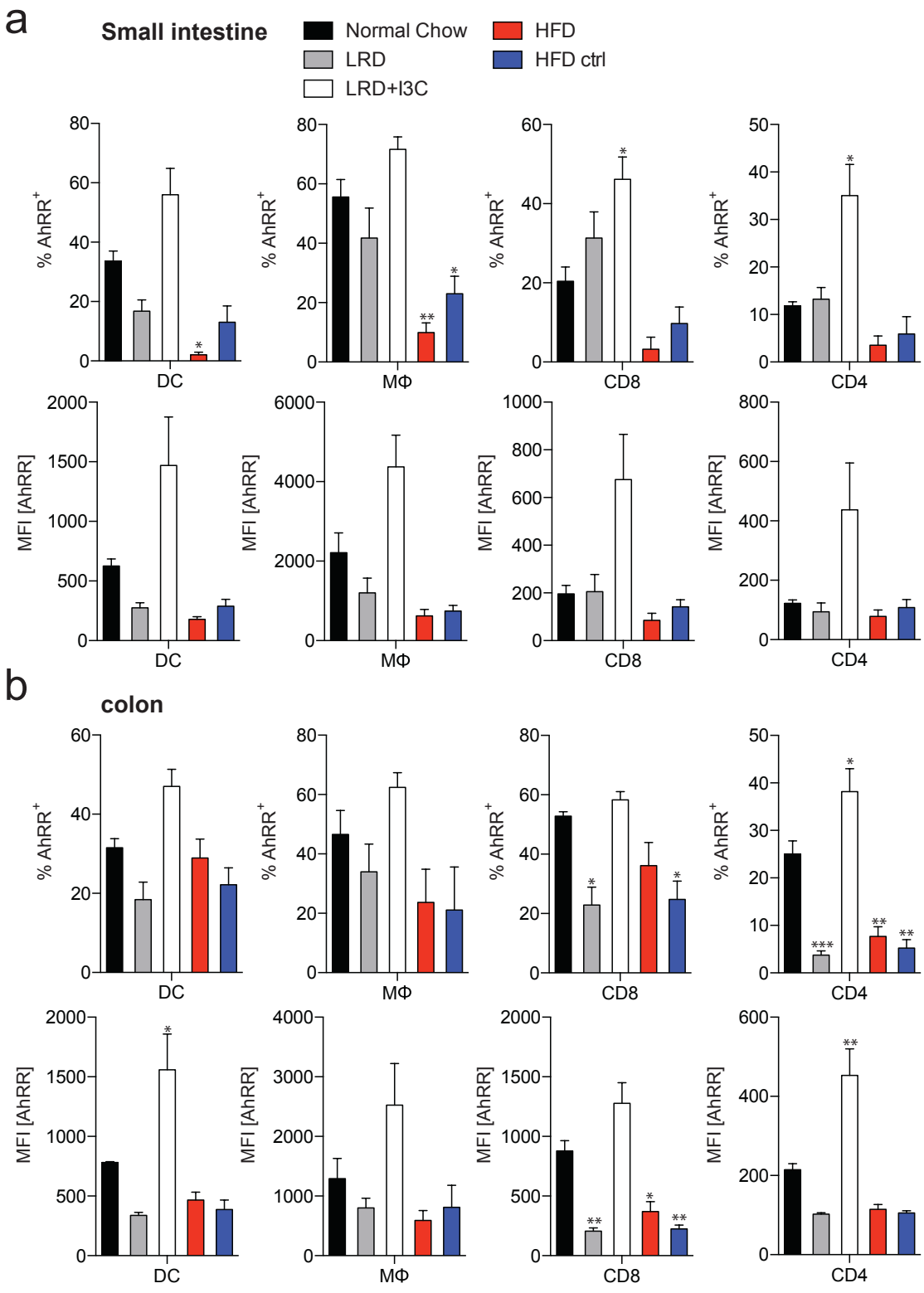

Figure 5.11: HFD and HFD ctrl reduce AhRR expression in immune cells of the lamina propria
AhRR$^{E/+}$ mice were kept under different dietary conditions for four weeks. (a)/(b) DCs, MΦ, CD8$^+$ T cells and CD4$^+$ T cells were isolated from the lamina propria of SI and colon. Cells were analyzed for the frequency of AhRR$^+$ cells and AhRR MFI via flow cytometry. Data is pooled from two independent experiments (n=3-5). Results are shown as mean +/– SEM and significance was analyzed by one-way ANOVA corrected for multiple comparisons by the Bonferroni's method (*p<0.05, **p<0.01, ***p<0.001). LRD=ligand reduced diet, I3C=Indole-3-carbinol, HFD=high fat diet, HFD ctrl=HFD control, NC=normal chow

However, inductive effects of AhRR expression in LRD+I3C fed mice were as strong as observed before. Expression intensity (MFI) of the AhRR in LRD+I3C fed mice was even higher than in normal chow fed mice. Mice receiving HFD or HFD ctrl showed reduced frequencies of AhRR$^+$ cells in all cell types analyzed and lower MFI of the AhRR compared to normal chow and LRD+I3C fed mice (Fig.5.11), indicating clearly reduced AhR ligand concentration in these diets.

To check in more detail, whether HFD and HFD ctrl do not only influence AhRR expression in the lamina propria but also in the mLNs, DCs from mLNs were isolated and investigated for their AhRR expression in dependence of the different dietary conditions. In line with the observations made in the lamina propria, mLNs of mice fed with LRD, HFD and HFD ctrl had a significantly reduced frequency of AhRR$^+$ DCs. DCs of mLNs of normal chow and LRD+I3C fed mice both displayed high frequencies of AhRR$^+$ cells. The modification of AhRR expression by different diets was also reflected in the MFI indicating a reduction in the intensity of AhRR/EGFP expression per cell (Fig.5.12).

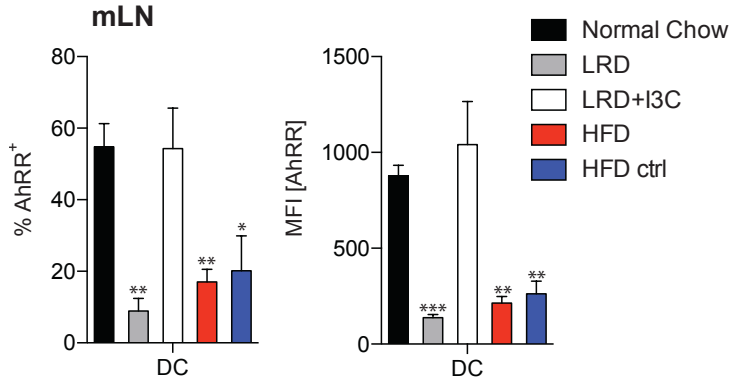

Figure 5.12: AhRR expression in DCs of the mesenteric lymph nodes (mLNs) is reduced in HFD and HFD ctrl fed mice
AhRR$^{E/+}$ mice were kept under different dietary conditions for four weeks. DCs were isolated from the mLNs and analyzed for the frequency of AhRR-expressing cells and for the mean fluorescent intensity (MFI). Data is pooled from two independent experiments (n=3-5). Results are shown as mean +/– SEM and significance was analyzed by one-way ANOVA corrected for multiple comparisons by the Bonferroni's method (*p<0.05, **p<0.01, ***p<0.001). LRD=ligand reduced diet, I3C=Indole-3-carbinol, HFD=high fat diet, HFD ctrl=HFD control, NC=normal chow

Besides lamina propria lymphocytes that did not show as strong differences in AhRR expression as seen in the previous experiments (Fig.5.8), AhRR expression of intraepithelial lymphocytes (IELs) was investigated. These cells are residing between the intestinal epithelial cells and are therefore the first immune cells in the gastrointestinal tract confronted with luminal antigens, including dietary products. Cells were isolated as described in the methods section and analyzed by flow cytometry. After setting a lymphocyte gate, CD45$^+$ cells were

analyzed for viability. Different IEL subsets were identified by the expression of either the TCRγ/δ or the TCRβ chain. Both populations were subsequently divided into CD8αα- and CD8αβ-positive cells resulting in four main IEL populations that were further analyzed for proportion of AhRR$^+$ cells as well as for the MFI of the AhRR (Fig.5.13).

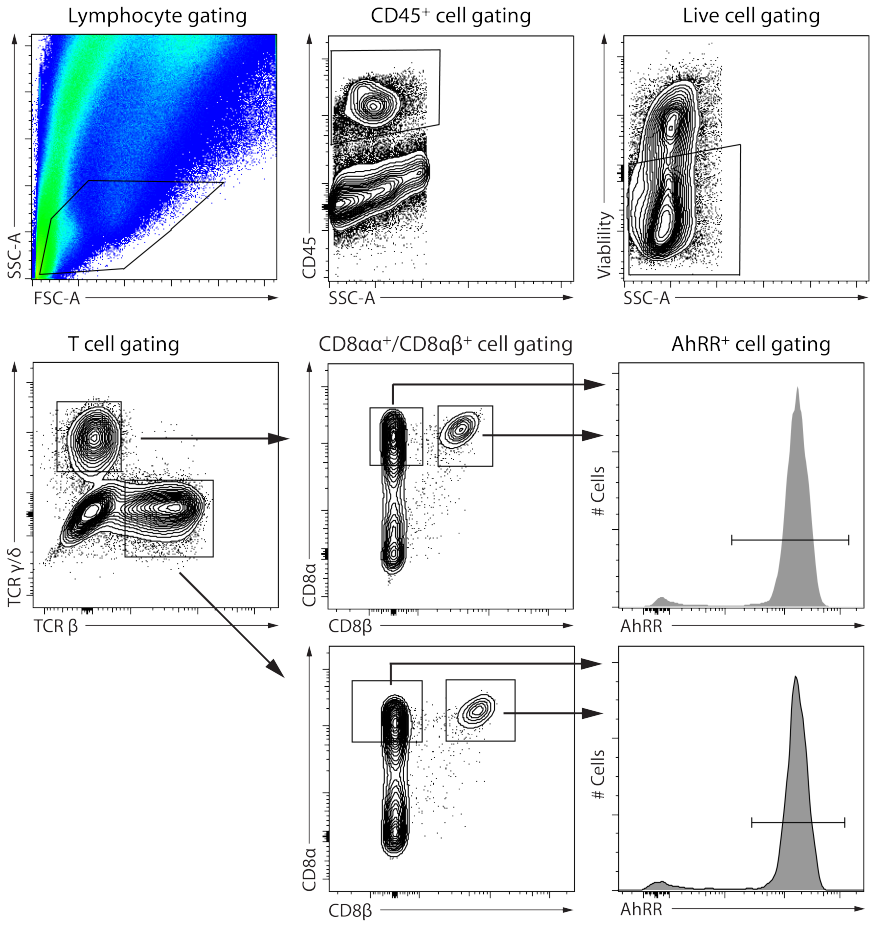

Figure 5.13: Gating strategy for intraepithelial lymphocytes (IELs)
Leukocytes were gated in the FSC/SSC diagram. CD45-positive, living cells were divided into TCRγδ- or TCRβ-positive T cells. Each population was afterwards divided based on expression of CD8 (CD8αα$^+$/CD8αβ$^+$). The four IEL subsets (TCRγδ$^+$CD8αα$^+$, TCRγδ$^+$CD8αβ$^+$, TCRβ$^+$CD8αα$^+$, TCRβ$^+$CD8αβ$^+$) were analyzed for their expression of the AhRR, here shown exemplary for the two CD8αα$^+$ IEL subsets.

IELs were isolated from the SI and colon. As already shown in previous studies[128], all IELs posses a high proportion of AhRR expressing cells in the SI and colon (Fig.5.14). TCRβ- and TCRγδ-expressing subsets contained about 80% to 90% of AhRR$^+$ cells in the SI (Fig.5.14a, top panel) and between 40% and 70% in the colon (Fig.5.14b, top panel).

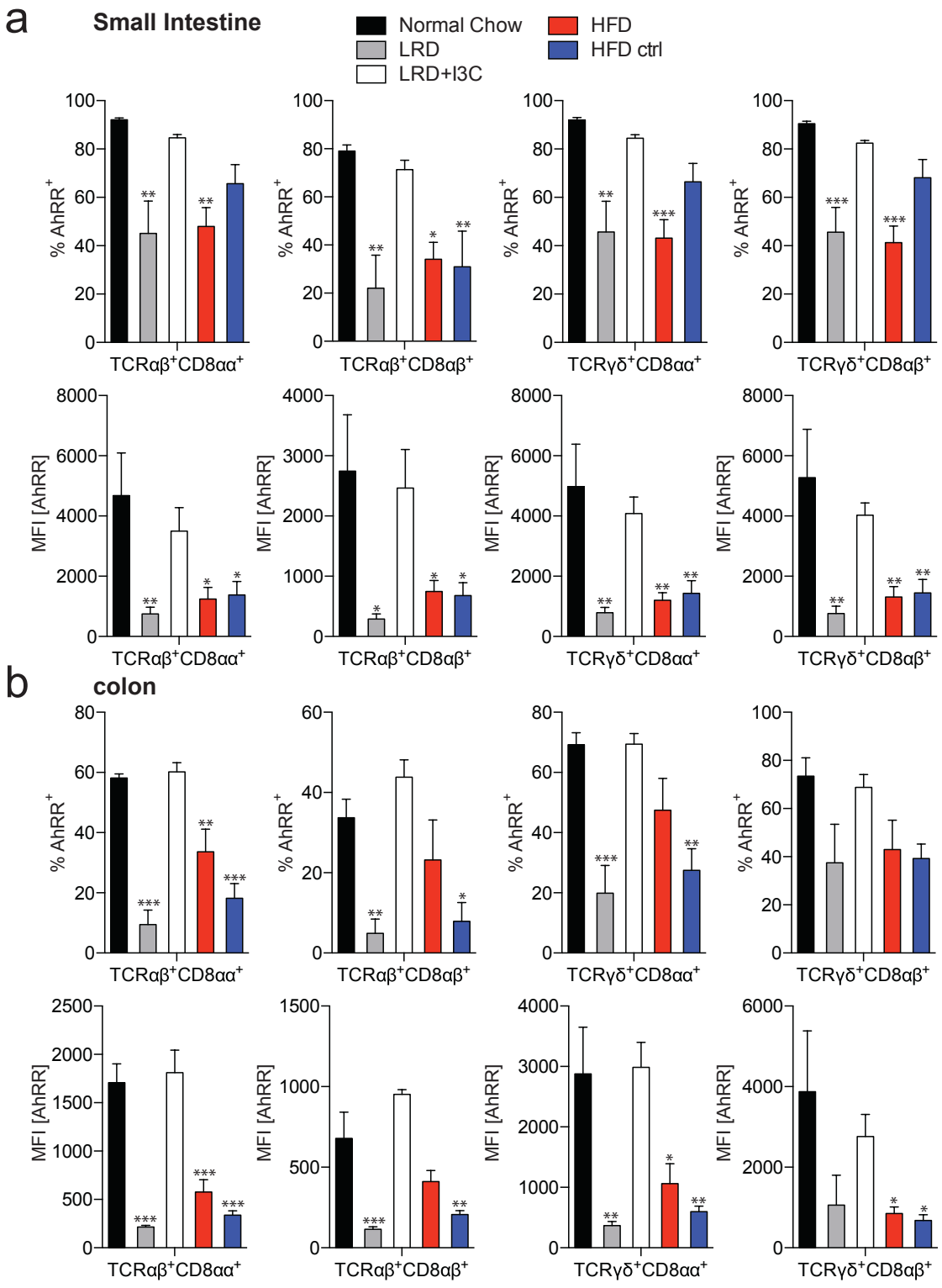

Figure 5.14: AhRR expression in intraepithelial lymphocytes (IELs) is reduced in HFD and HFD ctrl fed mice

AhRR$^{E/+}$ mice were kept under different dietary conditions for four weeks. IELs were isolated from the SI (a) and the colon (b) and analyzed by flow cytometry for AhRR expressing cells as well as the MFI of AhRR (gated according to Fig.5.13). Data is pooled from two independent experiments (n=5). Results are shown as mean +/– SEM and significance was analyzed by one-way ANOVA corrected for multiple comparisons by the Bonferroni's method (*p<0.05, **p<0.01, ***p<0.001). LRD=ligand reduced diet, I3C=Indole-3-carbinol, HFD=high fat diet, HFD ctrl=HFD control, NC=normal chow

As already observed in previous experiments for lamina propria and mLNs, mice fed with LRD showed severely reduced frequencies of $AhRR^+$ cells, whereas percentages of $AhRR^+$ cells were comparable high between mice on normal chow and LRD+I3C. Interestingly, frequencies of $AhRR^+$ cells in $AhRR^{E/+}$ animals fed with HFD or HFD ctrl, were similarly reduced as in mice on LRD. In line, also the intensity of AhRR expression (MFI) was similarly reduced in IELs of mice fed the LRD, HFD or HFD ctrl (Fig.5.14a/b, lower panel). Further, IELs from normal chow or LRD+I3C fed animals showed a consistently high MFI for AhRR, which was different from the unusual low AhRR expression of lamina propria immune cells from normal chow fed mice (Fig.5.11). These observations could be additionally made in both SI and colon.

In summary, feeding of both, HFD and HFD ctrl leads to reduced frequencies of $AhRR^+$ immune cells in the lamina propria, mLNs and IELs, indicating that these diets influence AhR signaling *in vivo*. This effect was overall slightly stronger in mLNs and in IELs in comparison to cells of the lamina propria. In line with previous experiments it could be shown that dietary AhR ligands have a profound effect on the MFI of the AhRR in immune cells of the gastrointestinal tract, in addition to reducing the frequency of AhRR expressing cells.

5.2.5 Histological analysis of AhRR expression in colon and skin

In addition to flow cytometric analysis, the influence of the different dietary conditions (NC, LRD, LRD+I3C, HFD, HFD ctrl) on AhRR expression was also investigated histologically. Cryosections of PFA-fixed colon and skin tissue samples were counterstained with DAPI. AhRR-expressing cells were identified by EGFP reporter expression in $AhRR^{E/+}$ mice.

AhRR/EGFP-positive cells could be readily detected in the colon of mice on normal chow and LRD+I3C (Fig.5.15a). However, expression of the EGFP reporter was strongly reduced in mice fed with LRD, HFD or HFD ctrl. In contrast, EGFP-expressing cells were equally detected in the skin of all five groups (Fig.5.15b). A slightly stronger AhRR/EGFP expression was detected in histological skin samples from mice fed with LRD+I3C.

In summary, these experiments illustrated that purified diets are reduced in AhR ligands and therefore lead to reduced expression of AhR target genes, here shown for the AhRR in immune cells of the gastrointestinal tract and skin. These experiments further underlined the crucial role of dietary AhR ligands for AhR target gene expression and suggest that low AhR ligand concentration in HFD and HFD ctrl might have a general influence in studies using these diets.

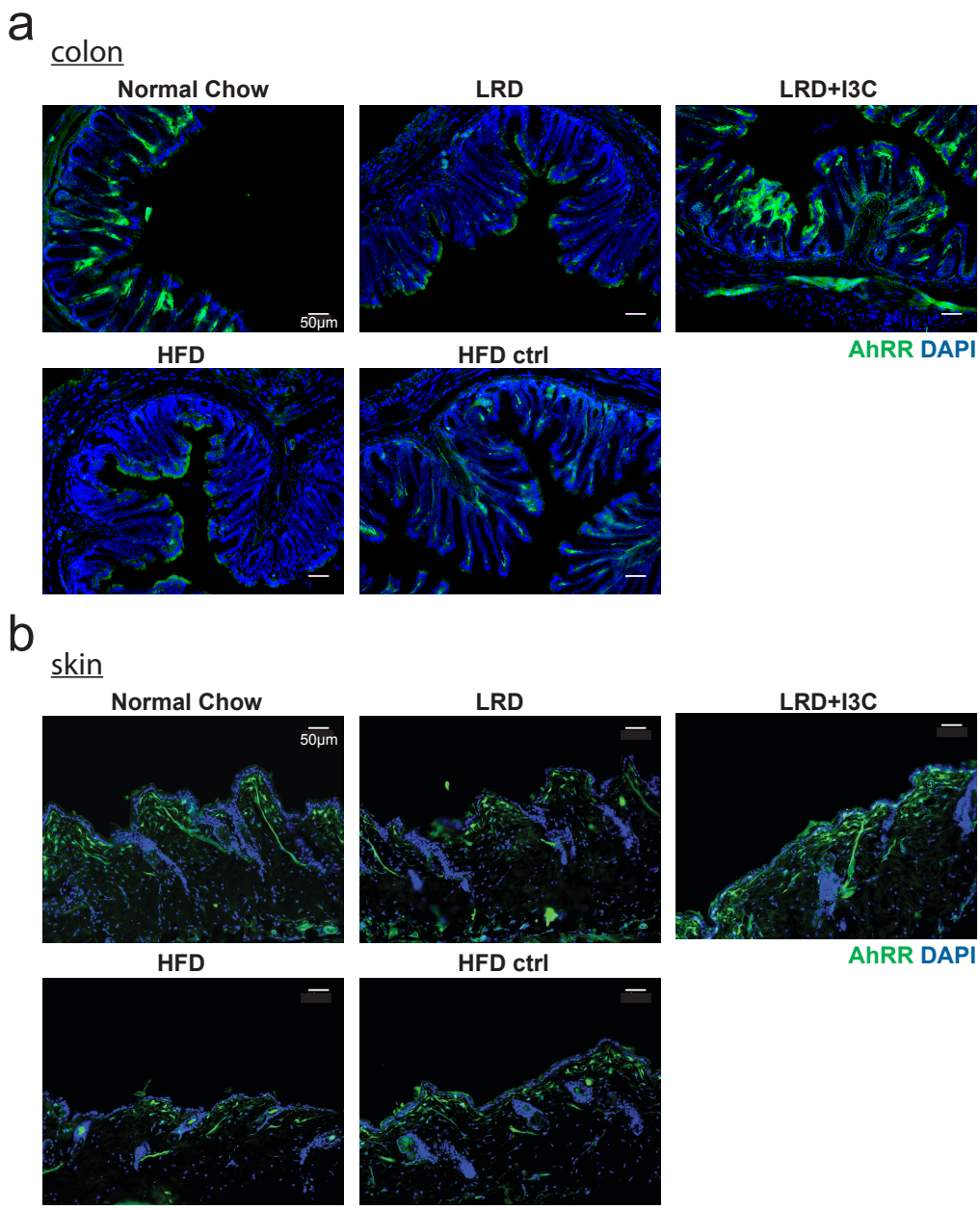

Figure 5.15: Histological analysis of AhRR expression in colon and skin of mice under different dietary conditions

AhRR$^{E/+}$ mice were fed with different diets (NC, LRD, LRD+I3C, HFD, HFD ctrl) for four weeks from weaning onwards. After PFA fixation, cryosections of the colon (a) and the skin (b) were stained with DAPI in addition to the endogenous EGFP reporter. Pictures are representative of at least three different mice from at least two independent experiments. LRD=ligand reduced diet, I3C=Indole-3-carbinol, HFD=high fat diet, HFD ctrl=HFD control, NC=normal chow, DAPI= 4′,6-Diamidin-2-phenylindol

5.2.6 AhR ligand reduced diet leads to higher intestinal permeability and higher susceptibility to DSS-induced colitis

The previous section highlighted that dietary AhR ligands have a profound influence on AhR activation and subsequent target gene expression. It has further been shown that the AhR and its activation is of great importance for functional gut immunity[119]. Another study demonstrated increased susceptibility for DSS colitis as a consequence of a reduction of dietary AhR ligands[121]. In this context, it is obvious to speculate that HFD and HFD ctrl might have similar consequences for the function of the intestinal immune system.

In order to investigate the integrity of the intestinal barrier under the influence of different diets containing or lacking AhR ligands, an intestinal permeability assay was performed. After feeding WT mice and AhRR-deficient mice with one of the five different diets for four weeks, intestinal permeability was assessed by oral application of FITC-dextran and measurement of the amount of FITC-dextran transmitted to the circulation. All mice that received FITC-dextran via oral gavage showed FITC fluorescence in the serum. This fluorescence was higher than background fluorescence in serum of mice that did not receive any FITC-dextran (Fig.5.16a) indicating transmission FITC-Dextran from the gut lumen to the serum. However, only mice that were fed with LRD showed significantly elevated FITC fluorescence compared to normal chow fed mice. Mice on LRD+I3C, HFD or HFD ctrl did not show increased intestinal permeability compared to normal chow fed mice. This observation could be made for WT mice as well as AhRR-knockout mice.

In order to investigate, if lack of dietary AhR ligands possibly influences the intestinal immune system and intestinal barrier under inflammatory conditions, C57BL/6 mice were fed with one of the five experimental diets for four weeks before treating them with 2% DSS in the drinking water for seven days, followed by five days of normal drinking water. Body weight changes over the course of the experiment were monitored in order to evaluate differences in colitis susceptibility. All mice lost weight from day three onwards, however, weight loss of mice on LRD was significantly higher in this initial phase of the colitis (Fig.5.16b). Over the course of the experiment the LRD group continued to lose more weight than the normal chow control group, finally resulting in an earlier exclusion of these animals from the experiment at day six. Mice on normal chow, HFD and LRD+I3C showed similar weight loss during DSS administration, however, the LRD+I3C group did not recover from colitis after changing to normal drinking water. These mice were consequently removed from the experiment at day ten.

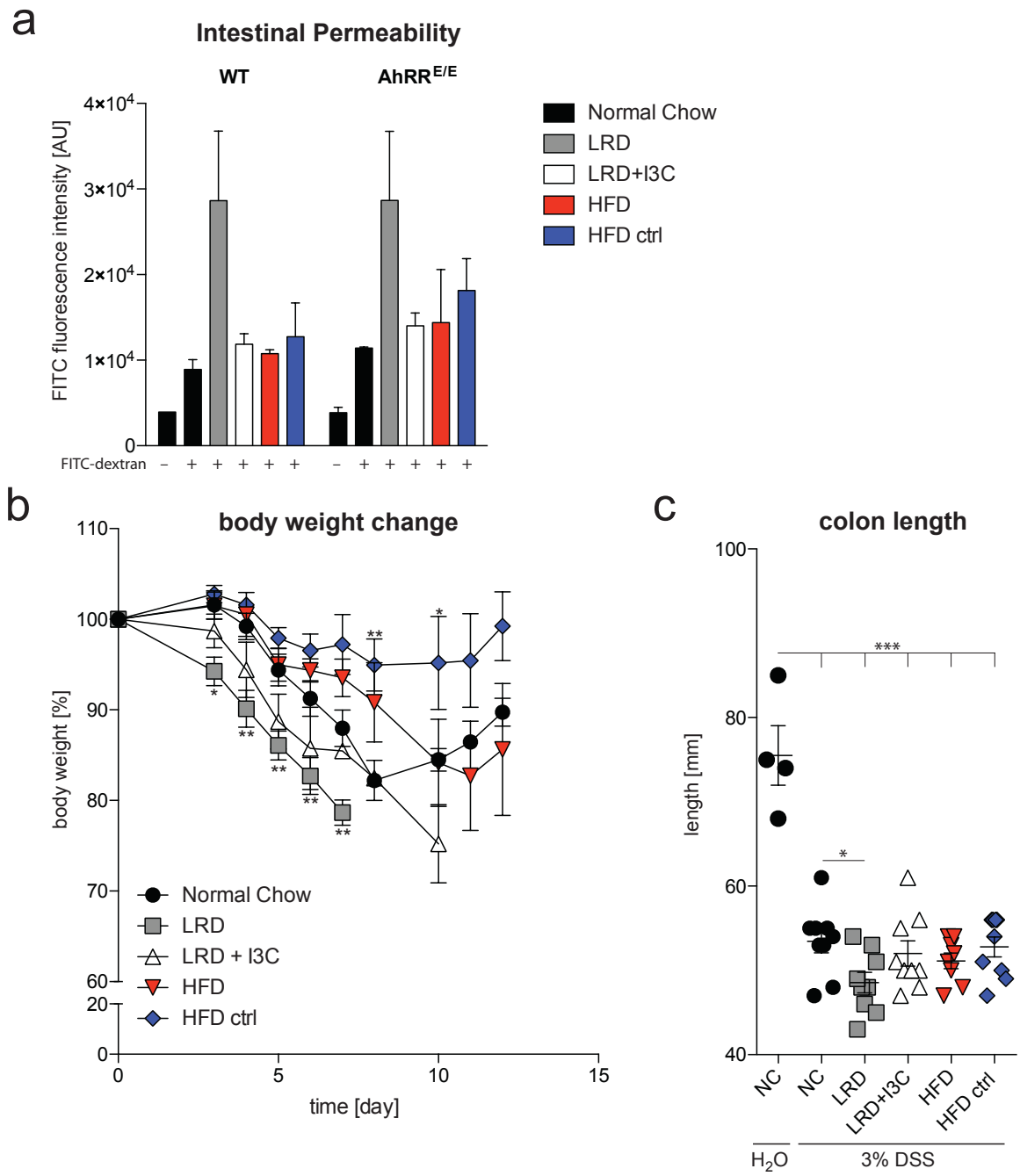

Figure 5.16: Dietary AhR ligands influence the intestinal barrier integrity and susceptibility to DSS-induced colitis

C57BL/6 and AhRR$^{E/E}$ mice were fed with different diets (NC, LRD, LRD+I3C, HFD, HFD ctrl) for four weeks. (a) Mice were fasted for four hours, orally gavaged with 600mg/kg FITC-dextran and four hours later FITC fluorescence in the serum was determined. (b) C57BL/6 mice were fed with different diets for four weeks and afterwards treated with 2% Dextran sodium sulfate (DSS) via the drinking water for seven days, followed by five days normal drinking water. Body weight was monitored over the course of the experiment. (c) C57BL/6 mice were treated for five days with 3% DSS and colon length was compared to WT mice just receiving water. Data is pooled from two independent experiments (n=2-9). Results are shown as mean +/– SEM and significance was analyzed by one-way ANOVA corrected for multiple comparisons by the Bonferroni's method (a, c) or by ordinary two-way ANOVA corrected for multiple comparisons by the Dunneet's method (b) (*p<0.05, **p<0.01, ***p<0.001). LRD=ligand reduced diet, I3C=Indole-3-carbinol, HFD=high fat diet, HFD ctrl=HFD control NC=normal chow

Interestingly, mice that were fed with HFD ctrl showed just mild colitis symptoms, indicated by minimal weight loss. In addition these mice showed complete recovery of body weight by the end of the experiment.

In order to further investigate, if besides changes in body weight and overall appearance during colitis, often referred to as disease activity index (DAI) (not shown), other differences in colitis susceptibility can be observed between mice fed the different diets, animals were treated with 3% DSS for five days in order to establish a severe inflammation. Colon length was measured at day five and compared to control animals that did not receive DSS. All DSS-treated mice showed highly significant differences in colon length compared to untreated control mice. Only LRD fed mice exhibited significant shorter colons compared to DSS-treated normal chow fed animals (Fig.5.16c), whereas this was not observed for the groups fed with LRD+I3C, HFD, or HFD ctrl.

In summary, these experiments confirmed previous studies indicating intestinal barrier defects and increased colitis susceptibility of mice fed with diet poor in AhR ligands. Intriguingly, neither a barrier defect nor increased colitis pathology was observed for mice fed with HFD or HFD ctrl, although previous experiments identified these diets as poorly activating the AhR. Interestingly, HFD ctrl even conferred a notable protection from DSS colitis.

5.2.7 Reduced dietary AhR ligands lead to altered cytokine production in DSS colitis

In order to understand the mechanisms responsible for the different disease outcome in mice fed with distinct diets, further analyses were conducted. To investigate the inflammatory response in colitis, myeloperoxidase (MPO) activity and fecal or serum Lipocalin-2 (LCN2) content were determined as surrogate markers[163,170]. Further, it was shown that disease severity is correlated with higher levels of proinflammatory cytokines in the serum, such as IL-6 or Il-1β [162].

MPO activity in colon tissue and LCN2 content in stool and serum after five days of acute 3% DSS colitis were compared to healthy control WT mice. All mice showed significantly upregulated MPO activity after treatment with DSS compared to control mice (Fig.5.17a). This effect appeared to be independent of dietary conditions. Also fecal and serum levels of LCN2 were elevated in mice treated with DSS, compared to untreated control mice (Fig.5.17b). Interestingly, these measurements revealed small differences between mice on different dietary conditions. While mice fed with HFD showed the highest levels of LCN2 in stool and serum, HFD ctrl fed mice had the lowest levels of LCN2. The amount of LCN2 was

relatively similar in stool and serum of LRD and LRD+I3C fed mice. These values were slightly decreased in stool and increased in serum compared to normal chow fed mice.

Taken together LCN2 and MPO proved to be valid surrogate markers to detect intestinal inflammation, however, no major differences could be detected between the groups fed with different diets. HFD fed mice showed the highest LCN2 levels despite not showing the strongest inflammatory reaction after DSS application. In contrast, low levels of LCN2 in HFD ctrl fed mice correlated with the reduced susceptibility of these mice to colitis as indicated by lesser weight loss.

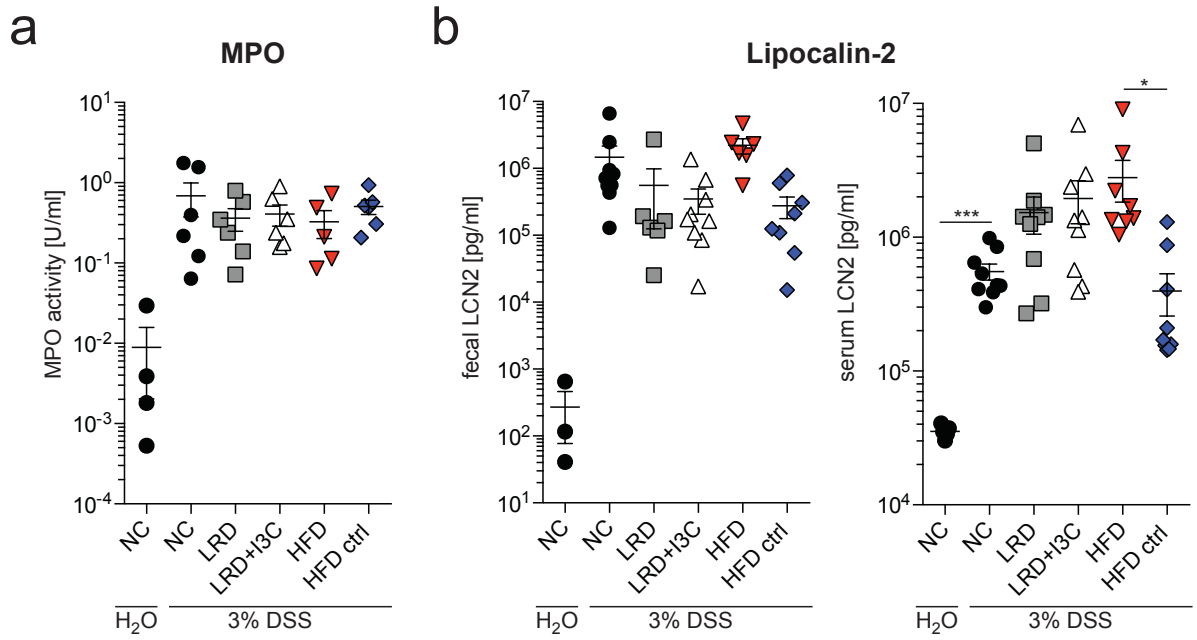

Figure 5.17: Influence of dietary AhR ligands on MPO activity and Lipocalin-2 (LCN2) levels
C57BL/6 mice were fed with different diets (NC, LRD, LRD+I3C, HFD, HFD ctrl) for four weeks and afterwards treated with 3% DSS in the drinking water for five days. (a) Myeloperoxidase (MPO) activity is measured in the colonic tissue of DSS treated mice and untreated control mice. (b) LCN2 levels were measured in stool lysates and serum of DSS-treated mice under different dietary conditions and untreated control mice. Data is pooled from two independent experiments (n=3-9). Results are shown as mean +/– SEM and significance was analyzed by ordinary one-way ANOVA and two-tailed students t-test. LRD=ligand reduced diet, I3C=Indole-3-carbinol, HFD=high fat diet, HFD ctrl=HFD control, NC=normal chow

To answer the question if quantitative differences in cytokine production might be associated with differential disease progression, protein lysates of colonic tissue after five days of 3% DSS colitis were analyzed for their cytokine profile. Disregarding some outliers, nearly all mice showed elevated cytokines levels in the colonic tissue after DSS treatment compared to untreated mice (Fig.5.18). This observation was consistent for IL-22, IL-17, CXCL1, IL-6 and

IL-1β. However, the degree of induction of certain cytokines varied selectively between the different dietary conditions. Mice on LRD showed only very low levels of IL-22 in the colon tissue. Mice on LRD+I3C, HFD and HFD ctrl had higher levels, despite not reaching the IL-22 levels of normal chow fed mice. IL-17 upregulation after colitis was strongest in LRD, LRD+I3C and HFD fed mice. CXCL1, IL-6 and IL-1β levels were regulated in a similar fashion: normal chow fed mice showed the highest levels of these cytokines, whereas animals on LRD and LRD+I3C had a markedly decreased colonic cytokine content. The degree of cytokine production of HFD and HFD ctrl fed mice was in between the aforementioned groups.

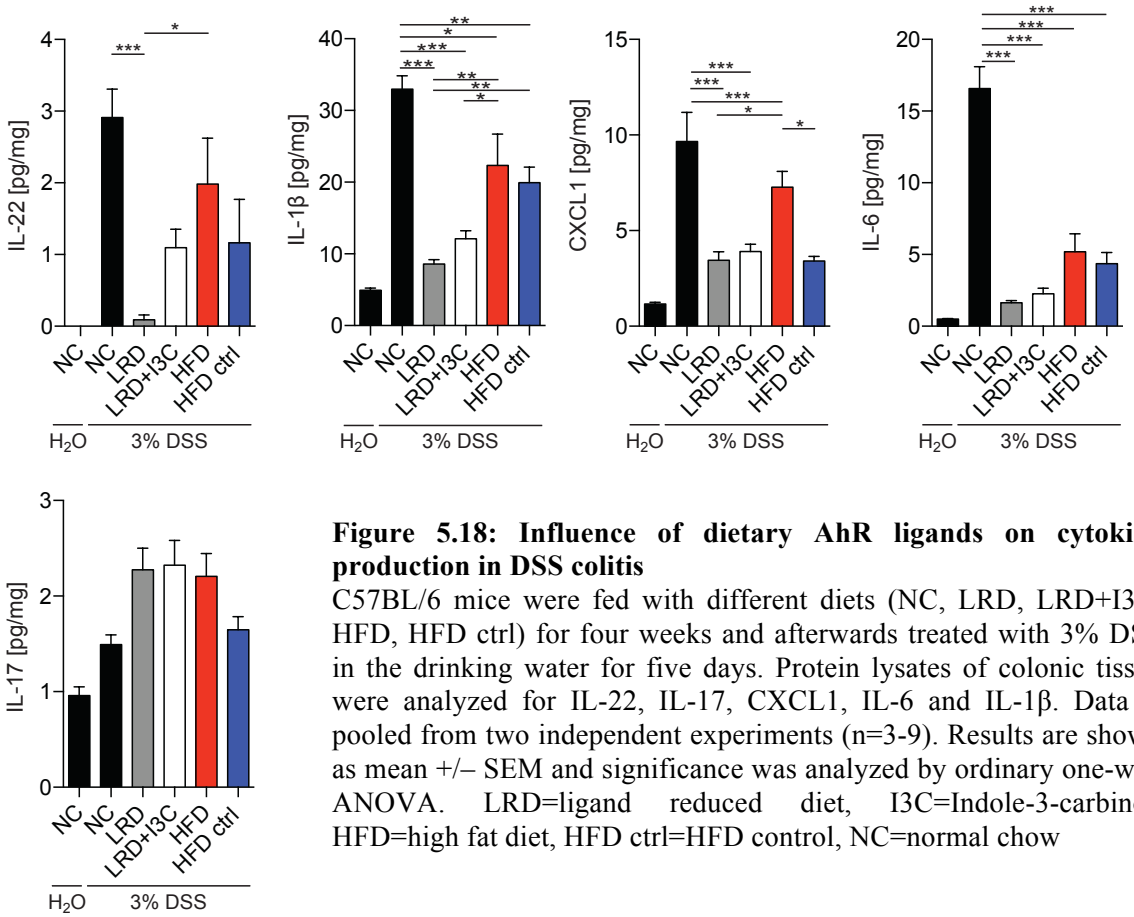

Figure 5.18: Influence of dietary AhR ligands on cytokine production in DSS colitis
C57BL/6 mice were fed with different diets (NC, LRD, LRD+I3C, HFD, HFD ctrl) for four weeks and afterwards treated with 3% DSS in the drinking water for five days. Protein lysates of colonic tissue were analyzed for IL-22, IL-17, CXCL1, IL-6 and IL-1β. Data is pooled from two independent experiments (n=3-9). Results are shown as mean +/– SEM and significance was analyzed by ordinary one-way ANOVA. LRD=ligand reduced diet, I3C=Indole-3-carbinol, HFD=high fat diet, HFD ctrl=HFD control, NC=normal chow

Overall only one clear correlation between proinflammatory cytokine production and disease outcome was observed. Thus, LRD fed mice displayed very low levels of the barrier beneficial cytokine IL-22, providing a possible explanation for the high susceptibility of these mice to DSS colitis.

Overall, these experiments demonstrated that expression of the AhRR and presumably also of other AhR target genes is largely driven by diet-derived AhR ligands. This was shown for intestinal immune cells and to a lesser extent also for immune cells in the skin. Further, it was

demonstrated that the single AhR ligand precursor I3C has the same if not a bigger potential in inducing AhR target genes than a variety of AhR ligands contained in the normal chow, although an AhR ligand dose effect cannot be ruled out. Changes in the intestinal microbiota had negligible effects on AhRR expression. Interestingly, also HFD and HFD ctrl exhibited low AhR activation, indicating a low content of AhR ligands in these diets. Nevertheless, only LRD affected intestinal barrier permeability and evoked high susceptibility to DSS colitis, possibly due to the presence of other barrier protective substances in HFD and HFD ctrl. Apart from a significant difference in the serum LCN2 levels after DSS treatment, there was no major difference in cytokine production comparing HFD and HFD ctrl.

5.2.8 Dietary AhR ligands change the composition of the intestinal microbiota

The composition of the gut microbiota has been shown to vary considerably depending on various factors, including the diet[84]. Recently, certain bacterial strains have been shown to have a big impact on DSS colitis susceptibility in mice[171]. In order to investigate if different dietary conditions and specifically dietary AhR ligands influence the intestinal gut microbiota and might explain different colitis susceptibilities the composition of the gut microbiota was determined by 16S ribosomal DNA sequencing. These experiments were performed in cooperation with the group of Haruko Takeyama from the TWIns Institute of the Waseda University in Tokyo.

The Ribosomal Database Project (RDP) Classifier is used to accurately classify 16S rDNA sequences into higher-order taxonomy. Comparison of different bacterial phyla present in WT mice receiving different diets revealed major differences between the groups (Fig.5.19a). Normal chow fed mice possessed around 80% *Bacteroidetes*, 15% of *Firmicutes* and a small population of *Proteobacteria*. LRD fed mice showed expansion of *Proteobacteria* and a reduced frequency of *Firmicutes*. Supplementation of I3C expanded *Firmicutes* at the cost of *Proteobacteria* and *Bacteroidetes*. HDF fed mice had a huge expansion of *Firmicutes* (60%), a smaller population of *Bacteroidetes* (30%) and only few *Proteobacteria*. Mice on HFD ctrl had around 40% to 50% *Bacteroidetes*, 30% to 40% *Firmicutes* and around 10% *Proteobacteria* (Fig.5.19a).

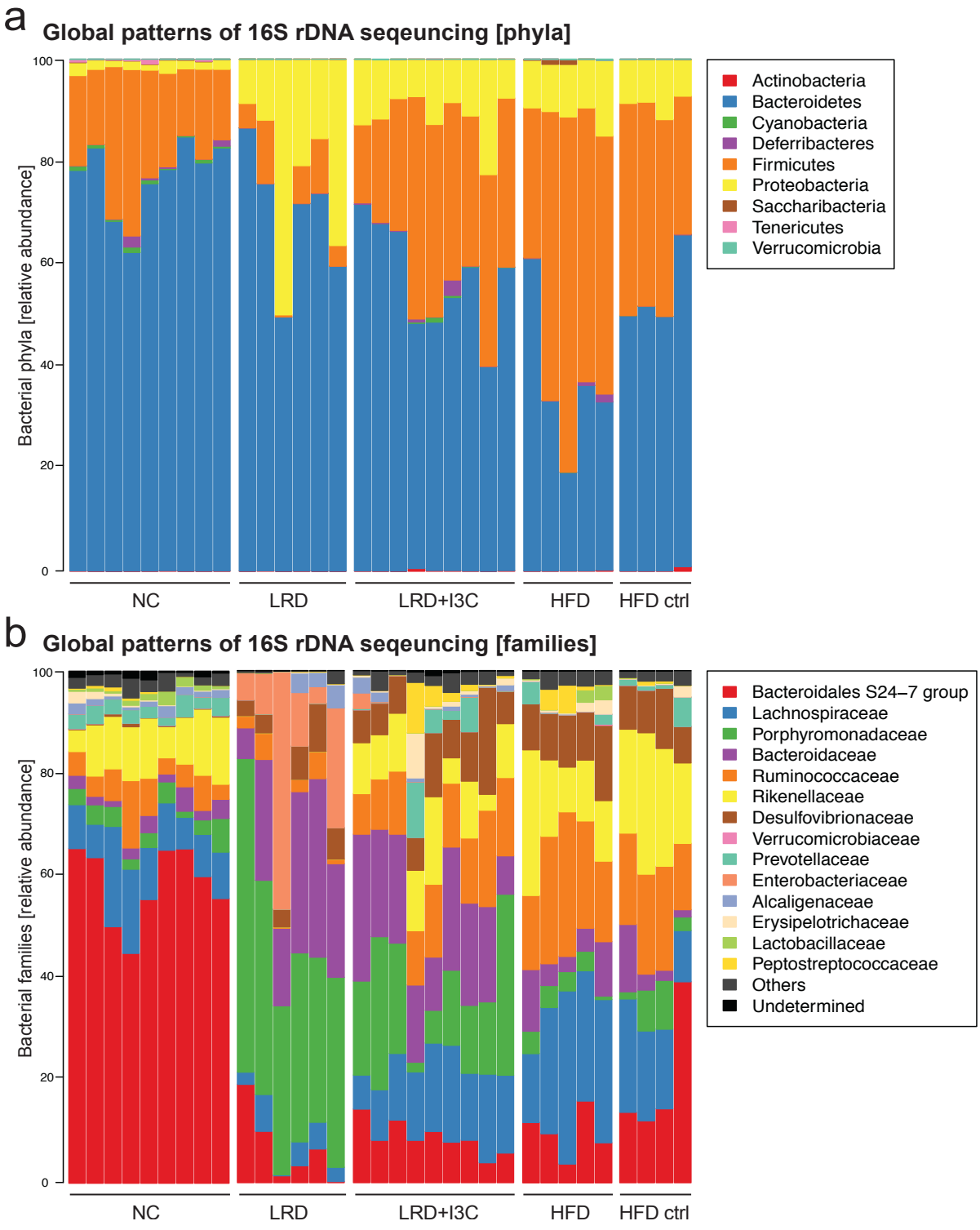

Figure 5.19: Different dietary conditions influence the intestinal microbiome composition
C57BL/6 mice were fed with different diets (NC, LRD, LRD+I3C, HFD, HFD ctrl) for four weeks. Stool samples were collected and genomic DNA was isolated. Bacterial 16S ribosomal DNA was PCR amplified and sequenced by Illumina MiSeq. Gut microbiome composition prediction was performed with the RDP-Classifier tool. (a) Relative abundance of bacterial phyla in C57BL/6 mice after feeding different diets for four weeks. (b) Relative abundance of bacterial families is shown for C57BL/6 mice. NC=normal chow, LRD=ligand reduced diet, I3C=Indole-3-carbinol, HFD=high fat diet, HFD ctrl=HFD control

Additionally, frequencies of bacterial families constituting the bacterial phyla were determined. Analysis of relative abundance of bacterial families revealed distinct differences between mice receiving different diets, while mice on the same diet had a similar microbial composition (Fig.5.19b). Normal chow fed animals had the biggest population of the *Bacteriodales S24-7 group* and a high representation of *Rikenellaceae*, both belonging to the *Bacteroidetes*. In addition, all normal chow fed mice had an expanded population of *Lachnospiraceae*, belonging to the *Firmicutes* phylum.

Mice on LRD had a big population of *Porphyromonadaceae* (*Bacteroidetes*). Moreover, LRD led to an expansion of *Bacteroidaceae* (*Bacteroidetes*), *Enterobacteriaceae* (*Proteobacteria*) and additionally *Desulfovibrionaceae* (Proteobacteira). *Enterobacteriaceae* were reduced in mice on LRD+I3C, but *Ruminococcaceae* (*Firmicutes*) and *Lachnospiraceae* (*Firmicutes*) were expanded compared to mice on LRD. Further, also *Desulfovibrionaceae* (Proteobacteira) were expanded by I3C supplementation (Fig.5.19b).

Mice on HFD and HFD ctrl showed a relative similar microbial composition on family level. All of these mice had big populations of *Lachnospiraceae*, *Ruminococcaceae* and *Rikenellaceae*. Frequency of *Porphyromonadaceae* was clearly reduced in comparison to LRD and LRD+I3C fed mice while the frequency of *Desulfovibrionaceae* was similar in LRD+I3C, HFD and HFD ctrl fed mice (Fig.5.19b).

Since dietary AhR ligands had a big influence on microbial composition in the intestine, relative abundance of bacterial families was compared between WT mice and AhRR-deficient mice ($AhRR^{E/E}$) in order to investigate, if presence of the AhRR has an influence on microbial composition. WT and $AhRR^{E/E}$ mice were compared under the influence of normal chow, LRD and LRD+I3C (Fig.5.20, Fig.5.21). No big differences in microbial composition were observed between WT and $AhRR^{E/E}$ mice fed mice receiving normal chow, LRD or LRD+I3C (Fig.5.20). Nevertheless, some small differences with regard to the appearance of bacterial families were observed comparing WT and $AhRR^{E/E}$ mice. Analysis of relative abundance of bacterial families in LRD fed mice revealed presence of *Prevotellaceae* in some of the $AhRR^{E/E}$ mice on LRD, which could not be observed in LRD fed WT mice. Interestingly, *Prevotellaceae* could be detected in LRD+I3C fed mice, independent of the genotype (Fig.5.20).

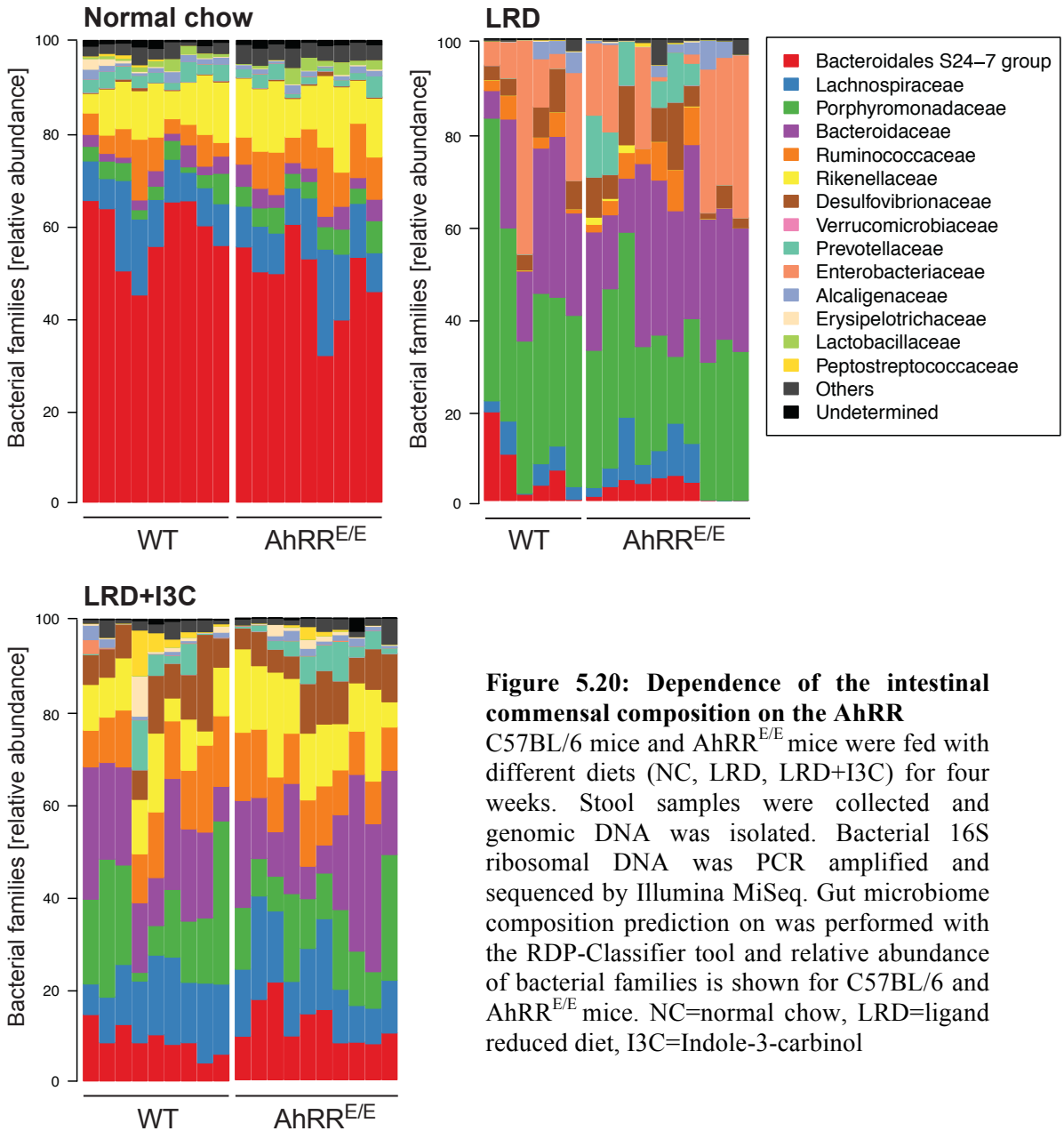

Figure 5.20: Dependence of the intestinal commensal composition on the AhRR
C57BL/6 mice and AhRR$^{E/E}$ mice were fed with different diets (NC, LRD, LRD+I3C) for four weeks. Stool samples were collected and genomic DNA was isolated. Bacterial 16S ribosomal DNA was PCR amplified and sequenced by Illumina MiSeq. Gut microbiome composition prediction on was performed with the RDP-Classifier tool and relative abundance of bacterial families is shown for C57BL/6 and AhRR$^{E/E}$ mice. NC=normal chow, LRD=ligand reduced diet, I3C=Indole-3-carbinol

The general similarity between WT and AhRR$^{E/E}$ mice was also reflected by principle component analysis (PCA) of weighted and unweighted UniFrac distance analysis. The analysis revealed one coherent population of mice receiving normal chow diet that was clearly distinct from mice receiving LRD or LRD+I3C (Fig.5.21). No genotype specific clustering could be observed using the PCA of UniFrac distance analysis. LRD fed mice were slightly more scattered in the PC analysis indicating a generally higher diversity between individual mice, but also no clear genetic differences in microbial composition (Fig.5.21). Mice on LRD+I3C showed a clearly different microbial composition from normal chow or LRD fed mice, but also no genotype specific clustering (Fig.5.21).

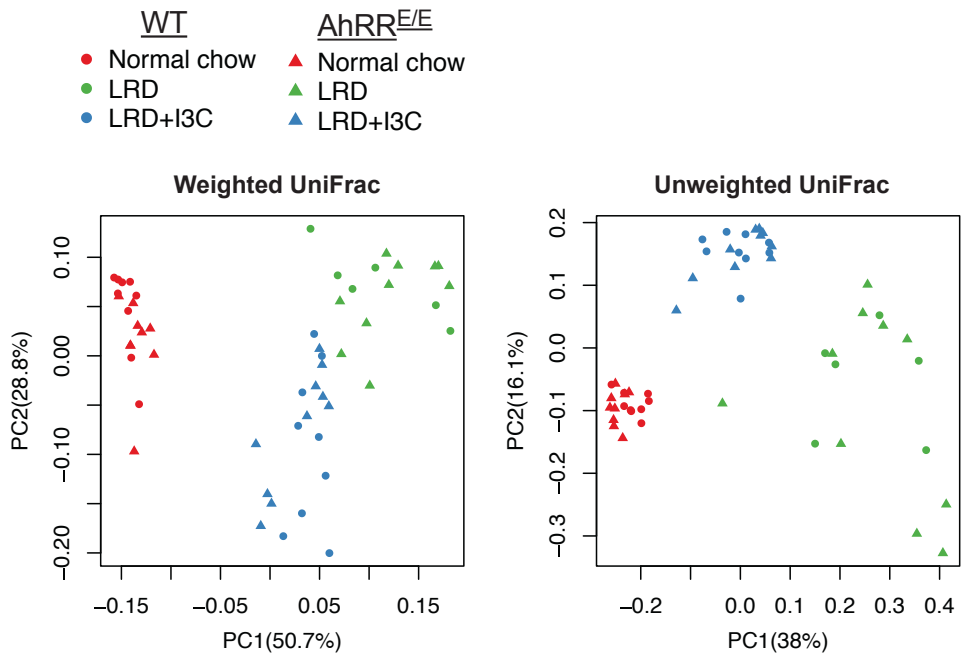

Figure 5.21: Dietary AhR ligands change the overall intestinal microbiota composition
C57BL/6 and AhRR$^{E/E}$ mice were fed with different diets (NC, LRD, LRD+I3C, HFD, HFD ctrl) for four weeks. Bacterial 16S rDNA was PCR amplified from stool samples and sequenced by Illumina MiSeq. Weighted and unweighted UniFrac distance analysis was used to determine differences in composition of the microbiota between mice on different diets. Principle component analysis of UniFrac distances was plotted for the indicated genotypes and diets.

In summary, this analysis revealed that dietary conditions severely change the microbiota of mice. Dietary AhR ligands but also other substances regulate these changes. However, only minor differences between WT and AhRR-deficient mice could be detected, suggesting that the AhRR does not impair the composition of the intestinal microbiota.

6 Discussion

The AhR has been extensively studied in the field of toxicology as an environmental sensor, as a receptor for xenobiotics and for its role in the detoxification of chemicals. More recently, the AhR has gained increasing interest in the field of immunology, since it is involved in mediating TCDD-induced immunosuppresion[172]. Expression of the AhR is widespread in cells of the immune system and particularly high in different cell types of barrier organs[110], in line with its main function as environmental sensor. In the gut mucosa the AhR has been shown to be essential as a transcription factor for maintaining IEL and ILC populations[123]. Mutations in the AhR have been further identified as a risk factor for IBD[143]. Moreover, different studies have shown that AhR-deficient mice are highly susceptible to colitis, largely as a consequence of the loss of IELs and ILCs[48,120,121].

The activity of the AhR is regulated by a negative feedback loop through the AhRR, which is a direct target gene of the AhR. In this thesis, the functional importance of the AhRR in the gut immune system was investigated. In the second part of the thesis the activation of the AhR by dietary AhR ligands and subsequent AhRR expression was examined. In addition, the functional importance of dietary AhR ligands for the intestinal immune system and the intestinal microbiota was investigated.

6.1 Regulation of gut immunity through the AhRR in homeostasis and in DSS-induced colitis

Studies in our group revealed that mice deficient for the AhRR ($AhRR^{E/E}$ mice) are more susceptible to DSS colitis than wild-type littermates[149]. This was somewhat surprising, since other studies already showed increased colitis susceptibility of AhR-deficient mice[119,120]. Hence, it is important to study why AhR and AhRR do not act anatgonistically and how both molecules contribute to intestinal barrier maintenance. Extensive research on the AhR and its role for the immune system showed that AhR-deficient mice are highly susceptible to DSS colitis due to an impaired maintenance of IELs and ILC3s[121,173]. Previous experiments by Dr. O. Brandstätter revealed that the presence of IELs in the intestine of AhRR-deficient mice was only moderately affected in comparison to AhR-deficient mice[121,149]. Only a relatively small reduction of colonic $CD8\alpha^{+}TCR\gamma\delta^{+}$ IELs was apparent in $AhRR^{E/E}$ mice which might partially contribute to the DSS colitis susceptibility of these mice. Further experiments showed that $AhRR^{E/E}$ mice had no elevated barrier permeability and no apparent changes in microbiota diversity, which could have additionally explained enhanced DSS colitis susceptibility. In addition, $AhRR^{E/E}$ mice showed reduced fecal IgA titers but elevated serum

IgA titers, indicative of a disturbed IgA production or defective migration of IgA-producing B cells, which might contribute to elevated colitis susceptibility[149]. However, it is not clear whether these collective findings alone explain the increased colitis susceptibility of AhRR$^{E/E}$ mice.

6.1.1 AhRR$^{E/E}$ mice do not exhibit reduced ILC3 frequency in the gut

Besides affecting the survival of ILC3s, lack of AhR signaling additionally impairs IL-22 production by ILC3s and Th17 cells in the intestine[123,174]. IL-22 has been described to be of great importance in the pathology of intestinal diseases, inhibiting inflammation and protecting the barrier against pathogens[175].

In the present work, reduced frequencies of NKp46^{+} and NKp46^{-} ILC3s could be confirmed in AhR knockout mice, however to a lesser extend as has been described previously[122]. In contrast, a normal presence of these cells was shown in the SI of AhRR$^{E/E}$ mice, suggesting a normal functionality of intestinal ILC3s in these mice. Indeed, resistance of AhRR$^{E/E}$ mice to infection with *Citrobacter Rodentium* has been shown, further supporting normal ILC3 function[128]. Therefore, a role for ILC3s in the susceptibility of AhRR$^{E/E}$ mice to DSS colitis seems rather unlikely. In line with the high AhR expression by ILC3s[174,176], these cells also comprised a high proportion of AhRR positive cells, as a direct target gene of the AhR. Around 80% of the NKp46^{+} ILC3s expressed the AhRR/EGFP reporter under homeostatic conditions. Interestingly, just 20% of the NKp46^{-} ILC3s expressed the AhRR indicating less AhR activation or expression in this cell population. Notably, in these experiments, only a slight reduction of the NKp46^{-} ILC3 subset in AhR$^{-/-}$ mice was apparent. Therefore, maintenance of ILC3s seems to be only partially dependent on AhR signaling. In this context, it is interesting to mention that Qiu et al, who initially described the loss of RORγt^{+}ILC3s in AhR$^{-/-}$ mice, observed residual lineage negative cells expressing RORγt in AhR$^{-/-}$ mice, presumably ILC3s[119]. It would hence be interesting to investigate the role of other transcriptional programs or molecules important for ILC maintenance in this context. In fact, besides AhR$^{-/-}$ mice, animals deficient for RORγt, CXCR6 or Rag2 and IL-2R show reduced ILC populations[177-179]. Incomplete loss of intestinal ILC3s might also be explained by a different intestinal microbiota. Reduced numbers of NKp46^{+} ILC3s in germ-free or antibiotic-treated mice indicated an effect of the microbiota on ILC development or survival[74,177]. These findings highlight the complex regulation of ILC survival after birth, presumably involving more signals than just the AhR pathway.

Since number of colonic IELs were just slightly reduced and small intestinal ILC3 frequencies were unchanged in AhRR$^{E/E}$ one might suggest that these cells are not critically involved in the elevated colitis susceptibility. However, previous studies showed that defective AhR signaling not only leads to loss of these cells but also to impaired functionality. Thus, additional analysis investigating ILC3 functionality, such as IL-22 and IL-17 production, is necessary to completely rule out a role of these cells.

6.1.2 AhRR-deficiency affects T helper cell differentiation in DSS colitis

The intestinal immune system has to respond to dangerous substances and infectious threats while remaining unresponsive to harmless food antigens or the commensal microbiota[1]. Likewise also T cells are either able to maintain immune tolerance in the gut mucosa or play a key role in the pathogenesis of IBD[38]. Unlike human disease, DSS colitis does not necessarily require T and B cells for development and has a bigger contribution of the innate immune system[180]. Nonetheless, T cells are still involved in the colitis pathology. Due to this reason the differentiation status of T cells during colitis was analyzed. Considering that Th17 cells and IL-22 production by Th17 and Th22 cells are regulated by AhR-activation[123], an involvement of AhRR in regulating the function and development of T cells is plausible. Analysis of the frequency of Th17, Th1, Tc17 and Tc1 cells in DSS colitis revealed that lack of the AhRR caused an enhanced differentiation of Th17 and Tc17 cells, whereas the frequency of the IFNγ-producing Th1 and Tc1 cells was reduced. While more Th17 cells could also be observed in AhR$^{-/-}$ mice, the increased frequency of Tc17 cells was exclusive for AhRR$^{E/E}$ mice. It has been previously shown that the AhR regulates Treg and Th17 differentiation in a ligand-dependent fashion[152]. Application of FCIZ has been shown to boost the differentiation of Th17 cells in *in vitro* studies as well as in an *in vivo* model of experimental autoimmune encephalomyelitis (EAE)[181]. Stronger AhR signaling in the absence of the AhRR might therefore lead to augmented intestinal Th17 cell differentiation and consequentially to a reduced frequency of other T helper cell subsets. As Th17 cells have been shown to infiltrate the inflamed gastrointestinal mucosa of CD and UC patients and produce an excess of Th17 related cytokines[182], the elevated frequency of Th17 and Tc17 cells in AhRR-deficient mice might be responsible for the stronger colitis. However, also protective effects of Th17 cytokines in colitis have been described. Blocking of IL-17A by antibody or genetic ablation exacerbates colitis symptoms, indicative of a protective effect of IL-17A[183]. Furthermore, the Th17-derived cytokine IL-22 has been attributed with tissue protective functions, indicating that Th17 cells might have a dual role. This phenomenon has also emerged as a general concept in Th17 cell biology, since it could be shown that exposure

to IL-23 confers pathogenic properties to Th17 cells, whereas absence of IL-23 results in induction of an inhibitory module in Th17 cells[184].

In vitro T cell differentiation studies performed by Dr. J. König could not show differences in Th17 and Th1 differentiation comparing WT and AhRR$^{E/E}$ mice[128], indicating that altered T cell differentiation *in vivo* is not T cell intrinsic. Therefore, we speculate that the intestinal microenvironment during DSS colitis might be changed in the absence of the AhRR and subsequently drive Th17/Tc17 cell differentiation. It has been shown that IL-6, TGFβ and IL-1β produced by antigen presenting cells, in particular monocytes and cDCs, promote polarization of naïve CD4$^+$ T cells into Th17 cells[182]. Indeed, assessment of the intestinal cytokine milieu in WT and AhRR$^{E/E}$ mice under homeostatic conditions and in DSS colitis revealed significantly higher IL-1β levels in untreated AhRR$^{E/E}$ mice, potentially contributing to the elevated frequency of Th17 cells observed in AhRR$^{E/E}$ mice during colitis. High IL-1β concentrations might facilitate the Th17/Tc17 differentiation early in the inflammation and therefore eventually result in more IL-17 producing effector T cells in colitis, although IL-1β levels were not significantly enhanced at day six. Mechanistically, it has been shown that IL-1β inhibits TGF-β-induced Foxp3 expression and additionally augments expression of the Th17 cell-specific transcription factors NFKBIZ and BATF[185]. In addition the AhR is able to regulate the balance of Treg and Th17 cell differentiation in a ligand dependent-fashion[152]. Therefore it might be possible that the enhanced Th17 cell frequency influences Treg numbers in AhRR$^{E/E}$ mice. However, experiments performed by Dr. O. Brandstätter showed no differences in Treg frequencies between AhRR$^{E/E}$ and WT mice in inflammation and under homeostatic conditions[149]. This argues against a misbalance in Th17/Tc17–Treg differentiation as an explanation for the elevated frequency of IL-17-producing T cells in AhRR$^{E/E}$ mice.

Tc17 cells have received only marginal attention, as they are a relative newly defined subset of CD8$^+$ T cells. In the current understanding, IL-6 and TGFβ together with activators of STAT3 and RORγt are necessary for the differentiation of Tc17 cells[186]. In humans, also the combination of IL-1β and IL-23 has been shown to induce the production of IL-17 in circulating CD8$^+$ T cells[187]. Therefore, it cannot be ruled out that IL-1β is important for the induction of Tc17 cells in mice as additional cytokine requirements for Tc17 cells in general appear to be similar to Th17 cells[188].

Intestinal tissue macrophages are potent producers of IL-1β, especially under inflammatory conditions, thus driving local differentiation but also expansion of Th17 cells[62,189,190]. Therefore, macrophages might be involved in driving Th17/Tc17-biased T cell differentiation

in AhRR$^{E/E}$ mice. In addition, also DCs are of importance in inducing Th17 responses in the intestine. Intestinal DCs are discriminated from macrophages by the lack of CD64 and F4/80 expression and are subdivided into four populations based on their expression of CD103 and CD11b[51]. To investigate the influence of these antigen-presenting cells on T cell differentiation, the frequencies of DCs and macrophages in the different compartments of the intestine were analyzed. However, no differences in macrophage frequencies in colon and SI were observed, indicating that the elevated IL-1β levels in AhRR$^{E/E}$ mice cannot be attributed to increased macrophage frequency. Therefore, it is likely that AhRR-deficient macrophages produce more IL-1β or that the absolute number of intestinal leukocytes is elevated, as the frequency of macrophages was unchanged. This has to be analyzed in more detail in future experiments.

AhRR-deficient mice showed elevated overall DC frequencies in the SI, whereas DC frequencies in the mLNs were reduced. This might hint at a migratory defect in AhRR$^{E/E}$ mice, preventing DCs from leaving the lamina propria to enter the mLNs[191]. Again these data do not give information about absolute cell numbers in the lamina propria and mLNs. Of note, the increased frequency of DCs in the SI correlated with the strongest Th17 and especially Tc17 induction in the SI, suggesting that DCs also have a local influence on T cell differentiation processes in the small intestinal lamina propria. DC subsets differ to some extent with regard to their ability to prime and polarize naïve CD4$^+$ and CD8$^+$ T cells. Especially CD103$^+$CD11b$^+$ DCs are potent Th17 inducers[192,193]. In addition, also the smaller population of CD103$^-$ DCs is able to promote Th1 or Th17 differentiation[54]. As none of the Th17 cell-inducing DC subsets was particularly expanded in WT and AhRR$^{E/E}$ mice, it seems unlikely that the stronger Th17/Tc17 differentiation is explained by expansion of one specific DC subpopulation.

In summary, *in vitro* studies highlighted that T cells in AhRR$^{E/E}$ mice do not have an intrinsic differentiation defect[128]. It is possible that enhanced Th17/Tc17 differentiation *in vivo* might be caused by an altered cytokine micromilieu in AhRR-deficient mice. More detailed analysis of DCs that accumulate in the SI of AhRR$^{E/E}$ mice and determination of the source of elevated IL-1β levels in AhRR$^{E/E}$ mice could extend the current understanding of the molecular processes leading to elevated susceptibility in AhRR$^{E/E}$ mice.

6.1.3 AhRR expression in macrophages and neutrophils is dispensable for protection against colitis

Although the frequency of macrophages was unchanged in $AhRR^{E/E}$ mice, a role of these cells for colitis susceptibility in AhRR-deficient mice cannot be excluded. Macrophages are potent innate effector cells, eliminating invading bacteria, dead epithelial cells and apoptotic material[1]. Further, macrophages are important for maintaining intestinal homeostasis through their cyclo-oxygenase (COX)2-dependent prostaglandin production and secondary expansion of regulatory T cells through IL-10[51,194]. It has further been shown previously that depletion of macrophages enhances the susceptibility to DSS colitis[195]. In order to investigate more closely, if the lack of AhRR expression in macrophages is responsible for enhanced colitis susceptibility, a cell type-specific knockout of the AhRR was generated. $AhRR^{fl/fl}$ mice were crossed to LysM-Cre mice[145], resulting in deletion of the AhRR in all lysozyme M-expressing cells, comprising macrophages and neutrophils. As previous experiments showed no expression of the AhRR in bone-marrow neutrophils (unpublished observation), the lack of AhRR in neutrophils should not have a major input. $AhRR^{fl/fl}$LysM-Cre mice did not show enhanced weight loss after colitis induction in contrast to complete AhRR-deficient mice. All other parameters did not reveal any significant differences between WT, $AhRR^{E/E}$ and $AhRR^{fl/fl}$LysM-Cre mice. This was unexpected and might be explained by a change in the DSS colitis model. In contrast to previous experiments with 5% DSS over the course of six days, these experiments were performed with 3% DSS over the course of seven days, followed by a five day recovery phase, in which mice received normal drinking water. Administration of a lower DSS dose prevented exacerbated weight loss and allowed us to extend the experiment in order to monitor potentially small differences in colitis severity between $AhRR^{fl/fl}$LysM-Cre mice and WT mice or $AhRR^{E/E}$ mice that become more obvious when putting mice back on normal water after DSS administration[196,197]. However, in the recovery phase obvious signs of colitis were ameliorated, resulting in a milder phenotype also in $AhRR^{E/E}$ mice. Although the weight curve indicates that $AhRR^{fl/fl}$LysM-Cre mice are as affected as WT mice, future experiments using the 5% DSS colitis model will be necessary to clearly define the differences in colitis susceptibility between $AhRR^{E/E}$ and $AhRR^{fl/fl}$LysM-Cre mice.

The high frequency of macrophages expressing the AhRR suggests a great importance of the repressor in regulating AhR driven processes. As normal colitis development was observed by knocking out the AhRR in macrophages and neutrophils, it is conceivable that AhR ligand degradation through cytochrome p450 enzymes or AhR-activity inhibition through TiPARP

might substitute for the AhRR and ensure a properly balanced AhR signaling[105,111]. It is also conceivable that a cooperation of several different cell types with AhRR-deficiency is necessary to observe any effects in DSS colitis.

The phenotype of $AhRR^{fl/fl}$LysM-Cre mice cannot be easily awarded to one of the two affected cell types, but more collectively to all $LysM^{+}$ cells. Although neutrophils did not show expression of AhRR under homeostatic conditions (unpublished observation), it cannot be fully excluded that the AhRR is of functional importance for neutrophils under inflammatory conditions in DSS colitis. The experiments conducted with $AhRR^{fl/fl}$LysM-Cre mice did not show differences to WT mice with regard to intestinal inflammation. MPO activity in colon tissue, which is generally associated with influx of neutrophils and concomitant inflammation, was not elevated (Data not shown), which might again be partially attributed to late analysis in the colitis model used here. Further, no differences in histological scores, inflammatory serum cytokine levels and fecal and serum Lipocalin-2 levels were apparent. Application of the 5% DSS colitis model will be necessary to ultimately clarify, if there are differences in colitis susceptibility between $AhRR^{fl/fl}$LysM-Cre and WT mice.

Overall these experiments revealed that lack of AhRR in $LysM^{+}$ cells, namely macrophages and neutrophils, does not influence DSS colitis susceptibility in the low dose DSS colitis model after recovery phase. This might be either explained by a negligible role of the AhRR for the function of macrophages and neutrophils or by the colitis model itself as well as the time point of analysis. This issue needs to be addressed in future studies.

6.2 Dietary AhR ligands have a profound influence on AhR signaling and immune function in barrier organs

AhR ligands are of various origins. Oxidation and chemical condensation of dietary tryptophan leads to formation of the high affinity AhR ligand FICZ. Further tryptophan-derived AhR ligands are kynurenine, derived from the indoleamine 2,3-dioxygenase (IDO) and tryptophan 2,3-dioxygenase (TDO) metabolism, and indoles generated by bacterial tryptophan metabolism. Furthermore, the phytochemical indole-3-carbinol (I3C) is converted to the AhR ligands indolo-[3,2-b]-carbazole (ICZ) and 3,3′-diindolylmethane (DIM) under influence of the stomach acid[114,168]. It is interesting to speculate, which ligands drive the AhR pathway and the high expression of the AhRR during steady state. The ligand sources that should be considered in this context are dietary, bacterial metabolism-derived and endogenous AhR ligands. In particular the influence of different dietary conditions on the intestinal

immune system, intestinal barrier integrity and gut microbiome composition was investigated in this thesis.

6.2.1 AhR target gene expression is mainly driven by dietary AhR ligands

This study demonstrated that changes in composition and amount of intestinal commensals by oral antibiotic treatment have no influence on the AhRR expression in intestinal immune cells. Depletion of the resident intestinal microbiota in general has been shown to have diverse effects on the AhR signaling pathway. For example, reduction of tryptophan metabolizing bacteria, such as certain Lactobacilli strains, might result in reduced AhR ligand supply and thereby decreased AhR activation and target gene transcription[77]. However, AhRR expression in immune cells of the lamina propria and the mLNs was not affected by antibiotic treatment suggesting that AhR ligand providing bacterial strains might not have been fully depleted or are not present in the microbiota of the animals analyzed in this study. While truly germfree or axenic mice are free of all microorganisms and kept in controlled isolators, a broad spectrum-antibiotic approach cannot remove 100% of all gut bacteria, as shown by at least two independent studies[198,199]. Another explanation might be that bacterial derived AhR ligands are not quantitatively involved in activating AhR signaling and that therefore removing the intestinal microbiota does not influence AhRR expression. Indeed, indoles derived from bacterial metabolism are only low affinity AhR activators, as opposed to FICZ or I3C[114]. This study focused on AhRR expression in immune cells as indicator for AhR activation. However, it is still conceivable that other AhR target genes, for example *cyp1a1*, and other cells like intestinal epithelial cells might be more affected by antibiotic treatment. A recent study by Schiering *et al.* highlighted that expression of *cyp1a1* is particularly important in intestinal epithelial cells as opposed to T and B cells[200]. Future experiments should focus on the influence of oral antibiotic treatment on additional AhR target genes in an organ and cell-type specific manner.

In contrast to antibiotic treatment, feeding a purified diet reduced in plant-derived phytochemicals and consequently AhR ligands strongly reduced AhRR expression in immune cells of the intestine, indicating that AhRR expression is controlled by foodborne AhR ligands. Additionally, it was shown that also *cyp1a1* was strongly downregulated in mice receiving LRD. However, the presence of residual AhRR expressing cells, especially in SI and PPs, indicates the existence of other AhR ligands in the diet or endogenous metabolites that activate the AhR and thereby induce AhRR expression. An alternative explanation might be that in absence of diet-derived phytochemicals, intestinal bacteria are able to compensate

lack of dietary AhR ligands by efficiently metabolizing dietary tryptophan and providing AhR ligands. The considerably lower AhRR expression levels in the more distant parts of the gastrointestinal tract (colon, mLNs) might be a consequence of consumption of residual dietary tryptophan or phytochemicals in the upper parts of the gastrointestinal tract.

Addition of I3C to the diet led to similar frequencies of AhRR-expressing cells as in normal chow fed mice. The I3C degradation products ICZ and DIM have been shown to be potent AhR activators leading to high expression of *cyp1a1*[201]. Addition of I3C to LRD restores frequencies of AhRR-expressing cells, indicating that one or two AhR ligands can substitute for a variety of ligands present in normal chow. Notably, in some experiments even higher frequencies of AhRR expressing cells and higher MFI of the AhRR in mice on LRD+I3C compared to normal chow were noted. It has to be clarified, if higher frequencies of AhRR-expressing immune cells in mice receiving LRD+I3C are due to the high affinity of ICZ to the AhR or due to the higher AhR ligand dose. The I3C concentration in LRD was chosen according to published work[120]. However, neither the concentration of other substances with AhR activating properties in the LRD nor AhR ligand content in the normal chow is known. It is also possible that I3C influences AhRR expression via other pathways than AhR. I3C has been shown to interact with numerous other nuclear receptors like the estrogen and androgen receptor and modulates multiple signaling pathways, which could influence gene expression independently of the AhR[202,202].

Interestingly, AhRR expression of immune cells in the skin was also influenced by dietary AhR ligands, suggesting a systemic effect of foodborne AhR ligands. Nevertheless, the effects were not as strong as in the intestine, as proportions of AhRR-expressing γδ T cells in epidermis and dermis were independent of dietary conditions. Yet the MFI of the AhRR in γδ T cells was reduced in LRD fed mice. Langerhans cells showed a reduced frequency of AhRR positive cells and lower AhRR fluorescence intensity in mice fed with LRD. Similar to intestinal immune cells, diet supplementation with I3C restored frequency of $AhRR^+$ cells in the skin and led to even higher MFI values of the AhRR as observed in normal chow fed mice. As in the gastrointestinal tract, AhR ligands are also abundant in the skin, controlling AhR target gene expression. AhR activators in the skin can be derived from dietary plants, the skin microbiota or can be endogenously produced [95,203]. Moreover, UVB irradiation can induce FICZ as an intracellular tryptophan photoproduct, which in turn activates the AhR[204]. The relatively lower relevance of dietary Ahr ligands in the skin indicates that physiological AhR activation in the skin may be induced by different sources of AhR ligands. While the contribution of diet-derived compounds is very strong in the intestine, endogenous AhR

ligands from the tryptophan metabolism might be the crucial activators of AhR target gene expression and therefore AhRR expression in the skin. Moreover, another feasible hypothesis is that AhRR expression in the skin might be partially independent of stimulation through AhR ligands or even independent of the AhR per se. This hypothesis is supported by previous experiments that revealed a high frequency of residual AhRR expressing cells in mice deficient for the AhR[128], implying that AhRR induction in skin might occur independent of the AhR. However, until now other pathways activating AhRR in absence of AhR have not been identified. Interestingly, the promoter sequence of the AhRR contains three GC box sequences and one NF-κB site in addition to XRE sites[205], suggesting the possibility of AhRR induction by other transcription factors than AhR. Thus, it is very likely that AhRR expression can also be regulated independently of the AhR in a tissue and cell type-specific fashion. Nonetheless, I3C was able to increase AhRR expression in the skin in comparison to normal chow fed mice, which might be explained by high affinity of ICZ or by the AhR ligand dose.

In summary, these experiments highlighted that dietary AhR ligands are strong activators of the AhR signaling pathway. Moreover, the influence of dietary AhR ligands on AhRR expression is largely organ and cell type-specific. Surprisingly, the microbiota itself seemingly had no influence on AhRR expression.

6.2.2 Modified diets change AhRR expression through altered activation of the AhR signaling pathway

Since more than 40 years, scientists work on establishing guidelines for experimental nutrition that help to standardize studies among laboratories[206]. The common method for standardization is the usage of purified diets that are formulated with a restricted set of ingredients. Soybean protein isolate and casein are used as protein sources, sugar and starch as carbohydrate sources, vegetable oil and lard as fat sources and pure cellulose as source of fiber. In addition inorganic salts and vitamins are added[207]. The AIN76 purified diet, which was replaced by the improved AIN93G and AIN93M in 1993[207], was published by the National Institutes of Health (NIH) in 1977 as the first purified diet to be used as standard reference diet for rodents[208]. Widely used diets in the rapidly advancing field of immunometabolism are high fat diet (HFD) and a matched control diet (HFD ctrl), recommended by the manufacturer. Surprisingly, experiments in an initially unrelated project in our laboratory revealed strong influences of these diets on AhRR expression. To analyze

this further, a systematic comparison between HFD, HFD ctrl, normal chow, LRD and LRD+I3C was carried out.

The percentage of AhRR-expressing cells and MFI of AhRR expression was investigated in IELs and immune cells of the lamina propria and the mLNs. The strongest influence of dietary AhR ligands, independent of which diet was used, could be observed on IELs. A plausible explanation for this phenomenon might be the close proximity of IELs to the gut lumen, facilitating exposure of these cells to dietary components. The strongest reduction in the proportion of $AhRR^+$ IELs could be observed for mice fed with LRD. Confirming previous findings, LRD+I3C fed mice displayed similar $AhRR^+$ cell frequencies and AhRR expression levels as normal chow fed mice, pointing out a similar AhR activation through I3C supplementation and naturally occurring flavonoids and phytochemicals in grain based diet. As expected, mice fed with HFD and HFD ctrl had equally low frequencies of AhRR-expressing IELs as mice fed with LRD, confirming that HFD and HFD ctrl are low in AhR ligand concentration.

Analysis of AhRR-expressing cells in the lamina propria in a setup with all five different dietary conditions revealed the same tendencies as observed for the IELs, although reduction of AhRR expression through purified diets (LRD, HFD and HFD ctrl) in comparison to normal chow was not as strong as in the previous experiments. In contrast, clearly elevated frequencies and MFI values were observed in the experimental group receiving LRD+I3C. Interestingly, in particular the frequency of AhRR expressing cells in the animals receiving normal chow diet was lower as previously observed. 80% of the $CD8^+$ T cells in the SI of the first experiments expressed the AhRR, while only 20% of the $CD8^+$ T cells in the second comparison expressed the AhRR. This difference could possibly be attributed to experimental variations, however only in the normal chow fed group. Neither the normal chow manufacturer nor any other factor with regard to diet application, timing or handling has been changed, making this variation hard to explain.

DCs from mLNs showed the same tendencies and similar strong differences in frequency of $AhRR^+$ cells as observed for the IELs. Of note, mLN DCs showed much bigger differences in AhRR expression between the dietary groups than lamina propria lymphocytes isolated from the same mice. Especially frequency of $AhRR^+$ DCs in normal chow fed mice was as high as expected and not uncharacteristically low as observed in the lamina propria, suggesting AhRR expression differences in the lamina propria as a consequence of the cell isolation procedure or other technical aspects rather than reflecting a true effect through the diet.

Flow cytometric analysis of intestinal immune cells indicated that the reduction of AhRR$^+$ lymphocytes was slightly lower in HFD and HFD ctrl fed mice than in LRD fed mice. This observation might be explained by a higher concentration of residual AhR ligands in these diets compared to the LRD. However, the spectrum of AhR activating substances is very broad and structurally diverse AhR agonists lead to ligand-selective differences in gene expression[209]. Moreover, it is complicated to determine the amount of AhR ligands in a certain type of food. Combinations of methanol/water extraction, silica gel batch purification and several high-performance liquid chromatography (HPLC) steps have been used in this context before, and could therefore help to determine AhR ligand concentration in different diets. An alternative would be the usage of AhR reporter gene assays[116]. Similar to LRD also HFD and HFD ctrl influence AhRR expression not only in the gastrointestinal tract, but also in the skin, although to a lesser extent. However, detailed flow cytometric analysis of the influence of HFD and HFD ctrl on AhRR expression by immune cells in the skin has not been conducted yet.

Ssniff, the company producing the laboratory mouse diet used in this study, provides information about the amount of tryptophan in the experimental diet, whereas no information about plant-derived phytochemicals and other potential AhR activators are available. While LRD contains 0.22% tryptophan, HFD and HFD ctrl contain 0.31% and 0.23% tryptophan, respectively. However, it is debatable if this marginal difference in tryptophan content, especially the slightly higher concentration in HFD, might influence the AhRR expression to a measurable extent. Another potential source of AhR ligands might be the lard that is added to the HFD as a source of fat. As pig lard represents a natural product, it cannot be excluded that it also contains AhR activators. Studies could show that prostaglandins, which are lipid mediators derived from fatty acids that are abundant in HFD, are able to displace TCDD from the AhR binding site[210]. Although they are weak agonists, prostaglandins might represent a novel class of AhR activators, which might be specifically present in the HFD.

Judging AhR activation by expression of known AhR target genes is a well-accepted method in the field[101,200]. In order to understand the influence of dietary AhR ligands on AhR target gene expression in more depth, future studies and experiments should concentrate on additional target genes next to the AhRR[105], thereby improving reliability of the readout compared to just using AhRR. The enzymes of the cytochrome P450 family CYP1A1, CYP1A2 and CYP1B1 and also TiPARP are prime candidates that have been described to be strongly differentially regulated through the AhR and might therefore be investigated in more depth in future studies[211].

In summary, these experiment showed that HFD and HFD ctrl are almost equally reduced in AhR ligands as the prototypic ligand-reduced diet (AIN-93G), judged by the reduced expression of AhRR. Future studies using these diets should consider that reduced AhR activity could influence experimental settings.

6.2.3 AhR ligand reduced diets exercise different effects on the intestinal barrier function

Maintenance of ILCs and IELs, production of IL-22, resistance to *Citrobacter rodentium* infection, susceptibility to DSS-induced colitis and oral tolerance efficiency have been shown to depend on AhR activation by AhR ligands in the murine gut [119,120,212]. It has further been shown that AhR ligand exposure is linked to gastritis and colitis in humans[110]. Since we noticed that not only LRD but also HFD and HFD ctrl showed reduced AhR ligands, functional consequences of low AhR activation were investigated and compared between the different dietary groups.

Previous studies indicated that healthy $AhR^{-/-}$ mice do not show increased intestinal barrier permeability, tested by feeding FITC-dextran[121]. This finding was partly explained by a decreased epithelial cell turnover in $AhR^{-/-}$ mice, which might help keeping barrier integrity in absence of IELs and ILCs. Although feeding an AhR ligand reduced diet is believed to mimic the phenotype of $AhR^{-/-}$ mice, elevated transmission of FITC-dextran over the intestinal barrier could be observed for mice on LRD, but not with any other dietary condition. Thus, the lack of AhR ligands in diet affects barrier integrity already under homeostatic conditions. This defect could be rescued by the addition of I3C, which is in line with the literature, where I3C has been shown to act through the AhR in promoting normal intestinal immune function[114]. Interestingly, although having a strong influence on AhRR expression, HFD and HFD ctrl do not influence intestinal barrier permeability. Analysis of additional AhR target genes could potentially help to understand this aspect and clarify if more residual AhR ligands in HDF and HFD ctrl might explain the absence of elevated barrier permeability in mice fed with these two diets. Moreover, HFD and HFD ctrl might contain other immunostimulatory substances that support barrier function and thus substitute for the lack of AhR ligands.

Barrier integrity of mice under different dietary conditions was further tested by treatment with DSS to induce a strong colitis. Deficits in coping with DSS have been demonstrated already for mice receiving a diet that is low in AhR ligands[121]. Consistently, also in our experiments WT mice receiving LRD lost significantly more weight and showed elevated colon shortening. Interestingly, supplementation with I3C was not fully sufficient to rescue

mice from severe weight loss, which has been demonstrated in a previous study[121]. This might be explained by the utilization of different inbred mouse strains, which have shown very different susceptibilities to DSS-induced colitis[213]. A further explanation might be differences in gut microbiota composition. These have been shown to vary considerably between different animal facilities. Certain bacterial strains have recently been shown to have a big influence on DSS colitis susceptibility of mice[171]. It is additionally well known that colitogenic potential of DSS varies between vendors and manufacturing lot[180], offering another possible explanation for differences in DSS colitis between different laboratories.

In contrast, HFD and especially HFD ctrl fed mice showed protection against DSS-induced colitis, judged by reduced weight loss and disease symptoms. This observation is in line with other experiments, showing normal barrier function of these mice under homeostatic conditions. Hence, these results support the previously made hypothesis that HFD and HFD ctrl contain substances that confer protection against intestinal inflammation. For example it was shown that high content of dietary fiber protects against DSS-induced colitis[214]. Further, diet-induced changes in microbial composition might explain the relative mild colitis symptoms of mice on HFD and HFD ctrl, since changes in the microbial composition have been previously show to influence disease outcome in DSS colitis[171]. Despite differences with regard to loss of body weight, colon shortening and MPO values were similar in normal chow, HFD and HFD ctrl fed mice, indicating no differences in intestinal inflammation. Notably, LCN2 levels were highest in stool and serum of HFD fed mice. Recent studies identified LCN2 not only as a biomarker for intestinal inflammation, but also showed that LCN2 is produced by white adipose tissue and can control energy homeostasis and insulin sensitivity[215]. Interestingly WT mice on HFD ctrl displayed the lowest weight loss and the lowest LCN2 levels in stool and, especially, also in serum. On the one hand this can be explained by a lower degree of intestinal inflammation and better tolerance to DSS-induced colitis. On the other hand these mice probably possess less white adipose tissue, which would consequently lower the systemic LCN2 levels.

Cytokines characterizing acute DSS-induced colitis are mainly proinflammatory. However, also pro-resolving chemokines and cytokines that initiate tissue repair are markedly increased in DSS colitis[162]. Consistently, normal chow fed mice displayed the highest levels of proinflammatory cytokines and chemokines (IL-6, IL-1β and CXCL1,), but also showed the highest levels of the barrier protective cytokine IL-22. This counterbalance might explain why these mice develop a relative mild colitis accompanied with fast recovery from colitis. Higher susceptibility to DSS colitis in $AhR^{-/-}$ mice and mice receiving an AhR ligand reduced diet, is

attributed to the lack of IELs, ILC3s and lower IL-22 levels produced by ILC3s and Th17 cells[119]. This could be confirmed for LRD fed mice, as tissue IL-22 was strongly diminished after DSS colitis, while I3C supplementation elevated IL-22 levels, albeit not to the levels of normal chow fed mice. Interestingly, HFD and HFD ctrl fed mice displayed similar IL-22 levels as LRD+I3C fed mice. These results indicate that despite low dietary AhR ligand concentrations in HFD and HFD ctrl, production of IL-22 is sufficiently induced to protect from DSS-induced colitis. Future studies will focus on analyzing the frequencies of IELs and ILC3s after feeding HFD or HFD ctrl since they could be reduced as a consequence of low AhR ligand concentration. As mice on HFD ctrl were clearly protected from DSS symptoms compared to normal chow fed animals, it is intriguing to speculate if components of this diet might activate other pathways to maintain intestinal homeostasis and confer protection against DSS-induced colitis. One recently described candidate is the mammalian pregnane X receptor (PXR), which is a xenobiotic receptor expressed in IECs. The PXR has recently been linked to processes like cell migration, cell survival and apoptosis, all of which are key functions of IECs. It could be shown that activation of the PXR enhaces intestinal epithelial cell migration and wound healing and thereby contributes to intestinal mucosal barrier function[216,217]. Although much less is known about endogenous PXR ligands and their physiological role, recent studies have identified that similar to the AhR, tryptophan metabolites activate the PXR pathway and control barrier function[218].

In summary, feeding mice with HFD and HFD ctrl does not lead to elevated colitis susceptibility in contrast to LRD, despite similar low activation of the AhR. Therefore it is likely that other mechanisms independent of AhR ligands convey protection against DSS-induced colitis in HFD and HFD ctrl fed mice.

6.2.4 Dietary composition contributes to the composition of the intestinal microbiota and the functionality of the intestinal immune system

The composition of the gut microbiota is specific for every individual and has a profound impact on health. However, the interplay between microbiota and the host organism is still not fully understood[84]. Factors that influence the composition of the microbiota are host genetics, general lifestyle, medication, health/disease and the diet. Therefore, it was interesting to assess, whether the different diets used during this study have an influence on the composition of the intestinal gut microbiota. The utilized diets have been chosen due to their content or absence of AhR ligands. Previous studies could already show a role for the AhR in intestinal microbe composition and functionality[219]. The experiments performed in this thesis

highlighted that the dietary AhR activator I3C has a strong influence on the composition of the intestinal microbiota, since mice fed with LRD+I3C had a very different composition of microbial phyla and families than mice on LRD. While frequencies of *Bacteroidetes* were similar between both diets, LRD fed mice displayed an expansion of *Proteobacteria*, whereas supplementation with I3C expanded Firmicutes at the expense of the *Proteobacteria*. *Proteobacteria*, with *Enterobacteriaceae* being the dominant family within this phylum, are generally expanded in IBD patients and may induce IBD in genetically susceptible individuals[220,221]. These observations might also explain the highest DSS colitis susceptibility in LRD fed mice, because they had the highest abundance of *Proteobacteria* and *Enterobacteriaceae*. In humans, *Firmicutes* have been identified as dominant producers of butyrate, supplying energy to the gut epithelium and influencing immune cell functions[222]. Butyrate can limit intestinal inflammation by promoting the formation of Tregs[223]. Further, macrophages have been shown to produce less proinflammatory cytokines if treated with butyrate[224]. Thus, expansion of *Firmicutes* by application of dietary I3C might lead to suppression of intestinal inflammation through butyrate, partially explaining the positive effect of I3C on DSS colitis susceptibility. Future experiments should therefore focus on dissecting microbiota-derived metabolites and how they change upon different dietary conditions.

Despite low AhR ligand concentration in HFD and HFD ctrl, mice receiving these diets did not show elevated susceptibility to DSS colitis, as observed in mice on LRD. The composition of the gut microbiota of HFD and HFD ctrl fed mice was very different from mice receiving LRD and more resembled the composition of bacteria in LRD+I3C fed mice, at least on phylum level. Both diets led to a relative expansion of *Firmicutes* and a reduction of *Proteobacteria*, similar to the I3C supplemented diet. Positive effects coming from the *Firmicutes* might therefore also explain the resistance to DSS-induced colitis of HFD and HFD ctrl fed mice. One family member of the *Firmicutes* phylum specifically expanded in HFD fed mice was the *Lachnospiraceae*. Interestingly, these bacteria have been shown to be depleted in patients with CD and UC[79]. Furthermore, strains of the *Lachnospiraceae* have been described to have beneficial effects, limiting DSS- or *Clostridium difficile*-induced intestinal inflammation[225,226]. The positive effects of *Lachnospiraceae* have also been previously explained by a high production of butyrate by these bacterial family[227]. Hence, expansion of *Lachnospiraceae* in HFD fed mice might explain the relative mild DSS colitis, despite low AhR ligands within the diet. However, the dietary components of the HFD responsible for this expansion process need to be further investigated. Candidates might be

dietary fibers, which increase short chain fatty acid production by the microbiota preventing growth of potentially pathogenic bacteria of the *Enterobacteriaceae*[228]. Another plausible candidate for this phenomenon might be dietary sugars. While complex carbohydrates increase levels of beneficial *Bifidobacteria* spp.[229] refined sugars mediate overgrowth of opportunistic bacteria like *C. difficile*[230]. If and how these substances influence composition of intestinal microbiota will be subject of future studies.

Another interesting observation could be made comparing WT and AhRR$^{E/E}$ mice on LRD. Although PCA of UniFrac distances could not detect general differences between WT and AhRR$^{E/E}$ mice, AhRR$^{E/E}$ mice harbored a population of *Prevotellaceae* that was not detected in WT mice. Intriguingly, this population was only apparent in absence of dietary AhR ligands in mice fed with LRD, suggesting that expansion of *Prevotellaceae* may depend on some residual AhR signaling, which is enhanced in absence of the AhRR. Of note, *Prevotellaceae* could be detected in WT and AhRR$^{E/E}$ mice on LRD+I3C, indicating that the stronger AhR signaling in these animal leads to selective expansion, independent of the presence of the AhRR. Since *Prevotellaceae* could not be detected in normal chow fed mice, also the type of AhR ligand and possibly the concentration could to be important for their expansion. A connection of AhR signaling and *Prevotellaceae* has not been described yet. *Prevotela spp*. have been described as pathobionts, causing disease when the host immunity is perturbed[231]. As AhRR$^{E/E}$ mice show a generally elevated DSS colitis susceptibility, presence of a commensal pathobiont might contribute to the disease. However, elevated colitis susceptibility has been shown for mice on normal chow diet, whereas genotype specific appearance of *Prevotellaceae* could be shown for AhRR$^{E/E}$ mice on LRD. If a true connection between *Prevotellaceae* and AhR signaling exists and what functional consequences this might have, needs to be investigated in future studies.

In summary, these experiments showed that dietary AhR ligands have a strong influence on the composition of the intestinal microbiota, which can in turn influence the immune system of the harboring organism. The lack of the AhRR seems to rather influence individual bacterial families under specific circumstances than induce global changes in microbiota composition. Additionally, other dietary components contained in HFD and HFD ctrl have the potential to change microbial composition and influence the immune system. Future studies will focus on, which substances in these diets induce microbial changes and how this alters DSS colitis susceptibility.

7 References

1. Murphy, K. & Weaver, C. *Janeway's Immunobiology*. (Garland Science, 2016).
2. Parkin, J. & Cohen, B. An overview of the immune system. *Lancet* **357,** 1777–1789 (2001).
3. Delves, P. J. & Roitt, I. M. The immune system. First of two parts. *N. Engl. J. Med.* **343,** 37–49 (2000).
4. Brubaker, S. W., Bonham, K. S., Zanoni, I. & Kagan, J. C. Innate immune pattern recognition: a cell biological perspective. *Annu. Rev. Immunol.* **33,** 257–290 (2015).
5. Netea, M. G. *et al.* Trained immunity: A program of innate immune memory in health and disease. *Science* **352,** aaf1098 (2016).
6. Kaech, S. M., Hemby, S., Kersh, E. & Ahmed, R. Molecular and functional profiling of memory CD8 T cell differentiation. *Cell* **111,** 837–851 (2002).
7. Bonilla, F. A. & Oettgen, H. C. Adaptive immunity. *J. Allergy Clin. Immunol.* **125,** S33–40 (2010).
8. Brandtzaeg, P., Kiyono, H., Pabst, R. & Russell, M. W. Terminology: nomenclature of mucosa-associated lymphoid tissue. *Mucosal Immunol* **1,** 31–37 (2008).
9. Macpherson, A. J. & Smith, K. Mesenteric lymph nodes at the center of immune anatomy. *J. Exp. Med.* **203,** 497–500 (2006).
10. Brucklacher-Waldert, V., Carr, E. J., Linterman, M. A. & Veldhoen, M. Cellular Plasticity of CD4+ T Cells in the Intestine. *Front Immunol* **5,** 488 (2014).
11. Fütterer, A., Mink, K., Luz, A., Kosco-Vilbois, M. H. & Pfeffer, K. The lymphotoxin beta receptor controls organogenesis and affinity maturation in peripheral lymphoid tissues. *Immunity* **9,** 59–70 (1998).
12. Mowat, A. M. Anatomical basis of tolerance and immunity to intestinal antigens. *Nat. Rev. Immunol.* **3,** 331–341 (2003).
13. Mowat, A. M. & Agace, W. W. Regional specialization within the intestinal immune system. *Nat. Rev. Immunol.* **14,** 667–685 (2014).
14. Randall, T. D. & Mebius, R. E. The development and function of mucosal lymphoid tissues: a balancing act with micro-organisms. *Mucosal Immunol* **7,** 455–466 (2014).
15. Montilla, N. A., Blas, M. P., Santalla, M. L. & Villa, J. Mucosal immune system: a brief review. *Inmunología* (2004).
16. Jung, C., Hugot, J.-P. & Barreau, F. Peyer's Patches: The Immune Sensors of the Intestine. *Int J Inflam* **2010,** 823710 (2010).
17. Pabst, O. *et al.* Cryptopatches and isolated lymphoid follicles: dynamic lymphoid tissues dispensable for the generation of intraepithelial lymphocytes. *Eur. J. Immunol.* **35,** 98–107 (2005).
18. Baptista, A. P., Olivier, B. J., Goverse, G. & Greuter, M. Colonic Patch and colonic SILT development are independent and differentially-regulated events. *Mucosal ...* (2013).
19. Kanamori, Y. *et al.* Identification of novel lymphoid tissues in murine intestinal mucosa where clusters of c-kit+ IL-7R+ Thy1+ lympho-hemopoietic progenitors develop. *J. Exp. Med.* **184,** 1449–1459 (1996).
20. Eberl, G. & Littman, D. R. Thymic origin of intestinal alphabeta T cells revealed by fate mapping of RORgammat+ cells. *Science* **305,** 248–251 (2004).
21. Pabst, O., Herbrand, H. & Friedrichsen, M. Adaptation of solitary intestinal lymphoid tissue in response to microbiota and chemokine receptor CCR7 signaling. *The Journal of ...* (2006).
22. Lorenz, R. G., Chaplin, D. D., McDonald, K. G., McDonough, J. S. & Newberry, R. D. Isolated lymphoid follicle formation is inducible and dependent upon lymphotoxin-sufficient B lymphocytes, lymphotoxin beta receptor, and TNF receptor I function. *J Immunol* **170,** 5475–5482 (2003).
23. Tsuji, M. *et al.* Requirement for lymphoid tissue-inducer cells in isolated follicle formation and T cell-independent immunoglobulin A generation in the gut. *Immunity* **29,** 261–271 (2008).
24. Knoop, K. A. & Newberry, R. D. Isolated Lymphoid Follicles are Dynamic Reservoirs for the Induction of Intestinal IgA. *Front Immunol* **3,** 84 (2012).
25. Goodman, T. & Lefrançois, L. Expression of the gamma-delta T-cell receptor on intestinal CD8+ intraepithelial lymphocytes. *Nature* **333,** 855–858 (1988).
26. Hayday, A., Theodoridis, E., Ramsburg, E. & Shires, J. Intraepithelial lymphocytes: exploring the Third Way in immunology. *Nature Immunology* **2,** 997–1003 (2001).
27. Cheroutre, H., Lambolez, F. & Mucida, D. The light and dark sides of intestinal intraepithelial lymphocytes. *Nat. Rev. Immunol.* **11,** 445–456 (2011).
28. Farstad, I. N. *et al.* Distribution of beta 7 integrins in human intestinal mucosa and organized gut-associated lymphoid tissue. *Immunology* **89,** 227–237 (1996).
29. MacDonald, T. T. The mucosal immune system. *Parasite Immunol.* **25,** 235–246 (2003).
30. Hayday, A. & Gibbons, D. Brokering the peace: the origin of intestinal T cells. *Mucosal Immunol* **1,** 172–174 (2008).
31. Izcue, A., Coombes, J. L. & Powrie, F. Regulatory lymphocytes and intestinal inflammation. *Annu. Rev. Immunol.* **27,** 313–338 (2009).
32. Uhlig, H. H. *et al.* Characterization of Foxp3+CD4+CD25+ and IL-10-secreting CD4+CD25+ T cells during cure of colitis. *J Immunol* **177,** 5852–5860 (2006).
33. Maynard, C. L. *et al.* Regulatory T cells expressing interleukin 10 develop from Foxp3+ and Foxp3- precursor cells in the absence of interleukin 10. *Nature Immunology* **8,** 931–941 (2007).
34. Weaver, C. T., Elson, C. O., Fouser, L. A. & Kolls, J. K. The Th17 pathway and inflammatory diseases of the intestines, lungs, and skin. *Annu Rev Pathol* **8,** 477–512 (2013).
35. Korn, T., Bettelli, E., Oukka, M. & Kuchroo, V. K. IL-17 and Th17 Cells. *Annu. Rev. Immunol.* **27,** 485–517 (2009).

36. Ahern, P. P. *et al.* Interleukin-23 drives intestinal inflammation through direct activity on T cells. *Immunity* **33,** 279–288 (2010).
37. Zhu, J., Yamane, H. & Paul, W. E. Differentiation of effector CD4 T cell populations (*). *Annu. Rev. Immunol.* **28,** 445–489 (2010).
38. van Wijk, F. & Cheroutre, H. Mucosal T cells in gut homeostasis and inflammation. *Expert Rev Clin Immunol* **6,** 559–566 (2010).
39. Xu, H., Wang, X. & Veazey, R. S. Th17 Cells Coordinate with Th22 Cells in Maintaining Homeostasis of Intestinal Tissues and both are Depleted in SIV-Infected Macaques. *J AIDS Clin Res* **5,** (2014).
40. Akdis, M., Palomares, O., van de Veen, W., van Splunter, M. & Akdis, C. A. TH17 and TH22 cells: a confusion of antimicrobial response with tissue inflammation versus protection. *J. Allergy Clin. Immunol.* **129,** 1438–49– quiz1450–1 (2012).
41. Kaplan, M. H., Hufford, M. M. & Olson, M. R. The development and in vivo function of T helper 9 cells. *Nat. Rev. Immunol.* **15,** 295–307 (2015).
42. Spits, H. & Cupedo, T. Innate Lymphoid Cells: Emerging Insights in Development, Lineage Relationships, and Function. *Annu. Rev. Immunol.* **30,** 647–675 (2012).
43. Fuchs, A. *et al.* Intraepithelial type 1 innate lymphoid cells are a unique subset of IL-12- and IL-15-responsive IFN-γ-producing cells. *Immunity* **38,** 769–781 (2013).
44. Klose, C. S. N. *et al.* A T-bet gradient controls the fate and function of CCR6-RORγt+ innate lymphoid cells. *Nature* **494,** 261–265 (2013).
45. Spits, H. *et al.* Innate lymphoid cells |[mdash]| a proposal for uniform nomenclature. *Nat. Rev. Immunol.* **13,** 145–149 (2013).
46. McKenzie, A. N. J., Spits, H. & Eberl, G. Innate Lymphoid Cells in Inflammation and Immunity. *Immunity* **41,** 366–374 (2014).
47. Eberl, G., Colonna, M., Di Santo, J. P. & McKenzie, A. N. J. Innate lymphoid cells. Innate lymphoid cells: a new paradigm in immunology. *Science* **348,** aaa6566 (2015).
48. Buonocore, S. *et al.* Innate lymphoid cells drive interleukin-23-dependent innate intestinal pathology. *Nature* **464,** 1371–1375 (2010).
49. Bradford, B. M., Sester, D. P., Hume, D. A. & Mabbott, N. A. Defining the anatomical localisation of subsets of the murine mononuclear phagocyte system using integrin alpha X (Itgax, CD11c) and colony stimulating factor 1 receptor (Csf1r, CD115) expression fails to discriminate dendritic cells from macrophages. *Immunobiology* **216,** 1228–1237 (2011).
50. McDole, J. R. *et al.* Goblet cells deliver luminal antigen to CD103+ dendritic cells in the small intestine. *Nature* **483,** 345–349 (2012).
51. Cerovic, V., Bain, C. C., Mowat, A. M. & Milling, S. W. F. Intestinal macrophages and dendritic cells: what's the difference? *Trends Immunol.* **35,** 270–277 (2014).
52. Bekiaris, V., Persson, E. K. & Agace, W. W. Intestinal dendritic cells in the regulation of mucosal immunity. *Immunol. Rev.* **260,** 86–101 (2014).
53. Tamoutounour, S. *et al.* CD64 distinguishes macrophages from dendritic cells in the gut and reveals the Th1-inducing role of mesenteric lymph node macrophages during colitis. *Eur. J. Immunol.* **42,** 3150–3166 (2012).
54. Cerovic, V. *et al.* Intestinal CD103(-) dendritic cells migrate in lymph and prime effector T cells. *Mucosal Immunol* **6,** 104–113 (2013).
55. Schulz, O., Jaensson, E., Persson, E. K. & Liu, X. Intestinal CD103+, but not CX3CR1+, antigen sampling cells migrate in lymph and serve classical dendritic cell functions. *Journal of ...* (2009).
56. Rivollier, A., He, J., Kole, A., Valatas, V. & Kelsall, B. L. Inflammation switches the differentiation program of Ly6Chi monocytes from antiinflammatory macrophages to inflammatory dendritic cells in the colon. *Journal of Experimental Medicine* **209,** 139–155 (2012).
57. Bain, C. C. *et al.* Resident and pro-inflammatory macrophages in the colon represent alternative context-dependent fates of the same Ly6Chi monocyte precursors. *Mucosal Immunol* **6,** 498–510 (2013).
58. Varol, C. *et al.* Intestinal lamina propria dendritic cell subsets have different origin and functions. *Immunity* **31,** 502–512 (2009).
59. Varol, C. *et al.* Monocytes give rise to mucosal, but not splenic, conventional dendritic cells. *J. Exp. Med.* **204,** 171–180 (2007).
60. Vallon-Eberhard, A., Landsman, L., Yogev, N., Verrier, B. & Jung, S. Transepithelial pathogen uptake into the small intestinal lamina propria. *J Immunol* **176,** 2465–2469 (2006).
61. Ueda, Y. *et al.* Commensal microbiota induce LPS hyporesponsiveness in colonic macrophages via the production of IL-10. *Int. Immunol.* **22,** 953–962 (2010).
62. Shaw, M. H., Kamada, N., Kim, Y.-G. & Núñez, G. Microbiota-induced IL-1β, but not IL-6, is critical for the development of steady-state TH17 cells in the intestine. *Journal of Experimental Medicine* **209,** 251–258 (2012).
63. Fournier, B. M. & Parkos, C. A. The role of neutrophils during intestinal inflammation. *Mucosal Immunol* **5,** 354–366 (2012).
64. Maloy, K. J. & Powrie, F. Intestinal homeostasis and its breakdown in inflammatory bowel disease. *Nature* **474,** 298–306 (2011).
65. Cerutti, A. Location, location, location: B-cell differentiation in the gut lamina propria. *Mucosal Immunol* **1,** 8–10 (2008).
66. Mesin, L., Sollid, L. M. & Di Niro, R. The intestinal B-cell response in celiac disease. *Front Immunol* **3,** 313 (2012).
67. Rooks, M. G. & Garrett, W. S. Gut microbiota, metabolites and host immunity. *Nat. Rev. Immunol.* **16,** 341–352 (2016).
68. Eckburg, P. B. *et al.* Diversity of the human intestinal microbial flora. *Science* **308,** 1635–1638 (2005).

69. Nguyen, T. L. A., Vieira-Silva, S., Liston, A. & Raes, J. How informative is the mouse for human gut microbiota research? *Dis Model Mech* **8,** 1–16 (2015).
70. Turnbaugh, P. J. *et al.* The human microbiome project. *Nature* **449,** 804–810 (2007).
71. Maurice, C. F. & Turnbaugh, P. J. Quantifying the metabolic activities of human-associated microbial communities across multiple ecological scales. *FEMS Microbiol. Rev.* **37,** 830–848 (2013).
72. Smythies, L. E. *et al.* Human intestinal macrophages display profound inflammatory anergy despite avid phagocytic and bacteriocidal activity. *J. Clin. Invest.* **115,** 66–75 (2005).
73. Wu, H.-J. & Wu, E. The role of gut microbiota in immune homeostasis and autoimmunity. *Gut Microbes* **3,** 4–14 (2012).
74. Sanos, S. L. *et al.* RORgammat and commensal microflora are required for the differentiation of mucosal interleukin 22-producing NKp46+ cells. *Nature Immunology* **10,** 83–91 (2009).
75. Gaboriau-Routhiau, V. *et al.* The key role of segmented filamentous bacteria in the coordinated maturation of gut helper T cell responses. *Immunity* **31,** 677–689 (2009).
76. Mazmanian, S. K., Liu, C. H., Tzianabos, A. O. & Kasper, D. L. An immunomodulatory molecule of symbiotic bacteria directs maturation of the host immune system. *Cell* **122,** 107–118 (2005).
77. Zelante, T. *et al.* Tryptophan catabolites from microbiota engage aryl hydrocarbon receptor and balance mucosal reactivity via interleukin-22. *Immunity* **39,** 372–385 (2013).
78. Liu, L. *et al.* Polyamines regulate E-cadherin transcription through c-Myc modulating intestinal epithelial barrier function. *Am. J. Physiol., Cell Physiol.* **296,** C801–10 (2009).
79. Frank, D. N. *et al.* Molecular-phylogenetic characterization of microbial community imbalances in human inflammatory bowel diseases. *Proc. Natl. Acad. Sci. U.S.A.* **104,** 13780–13785 (2007).
80. Manichanh, C. *et al.* Reduced diversity of faecal microbiota in Crohn's disease revealed by a metagenomic approach. *Gut* **55,** 205–211 (2006).
81. Gophna, U., Sommerfeld, K., Gophna, S., Doolittle, W. F. & Veldhuyzen van Zanten, S. J. O. Differences between tissue-associated intestinal microfloras of patients with Crohn's disease and ulcerative colitis. *J. Clin. Microbiol.* **44,** 4136–4141 (2006).
82. Scanlan, P. D., Shanahan, F., O'Mahony, C. & Marchesi, J. R. Culture-independent analyses of temporal variation of the dominant fecal microbiota and targeted bacterial subgroups in Crohn's disease. *J. Clin. Microbiol.* **44,** 3980–3988 (2006).
83. Peterson, D. A., Frank, D. N., Pace, N. R. & Gordon, J. I. Metagenomic approaches for defining the pathogenesis of inflammatory bowel diseases. *Cell Host Microbe* **3,** 417–427 (2008).
84. Graf, D. *et al.* Contribution of diet to the composition of the human gut microbiota. *Microb. Ecol. Health Dis.* **26,** 26164 (2015).
85. Schnorr, S. L. *et al.* Gut microbiome of the Hadza hunter-gatherers. *Nat Commun* **5,** 3654 (2014).
86. Hoeffel, G. *et al.* Adult Langerhans cells derive predominantly from embryonic fetal liver monocytes with a minor contribution of yolk sac-derived macrophages. *Journal of Experimental Medicine* **209,** 1167–1181 (2012).
87. Ginhoux, F. *et al.* Langerhans cells arise from monocytes in vivo. *Nature Immunology* **7,** 265–273 (2006).
88. Tamoutounour, S. *et al.* Origins and functional specialization of macrophages and of conventional and monocyte-derived dendritic cells in mouse skin. *Immunity* **39,** 925–938 (2013).
89. Pasparakis, M., Haase, I. & Nestle, F. O. Mechanisms regulating skin immunity and inflammation. *Nat. Rev. Immunol.* **14,** 289–301 (2014).
90. Mosser, D. M. & Edwards, J. P. Exploring the full spectrum of macrophage activation. *Nat. Rev. Immunol.* **8,** 958–969 (2008).
91. Jakubzick, C., Gautier, E. L., Gibbings, S. L. & Sojka, D. K. Minimal differentiation of classical monocytes as they survey steady-state tissues and transport antigen to lymph nodes. *Immunity* (2013).
92. St John, A. L. *et al.* Immune surveillance by mast cells during dengue infection promotes natural killer (NK) and NKT-cell recruitment and viral clearance. *Proc. Natl. Acad. Sci. U.S.A.* **108,** 9190–9195 (2011).
93. Gebhardt, T. *et al.* Different patterns of peripheral migration by memory CD4+ and CD8+ T cells. *Nature* **477,** 216–219 (2011).
94. Mueller, S. N., Zaid, A. & Carbone, F. R. Tissue-resident T cells: dynamic players in skin immunity. *Front Immunol* **5,** 332 (2014).
95. Esser, C., Bargen, I., Weighardt, H., Haarmann-Stemmann, T. & Krutmann, J. Functions of the aryl hydrocarbon receptor in the skin. *Semin Immunopathol* **35,** 677–691 (2013).
96. Sumaria, N. *et al.* Cutaneous immunosurveillance by self-renewing dermal gammadelta T cells. *Journal of Experimental Medicine* **208,** 505–518 (2011).
97. Villanova, F. *et al.* Characterization of innate lymphoid cells in human skin and blood demonstrates increase of NKp44+ ILC3 in psoriasis. *J. Invest. Dermatol.* **134,** 984–991 (2014).
98. Burbach, K. M., Poland, A. & Bradfield, C. A. Cloning of the Ah-receptor cDNA reveals a distinctive ligand-activated transcription factor. *Proc. Natl. Acad. Sci. U.S.A.* **89,** 8185–8189 (1992).
99. Bersten, D. C., Sullivan, A. E., Peet, D. J. & Whitelaw, M. L. bHLH-PAS proteins in cancer. *Nature Reviews Cancer* **13,** 827–841 (2013).
100. Flaveny, C. A., Murray, I. A., Chiaro, C. R. & Perdew, G. H. Ligand selectivity and gene regulation by the human aryl hydrocarbon receptor in transgenic mice. *Mol. Pharmacol.* **75,** 1412–1420 (2009).
101. Mulero-Navarro, S. & Fernandez-Salguero, P. M. New Trends in Aryl Hydrocarbon Receptor Biology. *Front Cell Dev Biol* **4,** 45 (2016).
102. Michael, A. K. & Partch, C. L. *bHLH-PAS proteins: functional specification through modular domain architecture*. (OA Biochem, 2013).
103. Zhou, L. AHR Function in Lymphocytes: Emerging Concepts. *Trends Immunol.* **37,** 17–31 (2016).
104. Salisbury, T. B. *et al.* Endogenous aryl hydrocarbon receptor promotes basal and inducible expression of tumor

necrosis factor target genes in MCF-7 cancer cells. *Biochem. Pharmacol.* **91,** 390–399 (2014).
105. MacPherson, L. *et al.* Aryl hydrocarbon receptor repressor and TiPARP (ARTD14) use similar, but also distinct mechanisms to repress aryl hydrocarbon receptor signaling. *Int J Mol Sci* **15,** 7939–7957 (2014).
106. MacPherson, L. *et al.* 2,3,7,8-Tetrachlorodibenzo-p-dioxin poly(ADP-ribose) polymerase (TiPARP, ARTD14) is a mono-ADP-ribosyltransferase and repressor of aryl hydrocarbon receptor transactivation. *Nucleic Acids Res.* **41,** 1604–1621 (2013).
107. Kazlauskas, A., Poellinger, L. & Pongratz, I. The immunophilin-like protein XAP2 regulates ubiquitination and subcellular localization of the dioxin receptor. *Journal of Biological Chemistry* (2000).
108. Hankinson, O. The aryl hydrocarbon receptor complex. *Annu. Rev. Pharmacol. Toxicol.* **35,** 307–340 (1995).
109. Apetoh, L. *et al.* The aryl hydrocarbon receptor interacts with c-Maf to promote the differentiation of type 1 regulatory T cells induced by IL-27. *Nature Immunology* **11,** 854–861 (2010).
110. Esser, C. & Rannug, A. The aryl hydrocarbon receptor in barrier organ physiology, immunology, and toxicology. *Pharmacol. Rev.* **67,** 259–279 (2015).
111. Denison, M. S., Soshilov, A. A., He, G., DeGroot, D. E. & Zhao, B. Exactly the same but different: promiscuity and diversity in the molecular mechanisms of action of the aryl hydrocarbon (dioxin) receptor. *Toxicol. Sci.* **124,** 1–22 (2011).
112. Quintana, F. J. The aryl hydrocarbon receptor: a molecular pathway for the environmental control of the immune response. *Immunology* **138,** 183–189 (2013).
113. Denison, M. S., Pandini, A., Nagy, S. R. & Baldwin, E. P. Ligand binding and activation of the Ah receptor. *Chemico-biological …* (2002).
114. Hooper, L. V. You AhR what you eat: linking diet and immunity. *Cell* **147,** 489–491 (2011).
115. Wei, Y. D., Helleberg, H., Rannug, U. & Rannug, A. Rapid and transient induction of CYP1A1 gene expression in human cells by the tryptophan photoproduct 6-formylindolo[3,2-b]carbazole. *Chem. Biol. Interact.* **110,** 39–55 (1998).
116. Song, J. *et al.* A ligand for the aryl hydrocarbon receptor isolated from lung. *Proc. Natl. Acad. Sci. U.S.A.* **99,** 14694–14699 (2002).
117. Wincent, E. *et al.* Inhibition of cytochrome P4501-dependent clearance of the endogenous agonist FICZ as a mechanism for activation of the aryl hydrocarbon receptor. *Proc. Natl. Acad. Sci. U.S.A.* **109,** 4479–4484 (2012).
118. Moura-Alves, P. *et al.* AhR sensing of bacterial pigments regulates antibacterial defence. *Nature* (2014). doi:10.1038/nature13684
119. Qiu, J. *et al.* The aryl hydrocarbon receptor regulates gut immunity through modulation of innate lymphoid cells. *Immunity* **36,** 92–104 (2012).
120. Kiss, E. A. E. *et al.* Natural aryl hydrocarbon receptor ligands control organogenesis of intestinal lymphoid follicles. *Science* **334,** 1561–1565 (2011).
121. Li, Y. *et al.* Exogenous Stimuli Maintain Intraepithelial Lymphocytes via Aryl Hydrocarbon Receptor Activation. *Cell* **147,** 629–640 (2011).
122. Qiu, J. & Zhou, L. Aryl hydrocarbon receptor promotes RORγt+ Group 3 ILCs and controls intestinal immunity and inflammation. *Semin Immunopathol* **35,** 657–670 (2013).
123. Stockinger, B., Di Meglio, P., Gialitakis, M. & Duarte, J. H. The aryl hydrocarbon receptor: multitasking in the immune system. *Annu. Rev. Immunol.* **32,** 403–432 (2014).
124. Chmill, S., Kadow, S., Winter, M., Weighardt, H. & Esser, C. 2,3,7,8-Tetrachlorodibenzo-p-dioxin impairs stable establishment of oral tolerance in mice. *Toxicol. Sci.* **118,** 98–107 (2010).
125. Yeste, A., Nadeau, M., Burns, E. J., Weiner, H. L. & Quintana, F. J. Nanoparticle-mediated codelivery of myelin antigen and a tolerogenic small molecule suppresses experimental autoimmune encephalomyelitis. *Proc. Natl. Acad. Sci. U.S.A.* **109,** 11270–11275 (2012).
126. Haarmann-Stemmann, T. & Abel, J. The arylhydrocarbon receptor repressor (AhRR): structure, expression, and function. *Biological Chemistry* **387,**
127. Evans, B. R. *et al.* Repression of aryl hydrocarbon receptor (AHR) signaling by AHR repressor: role of DNA binding and competition for AHR nuclear translocator. *Mol. Pharmacol.* **73,** 387–398 (2008).
128. Brandstätter, O. *et al.* Balancing intestinal and systemic inflammation through cell type-specific expression of the aryl hydrocarbon receptor repressor. *Sci Rep* **6,** 26091 EP –
129. Kappelman, M. D. *et al.* Direct health care costs of Crohn's disease and ulcerative colitis in US children and adults. *Gastroenterology* **135,** 1907–1913 (2008).
130. Halme, L. *et al.* Family and twin studies in inflammatory bowel disease. *World J. Gastroenterol.* **12,** 3668–3672 (2006).
131. Jostins, L. *et al.* Host-microbe interactions have shaped the genetic architecture of inflammatory bowel disease. *Nature* **491,** 119–124 (2012).
132. Duerr, R. H. *et al.* A genome-wide association study identifies IL23R as an inflammatory bowel disease gene. *Science* **314,** 1461–1463 (2006).
133. Buch, S. *et al.* A genome-wide association scan identifies the hepatic cholesterol transporter ABCG8 as a susceptibility factor for human gallstone disease. *Nat. Genet.* **39,** 995–999 (2007).
134. Kaser, A., Zeissig, S. & Blumberg, R. S. Inflammatory bowel disease. *Annu. Rev. Immunol.* **28,** 573–621 (2010).
135. Faria, A. M. C. & Weiner, H. L. Oral tolerance. *Immunol. Rev.* **206,** 232–259 (2005).
136. Iqbal, N. *et al.* T helper 1 and T helper 2 cells are pathogenic in an antigen-specific model of colitis. *J. Exp. Med.* **195,** 71–84 (2002).
137. Bamias, G. *et al.* New concepts in the pathophysiology of inflammatory bowel disease. *Ann. Intern. Med.* **143,** 895–904 (2005).
138. Műzes, G., Molnár, B., Tulassay, Z. & Sipos, F. Changes of the cytokine profile in inflammatory bowel diseases. *World J. Gastroenterol.* **18,** 5848–5861 (2012).

139. de Mattos, B. R. R. *et al.* Inflammatory Bowel Disease: An Overview of Immune Mechanisms and Biological Treatments. *Mediators Inflamm.* **2015,** 493012 (2015).
140. Monteleone, I., Sarra, M., Pallone, F. & Monteleone, G. Th17-related cytokines in inflammatory bowel diseases: friends or foes? *Curr. Mol. Med.* **12,** 592–597 (2012).
141. Taurog, J. D. *et al.* The germfree state prevents development of gut and joint inflammatory disease in HLA-B27 transgenic rats. *J. Exp. Med.* **180,** 2359–2364 (1994).
142. Hoentjen, F. *et al.* Antibiotics with a selective aerobic or anaerobic spectrum have different therapeutic activities in various regions of the colon in interleukin 10 gene deficient mice. *Gut* **52,** 1721–1727 (2003).
143. Liu, J. Z. *et al.* Association analyses identify 38 susceptibility loci for inflammatory bowel disease and highlight shared genetic risk across populations. *Nat. Genet.* **47,** 979–986 (2015).
144. Schmidt, J. V., Su, G. H. & Reddy, J. K. Characterization of a murine Ahr null allele: involvement of the Ah receptor in hepatic growth and development. in (1996).
145. Clausen, B. E., Burkhardt, C., Reith, W., Renkawitz, R. & Förster, I. Conditional gene targeting in macrophages and granulocytes using LysMcre mice. *Transgenic Res.* **8,** 265–277 (1999).
146. Dieleman, L. A. *et al.* Chronic experimental colitis induced by dextran sulphate sodium (DSS) is characterized by Th1 and Th2 cytokines. *Clin. Exp. Immunol.* **114,** 385–391 (1998).
147. Benson, J. M. & Shepherd, D. M. Dietary ligands of the aryl hydrocarbon receptor induce anti-inflammatory and immunoregulatory effects on murine dendritic cells. *Toxicological Sciences* **124,** 327–338 (2011).
148. Monteleone, I., MacDonald, T. T., Pallone, F. & Monteleone, G. The aryl hydrocarbon receptor in inflammatory bowel disease. *Current Opinion in Gastroenterology* **28,** 310–313 (2012).
149. Brandstätter, O. Expression und Funktion des Arylhydrocarbon Rezeptor Repressor (AhRR) im darmassoziierten Immunsystem. (Rheinische Friedrich-Wilhelms-Universität Bonn).
150. Lee, J. S. *et al.* AHR drives the development of gut ILC22 cells and postnatal lymphoid tissues via pathways dependent on and independent of Notch. *Nature Immunology* **13,** 144–151 (2012).
151. Spits, H. & Di Santo, J. P. The expanding family of innate lymphoid cells: regulators and effectors of immunity and tissue remodeling. *Nature Immunology* **12,** 21–27 (2011).
152. Quintana, F. J. *et al.* Control of T(reg) and T(H)17 cell differentiation by the aryl hydrocarbon receptor. *Nature* **453,** 65–71 (2008).
153. Singh, N. P. *et al.* Activation of aryl hydrocarbon receptor (AhR) leads to reciprocal epigenetic regulation of FoxP3 and IL-17 expression and amelioration of experimental colitis. *PLoS ONE* **6,** e23522 (2011).
154. Veldhoen, M., Hocking, R. J., Atkins, C. J., Locksley, R. M. & Stockinger, B. TGFbeta in the context of an inflammatory cytokine milieu supports de novo differentiation of IL-17-producing T cells. *Immunity* **24,** 179–189 (2006).
155. Bettelli, E. *et al.* Reciprocal developmental pathways for the generation of pathogenic effector TH17 and regulatory T cells. *Nature* **441,** 235–238 (2006).
156. Mangan, P. R., Harrington, L. E., O'quinn, D. B. & Helms, W. S. Transforming growth factor-[beta] induces development of the TH17 lineage. *Nature* (2006).
157. Wilson, N. J. *et al.* Development, cytokine profile and function of human interleukin 17-producing helper T cells. *Nature Immunology* **8,** 950–957 (2007).
158. Yang, L. *et al.* IL-21 and TGF-beta are required for differentiation of human T(H)17 cells. *Nature* **454,** 350–352 (2008).
159. Manel, N., Unutmaz, D. & Littman, D. R. The differentiation of human T(H)-17 cells requires transforming growth factor-beta and induction of the nuclear receptor RORgammat. *Nature Immunology* **9,** 641–649 (2008).
160. Srenathan, U., Steel, K. & Taams, L. S. IL-17+ CD8+ T cells: Differentiation, phenotype and role in inflammatory disease. *Immunol. Lett.* **178,** 20–26 (2016).
161. Dinarello, C. A. Biologic basis for interleukin-1 in disease. *Blood* **87,** 2095–2147 (1996).
162. Alex, P. *et al.* Distinct cytokine patterns identified from multiplex profiles of murine DSS and TNBS-induced colitis. *Inflamm. Bowel Dis.* **15,** 341–352 (2009).
163. Chassaing, B. *et al.* Fecal lipocalin 2, a sensitive and broadly dynamic non-invasive biomarker for intestinal inflammation. *PLoS ONE* **7,** e44328 (2012).
164. Identification of a novel mechanism of regulationof Ah (dioxin) receptor function. 1–6 (1999).
165. Veldhoen, M. & Brucklacher-Waldert, V. Dietary influences on intestinal immunity. *Nat. Rev. Immunol.* **12,** 696–708 (2012).
166. Sartor, R. B. Therapeutic manipulation of the enteric microflora in inflammatory bowel diseases: antibiotics, probiotics, and prebiotics. *YGAST* **126,** 1620–1633 (2004).
167. Reikvam, D. H. *et al.* Depletion of murine intestinal microbiota: effects on gut mucosa and epithelial gene expression. *PLoS ONE* **6,** e17996 (2011).
168. Wincent, E. *et al.* The suggested physiologic aryl hydrocarbon receptor activator and cytochrome P4501 substrate 6-formylindolo[3,2-b]carbazole is present in humans. *J. Biol. Chem.* **284,** 2690–2696 (2009).
169. Furue, M., Takahara, M., Nakahara, T. & Uchi, H. Role of AhR/ARNT system in skin homeostasis. *Arch. Dermatol. Res.* **306,** 769–779 (2014).
170. Krawisz, J. E., Sharon, P. & Stenson, W. F. Quantitative assay for acute intestinal inflammation based on myeloperoxidase activity. Assessment of inflammation in rat and hamster models. *YGAST* **87,** 1344–1350 (1984).
171. Roy, U. *et al.* Distinct Microbial Communities Trigger Colitis Development upon Intestinal Barrier Damage via Innate or Adaptive Immune Cells. *Cell Rep* **21,** 994–1008 (2017).
172. Mimura, J. & Fujii-Kuriyama, Y. Functional role of AhR in the expression of toxic effects by TCDD. *Biochim. Biophys. Acta* **1619,** 263–268 (2003).
173. Qiu, J. *et al.* Group 3 Innate Lymphoid Cells Inhibit T-Cell-Mediated Intestinal Inflammation through Aryl Hydrocarbon Receptor Signaling and Regulation of Microflora. *Immunity* **39,** 386–399 (2013).

174. Cua, D. J. & Tato, C. M. Innate IL-17-producing cells: the sentinels of the immune system. *Nat. Rev. Immunol.* **10,** 479–489 (2010).
175. Parks, O. B., Pociask, D. A., Hodzic, Z., Kolls, J. K. & Good, M. Interleukin-22 Signaling in the Regulation of Intestinal Health and Disease. *Front Cell Dev Biol* **3,** 85 (2015).
176. Colonna, M. Interleukin-22-producing natural killer cells and lymphoid tissue inducer-like cells in mucosal immunity. *Immunity* **31,** 15–23 (2009).
177. Satoh-Takayama, N. *et al.* Microbial flora drives interleukin 22 production in intestinal NKp46+ cells that provide innate mucosal immune defense. *Immunity* **29,** 958–970 (2008).
178. Wang, Y. *et al.* Lymphotoxin beta receptor signaling in intestinal epithelial cells orchestrates innate immune responses against mucosal bacterial infection. *Immunity* **32,** 403–413 (2010).
179. Satoh-Takayama, N. *et al.* The chemokine receptor CXCR6 controls the functional topography of interleukin-22 producing intestinal innate lymphoid cells. *Immunity* **41,** 776–788 (2014).
180. Chassaing, B., Aitken, J. D., Malleshappa, M. & Vijay-Kumar, M. Dextran sulfate sodium (DSS)-induced colitis in mice. *Curr Protoc Immunol* **104,** Unit 15.25. (2014).
181. Duarte, J. H., Di Meglio, P., Hirota, K., Ahlfors, H. & Stockinger, B. Differential influences of the aryl hydrocarbon receptor on Th17 mediated responses in vitro and in vivo. *PLoS ONE* **8,** e79819 (2013).
182. Zenewicz, L. A., Antov, A. & Flavell, R. A. CD4 T-cell differentiation and inflammatory bowel disease. *Trends Mol Med* **15,** 199–207 (2009).
183. Ogawa, A., Andoh, A., Araki, Y., Bamba, T. & Fujiyama, Y. Neutralization of interleukin-17 aggravates dextran sulfate sodium-induced colitis in mice. *Clin. Immunol.* **110,** 55–62 (2004).
184. Yamamura, T. & Gran, B. *Multiple Sclerosis Immunology*. (Springer Science & Business Media, 2013).
185. Ikeda, S. *et al.* Excess IL-1 signaling enhances the development of Th17 cells by downregulating TGF-β-induced Foxp3 expression. *J Immunol* **192,** 1449–1458 (2014).
186. Liang, Y., Pan, H.-F. & Ye, D.-Q. Tc17 Cells in Immunity and Systemic Autoimmunity. *Int. Rev. Immunol.* **34,** 318–331 (2015).
187. Maggi, L. *et al.* CD161 is a marker of all human IL-17-producing T-cell subsets and is induced by RORC. *Eur. J. Immunol.* **40,** 2174–2181 (2010).
188. Nelson, M. H. *et al.* The inducible costimulator augments Tc17 cell responses to self and tumor tissue. *J Immunol* **194,** 1737–1747 (2015).
189. Chung, Y. *et al.* Critical regulation of early Th17 cell differentiation by interleukin-1 signaling. *Immunity* **30,** 576–587 (2009).
190. Atarashi, K. *et al.* ATP drives lamina propria T(H)17 cell differentiation. *Nature* **455,** 808–812 (2008).
191. Persson, E. K., Scott, C. L., Mowat, A. M. & Agace, W. W. Dendritic cell subsets in the intestinal lamina propria: Ontogeny and function. *Eur. J. Immunol.* n/a–n/a (2013). doi:10.1002/eji.201343740
192. Schlitzer, A. *et al.* IRF4 transcription factor-dependent CD11b+ dendritic cells in human and mouse control mucosal IL-17 cytokine responses. *Immunity* **38,** 970–983 (2013).
193. Persson, E. K. *et al.* IRF4 transcription-factor-dependent CD103(+)CD11b(+) dendritic cells drive mucosal T helper 17 cell differentiation. *Immunity* **38,** 958–969 (2013).
194. Pull, S. L., Doherty, J. M., Mills, J. C., Gordon, J. I. & Stappenbeck, T. S. Activated macrophages are an adaptive element of the colonic epithelial progenitor niche necessary for regenerative responses to injury. *Proc. Natl. Acad. Sci. U.S.A.* **102,** 99–104 (2005).
195. Qualls, J. E., Kaplan, A. M., van Rooijen, N. & Cohen, D. A. Suppression of experimental colitis by intestinal mononuclear phagocytes. *J. Leukoc. Biol.* **80,** 802–815 (2006).
196. Conway, K. L. *et al.* p40phox expression regulates neutrophil recruitment and function during the resolution phase of intestinal inflammation. *J Immunol* **189,** 3631–3640 (2012).
197. Rauch, I. *et al.* Type I interferons have opposing effects during the emergence and recovery phases of colitis. *Eur. J. Immunol.* **44,** 2749–2760 (2014).
198. Ellekilde, M. *et al.* Transfer of gut microbiota from lean and obese mice to antibiotic-treated mice. *Sci Rep* **4,** 5922 (2014).
199. Hansen, A. K. Antibiotic treatment of nude rats and its impact on the aerobic bacterial flora. *Lab. Anim.* **29,** 37–44 (1995).
200. Schiering, C. *et al.* Feedback control of AHR signalling regulates intestinal immunity. *Nature* **542,** 242–245 (2017).
201. Bjeldanes, L. F., Kim, J. Y., Grose, K. R., Bartholomew, J. C. & Bradfield, C. A. Aromatic hydrocarbon responsiveness-receptor agonists generated from indole-3-carbinol in vitro and in vivo: comparisons with 2,3,7,8-tetrachlorodibenzo-p-dioxin.
202. Busbee, P. B., Rouse, M., Nagarkatti, M. & Nagarkatti, P. S. Use of natural AhR ligands as potential therapeutic modalities against inflammatory disorders. *Nutr. Rev.* **71,** 353–369 (2013).
203. Hubbard, T. D., Murray, I. A. & Perdew, G. H. Indole and Tryptophan Metabolism: Endogenous and Dietary Routes to Ah Receptor Activation. *Drug Metab. Dispos.* **43,** 1522–1535 (2015).
204. Fritsche, E. *et al.* Lightening up the UV response by identification of the arylhydrocarbon receptor as a cytoplasmatic target for ultraviolet B radiation. *Proc. Natl. Acad. Sci. U.S.A.* **104,** 8851–8856 (2007).
205. Baba, T. *et al.* Structure and expression of the Ah receptor repressor gene. *J. Biol. Chem.* **276,** 33101–33110 (2001).
206. Barnard, D. E., Lewis, S. M., Teter, B. B. & Thigpen, J. E. Open- and closed-formula laboratory animal diets and their importance to research. *J. Am. Assoc. Lab. Anim. Sci.* **48,** 709–713 (2009).
207. Reeves, P. G., Nielsen, F. H. & Fahey, G. C. AIN-93 purified diets for laboratory rodents: final report of the American Institute of Nutrition ad hoc writing committee on the reformulation of the AIN-76A rodent diet. in **123,** 1939–1951 (1993).

208. Report of the American Institute of Nurtition ad hoc Committee on Standards for Nutritional Studies. *J. Nutr.* **107,** 1340–1348 (1977).
209. Denison, M. S. & Faber, S. C. And Now for Something Completely Different: Diversity in Ligand-Dependent Activation of Ah Receptor Responses. *Curr Opin Toxicol* **2,** 124–131 (2017).
210. Seidel, S. D. *et al.* Activation of the Ah receptor signaling pathway by prostaglandins. *J. Biochem. Mol. Toxicol.* **15,** 187–196 (2001).
211. Lo, R. & Matthews, J. High-resolution genome-wide mapping of AHR and ARNT binding sites by ChIP-Seq. *Toxicol. Sci.* **130,** 349–361 (2012).
212. Monteleone, I. *et al.* Aryl Hydrocarbon Receptor-Induced Signals Up-regulate IL-22 Production and Inhibit Inflammation in the Gastrointestinal Tract. *YGAST* **141,** 237–248.e1 (2011).
213. Mähler, M. *et al.* Differential susceptibility of inbred mouse strains to dextran sulfate sodium-induced colitis. *Am. J. Physiol.* **274,** G544–51 (1998).
214. Silveira, A. L. M. *et al.* Preventive rather than therapeutic treatment with high fiber diet attenuates clinical and inflammatory markers of acute and chronic DSS-induced colitis in mice. *Eur J Nutr* **56,** 179–191 (2017).
215. Jun, L. S., Siddall, C. P. & Rosen, E. D. A minor role for lipocalin 2 in high-fat diet-induced glucose intolerance. *Am. J. Physiol. Endocrinol. Metab.* **301,** E825–35 (2011).
216. Ranhotra, H. S. *et al.* Xenobiotic Receptor-Mediated Regulation of Intestinal Barrier Function and Innate Immunity. *Nucl Receptor Res* **3,** (2016).
217. Terc, J., Hansen, A., Alston, L. & Hirota, S. A. Pregnane X receptor agonists enhance intestinal epithelial wound healing and repair of the intestinal barrier following the induction of experimental colitis. *Eur J Pharm Sci* **55,** 12–19 (2014).
218. Venkatesh, M. *et al.* Symbiotic bacterial metabolites regulate gastrointestinal barrier function via the xenobiotic sensor PXR and Toll-like receptor 4. *Immunity* **41,** 296–310 (2014).
219. Murray, I. A., Nichols, R. G., Zhang, L., Patterson, A. D. & Perdew, G. H. Expression of the aryl hydrocarbon receptor contributes to the establishment of intestinal microbial community structure in mice. *Sci Rep* **6,** 33969 (2016).
220. Sasaki, M. & Klapproth, J.-M. A. The Role of Bacteria in the Pathogenesis of Ulcerative Colitis. *Journal of Signal Transduction* **2012,** 1–6 (2012).
221. Matsuoka, K. & Kanai, T. The gut microbiota and inflammatory bowel disease. *Semin Immunopathol* **37,** 47–55 (2015).
222. Cushing, K., Alvarado, D. M. & Ciorba, M. A. Butyrate and Mucosal Inflammation: New Scientific Evidence Supports Clinical Observation. *Clin Transl Gastroenterol* **6,** e108 (2015).
223. Furusawa, Y. *et al.* Commensal microbe-derived butyrate induces the differentiation of colonic regulatory T cells. *Nature* **504,** 446–450 (2013).
224. Chang, P. V., Hao, L., Offermanns, S. & Medzhitov, R. The microbial metabolite butyrate regulates intestinal macrophage function via histone deacetylase inhibition. *Proc. Natl. Acad. Sci. U.S.A.* **111,** 2247–2252 (2014).
225. Chen, L. *et al.* Corrigendum: NLRP12 attenuates colon inflammation by maintaining colonic microbial diversity and promoting protective commensal bacterial growth. *Nature Immunology* **18,** 1270 (2017).
226. Reeves, A. E., Koenigsknecht, M. J., Bergin, I. L. & Young, V. B. Suppression of Clostridium difficile in the gastrointestinal tracts of germfree mice inoculated with a murine isolate from the family Lachnospiraceae. *Infect. Immun.* **80,** 3786–3794 (2012).
227. Meehan, C. J. & Beiko, R. G. A phylogenomic view of ecological specialization in the Lachnospiraceae, a family of digestive tract-associated bacteria. *Genome Biol Evol* **6,** 703–713 (2014).
228. Zimmer, J. *et al.* A vegan or vegetarian diet substantially alters the human colonic faecal microbiota. *Eur J Clin Nutr* **66,** 53–60 (2012).
229. Pokusaeva, K., Fitzgerald, G. F. & van Sinderen, D. Carbohydrate metabolism in Bifidobacteria. *Genes Nutr* **6,** 285–306 (2011).
230. Berg, A. M., Kelly, C. P. & Farraye, F. A. Clostridium difficile infection in the inflammatory bowel disease patient. *Inflamm. Bowel Dis.* **19,** 194–204 (2013).
231. Ivanov, I. I. & Honda, K. Intestinal commensal microbes as immune modulators. *Cell Host Microbe* **12,** 496–508 (2012).

Publications

Böttcher JP, **Schanz O**, Wohlleber D, Abdullah Z, Debey-Pascher S, Staratschek-Jox A, Höchst B, Hegenbarth S, Grell J, Limmer A, Atreya I, Neurath MF, Busch DH, Schmitt E, van Endert P, Kolanus W, Kurts C, Schultze JL, Diehl L, Knolle PA. Liver-primed memory T cells generated under noninflammatory conditions provide anti-infectious immunity. Cell Rep. 2013 Mar 28;3(3):779-95. doi: 10.1016/j.celrep.2013.02.008.

Böttcher JP*, **Schanz O***, Garbers C, Zaremba A, Hegenbarth S, Kurts C, Beyer M, Schultze JL, Kastenmüller W, Rose-John S, Knolle PA. IL-6 trans-signaling-dependent rapid development of cytotoxic CD8+ T cell function. Cell Rep. 2014 Sep 11;8(5):1318-27. doi: 10.1016/j.celrep.2014.07.008. Epub 2014 Sep 4.

Brandstätter O*, **Schanz O***, Vorac J*, König J, Mori T, Maruyama T, Korkowski M, Haarmann-Stemmann T, von Smolinski D, Schultze JL, Abel J, Esser C, Takeyama H, Weighardt H, Förster I. Balancing intestinal and systemic inflammation through cell type-specific expression of the aryl hydrocarbon receptor repressor. Sci Rep. 2016 May 17;6:26091. doi: 10.1038/srep26091.

Wittlich M, Dudek M, Böttcher JP, **Schanz O**, Hegenbarth S, Bopp T, Schmitt E, Kurts C, Garbers C, Rose John S, Knolle PA, Wohlleber D. Liver sinusoidal endothelial cell cross-priming is supported by CD4 T cell-derived IL-2. J Hepatol. 2017 May;66(5):978-986. doi: 10.1016/j.jhep.2016.12.015.

Fülle L, Steiner N, Funke M, Gondorf F, Pfeiffer F, Siegl J, Opitz FV, Haßel SK, Erazo AB, **Schanz O**, Stunden HJ, Blank M, Gröber C, Händler K, Beyer M, Weighardt H, Latz E, Schultze JL, Mayer G, Förster I. RNA Aptamers Recognizing Murine CCL17 Inhibit T Cell Chemotaxis and Reduce Contact Hypersensitivity In Vivo. Mol Ther. 2017 Oct 13. pii: S1525-0016(17)30521-X. doi: 10.1016/j.ymthe.2017.10.005.

*Co-first author

Acknowledgments

I would like to sincerely thank everyone who helped me during the time of my PhD thesis with advice and support.

First of all I want to thank Prof. Dr. Irmgard Förster for accepting me as a PhD student, for mentoring and supervising my PhD project and for giving me thought-provoking impulses during my PhD project.

A very special thanks goes also to PD Dr. Heike Weighardt for giving very valuable scientific input whenever I needed it, for fruitful discussions and for finally putting a lot of work in proofreading my thesis.

I further want to thank Prof. Dr. Natalio Garbi for being the second referee for my PhD thesis.

I would like to thank all members of the AG Förster/AG Weighardt for great collaboration and constant support whenever I needed it. In particular I want to thank Olga Brandstätter for introducing me into the project and showing me all the things I needed to know to have an easy start into my PhD project. I further would like to thank Philip Hatzfeld for technical assistance with a lot of cell isolations and for the fun we had solving genetic problems. I also want to thank Laura Schlautmann for working with me side by side on this project during her Bachelor thesis, which led to some valuable results for both of our theses.

A special thanks goes to the group of Prof. Haruko Takeyama in Tokyo, who did valuable microbiome analysis for this thesis and also showed me a great time during my visit in 2016. I want to highlight Rieka Chijiiwa here, who especially during the final phase of the cooperation put a lot of effort in providing me with figures that I needed.

I want to thank my family and friends in Dortmund and Bonn who supported me during my whole studies, starting from the Bachelor in Molecular Biomedicine and finding a closure with the finish of my PhD.

Last but not least I want to thank Judith, not only for proofreading of my thesis and being patient with my moods during writing the thesis but also for a good time over all the years. You helped me to get my head off science when I needed to and not to loose my motivation during frustrating phases. Thank you for always being there for me.